

FLEXIBLE MULTIBODY DYNAMIC MODELING AND SIMULATION OF
RHEX HEXAPOD ROBOT WITH HALF CIRCULAR COMPLIANT LEGS

A THESIS SUBMITTED TO
THE GRADUATE SCHOOL OF NATURAL AND APPLIED SCIENCES
OF
MIDDLE EAST TECHNICAL UNIVERSITY

BY

GÖKHAN ORAL

IN PARTIAL FULFILLMENT OF THE REQUIREMENTS
FOR
THE DEGREE OF MASTER OF SCIENCE
IN
MECHANICAL ENGINEERING

NOVEMBER 2008

Approval of the thesis:

**FLEXIBLE MULTIBODY DYNAMIC MODELING AND SIMULATION OF
RHEX HEXAPOD ROBOT WITH HALF CIRCULAR COMPLIANT LEGS**

submitted by **GÖKHAN ORAL** in partial fulfillment of the requirements for the degree of **Master of Science in Mechanical Engineering Department, Middle East Technical University** by,

Prof. Dr. Canan Özgen
Dean, Graduate School of **Natural and Applied Sciences** _____

Prof. Dr. Sūha Oral
Head of Department, **Mechanical Engineering** _____

Assist. Prof. Dr. Yiğit Yazıcıoğlu
Supervisor, **Mechanical Engineering Dept., METU** _____

Assist. Prof. Dr. Afşar Saranlı
Co supervisor, **Electrical and Electronics Eng. Dept., METU** _____

Examining Committee Members:

Prof. Dr. Samim Ünlüsoy
Mechanical Engineering Dept., METU _____

Assist. Prof. Dr. Yiğit Yazıcıoğlu
Mechanical Engineering Dept., METU _____

Prof. Dr. Kemal İder
Mechanical Engineering Dept., METU _____

Assist. Prof. Dr. Buğra Koku
Mechanical Engineering Dept., METU _____

Assist. Prof. Dr.. Veysel Gazi
Electrical Engineering Dept., TOBB UNIVERSITY
OF ECONOMICS AND TECHNOLOGY _____

Date: _____ Nov 24, 2008

I hereby declare that all information in this document has been obtained and presented in accordance with academic rules and ethical conduct. I also declare that, as required by these rules and conduct, I have fully cited and referenced all material and results that are not original to this work.

Name, Last name : Gökhan Oral

Signature :

ABSTRACT

FLEXIBLE MULTIBODY DYNAMIC MODELING AND SIMULATION OF RHEX HEXAPOD ROBOT WITH HALF CIRCULAR COMPLIANT LEGS

Oral, Gökhan

M. S. in Department of Mechanical Engineering

Supervisor: Assist. Prof. Dr. Yiğit Yazıcıoğlu

Co-Supervisor: Assist. Prof. Dr. Afşar Saranlı

November, 2008, 130 pages

The focus of interest in this study is the RHex robot, which is a hexapod robot that is capable of locomotion over rugged, fractured terrain through statically and dynamically stable gaits while stability of locomotion is preserved. RHex is primarily a research platform that is based on over five years of previous research. The purpose of the study is to build a virtual prototype of RHex robot in order to simulate different behavior without manufacturing expensive prototypes. The virtual prototype is modeled in MSC ADAMS software which is a very useful program to simulate flexible multibody dynamical systems. The flexible half circular legs are modeled in a finite element program (MSC NASTRAN) and are embedded in the main model. Finally a closed loop control mechanism is built in MATLAB to be able to simulate real autonomous RHex robot. The interaction of MATLAB and MSC ADAMS softwares is studied.

Keywords: Multibody Dynamics Simulation, Finite Element Analysis, Flexible Multibody Dynamic Modeling,

ÖZ

YARIM DAİRE ŞEKLİNDEKİ ESNEK ALTI BACAKLI RHEX ROBOTUNUN ESNEK ÇOK GÖVDELİ DİNAMİK MODELLENMESİ VE SİMULASYONU

Oral, Gökhan

Yüksek Lisans Makine Mühendisliği Bölümü

Tez Yöneticisi: Y. Doç. Dr. Yiğit Yazıcıoğlu

Ortak Tez Yöneticisi: Assist. Prof. Dr. Afşar Saranlı

Kasım, 2008, 130 sayfa

Yarım daire şeklindeki esnek altı bacaklı Rhex robotu bozuk yüzeylerde dinamik stabilitesini koruyarak saniyede boyunun birkaç katı hızda ilerleyebilmektedir. Bu tezin amacı esnek çok gövdeli bir yapıya sahip olan Rhex robotunun dinamik modelinin oluşturulmasıdır. MSC ADAMS programı robotun ana dinamik modelinin oluşturulmasında kullanılmıştır. Esnek bacaklar sonlu eleman analizi programı olan MSC NASTRAN ile çözülmüş ve ana modele eklenmiştir. En son aşama olarak oluşturulan dinamik modelin MATLAB kontrol programı ile entegrasyonu tamamlanmış böylece otonom davranış sergileyebilen RHex robotunun tam modeli çıkarılmıştır. Prototip üreterek farklı davranışları ve farklı özellikteki parçaları robot üzerinde denemek çoğu zaman pahalı ve çok zaman gerektiren bir süreç olmuştur. Bu tezde karmaşık çok gövdeli altı bacaklı robot RHex'in sanal bir modeli oluşturulmuştur.

Anahtar kelimeler: Çok gövdeli dinamik modelleme, Sonlu eleman analizi, esnek çok gövdeli dinamik modelleme

ACKNOWLEDGEMENTS

I deeply thank to whom has participated within this study.

TABLE OF CONTENTS

ABSTRACT.....	iv
ÖZ.....	v
ACKNOWLEDGEMENTS	vi
CHAPTERS	
1. INTRODUCTION	1
1.1. Wheeled and Tracked Robots.....	4
1.2. Legged Robots.....	5
1.3. Present Day Legged Robots	9
1.3.1. Monopod Robots	9
1.3.2. Biped Robots	13
1.3.3. Quadruped Robots.....	16
1.3.4. Hexapod Robots	19
1.4. Flexible Multibody Dynamic Simulation	22
2. MECHANICAL DESIGN OF RHEX.....	28
2.1 Overall Description of the Design.....	28
2.2. Crash Frame	30
2.3. Base Frame.....	31
2.4. Motor mounting parts	34
2.5. The Flexible Legs	36
2.6. Inner Mounting Parts	37
2.6.1. Motor Driver Board Holder	38
2.6.2 Side Supports	39
2.6.3 PC104 Housing.....	39
3. FLEXIBLE MULTIBODY DYNAMIC SIMULATION	41
3.1. Motivation	41
3.2. ADAMS Software	42
3.3. Modeling RHex.....	43
3.4. ADAMS/Control Module	57
3.5. The complete and fully controllable model	64
4. CASE STUDIES.....	71

4.1. Simulation study with parameters in literature	71
4.2. Simulation trial with MATLAB interaction.....	77
4.3. Stable tripod walking with arbitrary parameters.....	82
4.4. The effect of leg compliance.....	88
4.4.1 Simulation run with 5 GPa Elastic Modulus	88
4.4.2 Simulation run with 10 GPa Elastic Modulus	92
4.5. The effect of t_{ratio} parameter.....	96
4.5.1. Simulation study with $t_{ratio}= 0.5$	96
4.5.2. Simulation study with $t_{ratio} = 1$	99
4.5.3. Simulation study with $t_{ratio} = 1.5$	102
4.5.4. Comparison of the three simulation results	104
4.6. The effect of Φ_s parameter	107
5. CONCLUSION	112
REFERENCES.....	115
APPENDICES	
A. VELOCITY INPUT FOR LEFT AND RIGHT TRIPOD FOR VALIDATION WITH THE LITERATURE RESULTS.....	122
B. VELOCITY INPUT FOR LEFT AND RIGHT TRIPOD FOR ARBITRARY PARAMETER SET.....	124
C. VELOCITY INPUT FOR LEFT AND RIGHT TRIPOD FOR $t_{ratio}= 0.5$	126
D. VELOCITY INPUT FOR LEFT AND RIGHT TRIPOD FOR $t_{ratio}= 1$...	127
E. VELOCITY INPUT FOR LEFT AND RIGHT TRIPOD FOR $t_{ratio}= 1.5$	128
F. VELOCITY INPUT FOR LEFT AND RIGHT TRIPOD FOR Φ_s PARAMETER.....	129

LIST OF FIGURES

FIGURES

Figure 1 Tracked and Wheeled Robot [3]	4
Figure 2 Raibert's Pogostick.....	11
Figure 3 ARL Monopod II Experiment Setup.....	12
Figure 4 WABOT-1.....	13
Figure 5 WABOT-2.....	14
Figure 6 ASIMO (Advanced Step in Innovative MObility).....	16
Figure 7 First Quadruped Machine.....	17
Figure 8 General Electric Quadruped	18
Figure 9 Phoney Poney	18
Figure 10 Scout I.....	19
Figure 11 OSU Hexapod.....	20
Figure 12 Boadicea.....	21
Figure 13 TUM Robot	21
Figure 14 Whegs I.....	21
Figure 15 Rhex - Compliant-Legged Hexapod Robot.....	22
Figure 16 ADAMS Model	24
Figure 17 Experimental Setup.....	24
Figure 18 Optimization of Crank Driver Mechanism Part.....	26
Figure 19 Durability Analysis of Spare-wheel Carrier.....	26
Figure 20 The base and crash frame assembly.....	29
Figure 21 The photograph of the main body of Rhex (base and crash frame) with motor and gearbox assemblies.....	29
Figure 22 The crash frame of RHex.....	30
Figure 23 The new motor mounting part.	31
Figure 24 The base frame.....	32
Figure 25 Frame Left Rail	33
Figure 26 Frame end angle	33
Figure 27 Frame middle angle	33
Figure 28 Frame assembly	34
Figure 29 Hip bearing seat and Hip bearing spacer.....	35
Figure 30 Exploded view of the motor mounting assembly.....	35
Figure 31 Leg mounted to the motor mounting assembly	36
Figure 32 The orientation of the multilayer fiberglass	37
Figure 33 Motor driver board holder.....	38
Figure 34 The final assembly of the robot.....	38
Figure 35 Side support.....	39
Figure 36 Side supports and PC104 housing assembly.....	39
Figure 37 Final assembly of the manufactured parts	40
Figure 38 Box model.....	44
Figure 39 CAD import from Patran.....	44

Figure 40	Import menu in ADAMS software	45
Figure 41	Import Menu in MSC PATRAN.....	46
Figure 42	Mesh properties definition.....	47
Figure 43	Tetrahedron element meshing with 1899 elements.....	48
Figure 44	Tetrahedron element meshing with 35811 elements.....	48
Figure 45	Create Node – The connection point	49
Figure 46	Node definition and connection.....	50
Figure 47	Material creation and property definition	51
Figure 48	Material assigning	51
Figure 49	Analysis settings-1	52
Figure 50	Analysis settings -2	53
Figure 51	Analysis settings-3	54
Figure 52	Function Builder Menu.....	55
Figure 53	Defined motions of the legs	56
Figure 54	Simple Pendulum Model	58
Figure 55	Assigning variables	58
Figure 56	Torque variable.....	59
Figure 57	Position variable	59
Figure 58	Assigning torque variable to the applied torque	60
Figure 59	Defining control plant.....	61
Figure 60	The final state of the control plant submenu.....	61
Figure 61	“Adams_sub” block, represents the simple pendulum system	62
Figure 62	Closed loop control of the angular position.....	63
Figure 63	Torque input to the legs.....	65
Figure 64	Definition of the inputs and outputs as a variable	65
Figure 65	Torque variable assignment	66
Figure 66	Angular Position of the Legs.....	66
Figure 67	Control Plant Definition.....	67
Figure 68	Final view of the Control Plant build menu.....	68
Figure 69	Calling m-file from MATLAB	68
Figure 70	A closed loop PID controller	69
Figure 71	Reference position presentation [44]	70
Figure 72	Forward body velocity for a simulation run with $t_c = 0.5s$,.....	72
Figure 73	Left and right tripod angular velocity profile	73
Figure 74	Angular position of left and right tripod	73
Figure 75	Position and Velocity of the body in X direction	74
Figure 76	Body fluctuation in y direction.....	75
Figure 77	Torque graph of one leg.....	76
Figure 78	Torque-speed curve of RE30 motor [48]	76
Figure 79	Velocity in x direction versus body fluctuation in y direction	77
Figure 80	Final ADAMS Sub Block	78
Figure 81	Reference angle input and real angular position of the leg in the same graph.....	80
Figure 82	The difference between reference and real angular position of the left tripod	80
Figure 83	The difference between reference and real angular position of the right tripod.....	81

Figure 84	Angular velocity profile of left and right tripods.....	83
Figure 85	Angular position profile of left and right tripod	83
Figure 86	Position and velocity of the body in x direction.....	84
Figure 87	Body fluctuation in y direction.....	85
Figure 88	Velocity in x direction versus body fluctuation in y direction	85
Figure 89	“ Φ ” angle of the body orientation	86
Figure 90	“ θ ” angle of the body orientation	87
Figure 91	Torque requirement of the left rear leg	87
Figure 92	Angular velocity input of the left and right tripods	88
Figure 93	Position and velocity in x direction.....	89
Figure 94	Body fluctuation in y direction.....	89
Figure 95	Velocity in x direction versus body fluctuation in y direction	90
Figure 96	“ θ ” angle of the body versus velocity in x direction.....	91
Figure 97	“ Φ ” angle of the body versus velocity in x direction	91
Figure 98	Torque requirement of one leg.....	92
Figure 99	Position and velocity in x direction of RHex with elastic modulus of leg 10 GPa.....	93
Figure 100	Body Fluctuation in “y” direction	94
Figure 101	Torque requirement of one leg for elastic modulus of 10 GPa...	95
Figure 102	The velocity profile comparison of the three simulation results..	95
Figure 103	The position of the body in x direction	96
Figure 104	The velocity of RHex in x direction.....	97
Figure 105	Body fluctuation in y direction	98
Figure 106	“ Φ ” angle of the body versus velocity in x direction.....	98
Figure 107	“ θ ” angle of the body versus velocity in x direction.....	99
Figure 108	Position of RHex in x direction	99
Figure 109	The velocity of RHex in x direction.....	100
Figure 110	The body fluctuation in y direction.....	100
Figure 111	“ Φ ” angle of the body versus velocity in x direction.....	101
Figure 112	“ θ ” angle of the body versus velocity in x direction.....	101
Figure 113	The position of RHex in x direction	102
Figure 114	The velocity of RHex in x direction.....	103
Figure 115	The body fluctuation in y direction.....	103
Figure 116	“ Φ ” angle of the body versus velocity in x direction.....	104
Figure 117	“ θ ” angle of the body versus velocity in x direction.....	104
Figure 118	The comparison of the displacement in x direction	105
Figure 119	The comparison of the velocity in x direction.....	106
Figure 120	The comparison of the body fluctuation in y direction.....	106
Figure 121	Angular velocities of left and right tripods	107
Figure 122	Position and velocity in x direction	108
Figure 123	Body fluctuation in y direction	109
Figure 124	“ Φ ” angle of the body versus velocity in x direction.....	109
Figure 125	“ θ ” angle of the body versus velocity in x direction.....	110
Figure 126	Screenshot of the start of the slow phase.....	110

CHAPTER 1

INTRODUCTION

Robots are wide range of devices with different levels of autonomy, intelligence, and mobility. They acquire sensory data, process the information, actuate motion and react to the external environment in a predictable and controllable manner. Robots with a high level of intelligence are capable of performing complex tasks autonomously. Their control architectures require more sophisticated design and implementation than those of robots with a low level of intelligence.

The complexity of robots shows differences according to the time that they have been invented. Mankind has long ago tried to build machines that looked like living beings or even resembled human beings. The beginning of robots may be traced to the Greek Engineer Ctesibius (c. 270 BC) who applied his knowledge of pneumatics and hydraulics to produce the first organ and water clocks with moving figures. Philo of Byzantium (c. 200 BC), one of the Ctesibius students, wrote “Mechanical Collection” describing his teacher’s work. Later, based on that book, Hero of Alexandria (c. AD 85) wrote “On Automatic Theaters, On Pneumatics and On Mechanics”, presenting the first well documented workable robots outside of mythology. The Greeks entertainment robots were designed for limited and repetitive jobs and didn’t have to perform more demanding functions. The Greeks had a specific word to name these machines: “automatos”. The current word automation is derived from this word and means “machine that imitates the figure and movements of an animate being” [1].

In the early ninth century the Khalif of Baghdad (786–833) assigned three men, to acquire all Greek texts that had been preserved by monasteries and scholars during the decline and fall of western civilization. They produced the large book *Kitab al-Hiyal* (The Book of Ingenious Devices) based on the works they collected. Over a hundred devices were described in that book. The next significant automation work was compiled by a Turkman, Badi'as-Zaman Isma'il bin Ar-Razzaz Al-Jazari (1150–1220), He gave detailed descriptions to the science of ingenious mechanisms and compilation or variation of existing designs besides . Al-Jazari may have constructed many of the mechanisms also.. Thus, the greatest contribution the Arabs made, besides preserving, disseminating and building on the work of the Greeks, was the concept of practical application. This was the key element that was missing in Greek robotic science [2].

The Renaissance revived not only the interest in Greek art and science, but also created a desire to compete with the ancients achievements. Inspired by this, Leonardo da Vinci (1452–1519) was actively engaged in verifying Greek reconstructions, an activity that no doubt inspired him to devise water powered organs and clocks equipped with *Jacque mart*, or Jack figures, for striking the hours.

In the 18th century mechanical puppets were first built in Europe. An established clock and watch making industry in Switzerland made available the skilled craftsmen and base technology needed to build those machines. The Scribe, the Draftsman and the Musician display a high degree of anthropomorphism for their time. Basically entertainment devices, the three figures were programmable through stacked cams, presenting sophisticated movements. Making their public debut in 1774, they were the work of Pierre Jaquet-Droz (1721-1790) and his assistants, chiefly Jean Frederic Leschat. The pioneer Jaquet-Droz created lasting examples of the craftsman's art. An early innovation was a tiny mechanical singing bird fitted into a snuffbox [2]. In 1801 Joseph Maria Jacquard introduced the next significant innovation

and invented the automatic draw loom. The draw loom would punch cards and was used to control the lifting of thread in fabric factories. This was the first invention to be able to store a program and control a machine.

Ever since, developments have mainly been driven to resemble physical aspects, although in the last few years, one of the main challenges in robotics has been to enrich these machines with a grade of intelligence in order to allow them to extract information from the environment and use that knowledge to carry out their tasks safely. Although it is not clear which of the previously mentioned devices should be considered the first robot, it is clear the origin of the term robot. This word was introduced in a play called R.U.R. (Rossum's Universal Robots), by a Czechoslovakian playwright named Karel Capek. R.U.R. was a play about human-like servants that were artificially created out of biological tissues to serve humans in factories and in the army. Capek called these artificial workers "robots", from the Czech word "robota", meaning slave work.

The robot evolution depends on the evolution on hardware. It has contributed to create robots with sensors and actuators which allow the imitation of the human beings and the animal's way of displacement. Concerning the software evolution, it has allowed supplying robots with intelligence and with the capability of learning and of mimicking the reasoning capacity and emotions of humans.

Today's robotic systems may be classified, generically, into two major areas:

- manipulation robotics
- mobile robotics.

Mobile robots have the capability to move around in their environment and are not fixed to one physical location. They could be classified according to the way that they use to move.

- Wheeled robots
- Tracked robots
- Legged robots

1.1. Wheeled and Tracked Robots

In the present state of civilization, locomotion using wheeled and tracked vehicles is dominant. Its use for performing the most varied tasks is so common that one might think this to be the only available or most effective way of locomotion. However, through a detailed analysis of the characteristics of this type of locomotion, it is possible to conclude that things are quite different.

Wheeled and tracked robots are capable of locomotion at very high speeds (Figure 1). Legged robots could not be considered as an alternative when the speed is the concern. It should be noted that wheeled vehicles demand paved or at least regular surfaces in order to move, being extremely fast and effective over these surfaces. At the same time these mechanisms can be simple and have light weight.

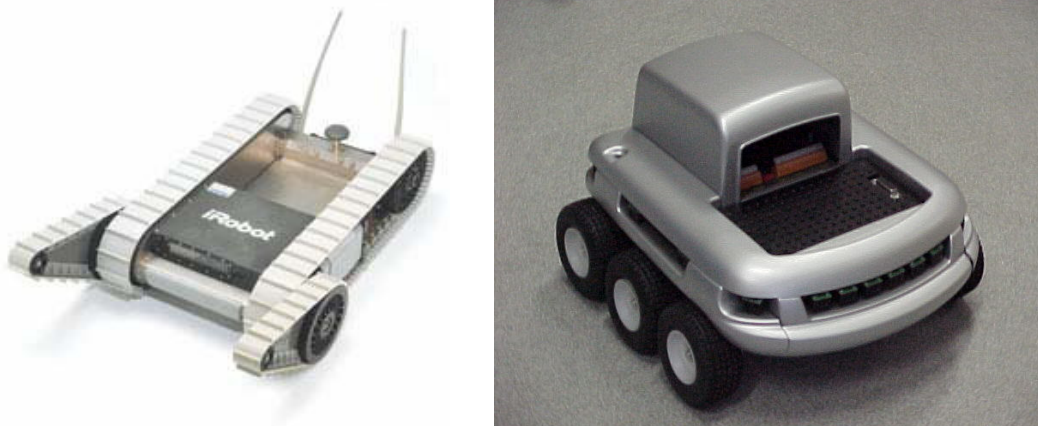


Figure 1 Tracked and Wheeled Robot [3]

On the other hand approximately half of the world's land mass is inaccessible to wheeled and tracked robots [3]. It is difficult, or even impossible, for wheeled vehicles to overcome large obstacles and surface unevenness. Even all-terrain vehicles can only pass over small obstacles and surface unevenness but at the cost of high energy consumption. An alternative is vehicles with tracked locomotion. Although they present increased mobility in difficult terrain they are not able to overcome many of the difficulties found, and energy consumption is relatively high. Wheeled mobile platforms provide sufficient robustness and energetic performance for many applications which are mostly indoor applications with structured environment such as transportation industry and service, customer support in museums and shops, cleaning large buildings and surveillance of buildings, when unstructured environment, highly broken and unstable terrain, is the concern legged robots are the only alternative.

1.2. Legged Robots

It might seem that there are already many existing mobile platforms, such as wheeled or tracked vehicles, which are capable of locomotion at very high speeds, and we need not necessarily consider legged locomotion as an alternative. Instead, one could argue that there are many, equally important and challenging problems to be solved at various other levels of abstraction, such as robot navigation, localization and mapping. Clearly, all of these problems are of great importance in robotic locomotion, and have received well deserved attention in the robotics literature. On the other hand, one must also note that the performance of traditional mobile robots largely results from the structured nature of their operating environments. In fact, approximately half of the world's land mass is inaccessible to such vehicles [3]. Robotic mobility over highly broken and unstable terrain requires legged machines. Even though for many applications, traditional wheeled platforms provide sufficient robustness and energetic performance, in the long run,

systems capable of operating in the widest variety of terrain conditions, will be legged robots. Nonetheless, legged platforms present many difficulties from an engineering point of view. Unlike traditional mobile robots, the control of these platforms requires a complete understanding of their dynamics. Most of their behavioral and energetic performance relies on the inherent properties of their mechanical structure, for which we currently have very few well developed analytical tools. The coordination of the large number of joints and the redundancy in the actuated degrees of freedom compared to the small number of task degrees of freedom, present novel challenges in the design of controllers for such systems. [4]

Legged locomotion vehicles present superior mobility in natural terrains, since these vehicles may use discrete footholds for each foot, in contrast to wheeled vehicles, which need a continuous support surface. Therefore, legged vehicles may move over irregular terrain, by varying their legs configuration in order to adapt themselves to surface irregularities. In addition, feet may establish contact with the ground at selected points in accordance with the terrain conditions. For these reasons, legs are inherently adequate systems for locomotion over irregular ground. When the vehicles move over soft surfaces, i.e. sandy soil, the ability to use discrete footholds in the ground can also improve the energy consumption, since they deform the terrain less than wheeled or tracked vehicles and, therefore, the energy needed to get out of depressions is lower [5]. Besides, the contact area between the foot and the ground can be made in such a way that the ground support pressure can be low. Moreover, the use of multiple degrees of freedom in the leg joints, allows legged vehicles to change their heading without slippage. It is also possible to vary the body height, introducing a damping and decoupling effect between terrain irregularities and the vehicle body. This is particularly true in the case that they move, for instance, over the outside surface of pipes, in order to increase their balance ability [6].

Another advantage that has recently been investigated, concerns failure tolerance during static stable locomotion. The consequence of a failure in one of the wheels of a wheeled vehicle is a severe loss of mobility, since all wheels on these kinds of vehicles should be in permanent contact with the ground during locomotion. However, legged vehicles may contain redundant legs and, therefore, can maintain static balance and continue locomotion even with one or more legs damaged [7], [8], [9], [10], [11].

Finally, it should be mentioned that legs can be used not only for locomotion, but also for other purposes. For instance, the body can be actively actuated while feet are fixed to the ground, working as an active support base to help the motion of a manipulator [12] or a tool [13] mounted on the body. As an alternative to the assembly of a manipulator on a robot body, multi-legged robots can use one or more of its legs to manipulate objects, as is possible with some animals (several animals use their legs to hold, manipulate and transport objects). As an example, Takita et al. (2003) [14] present a biped robot, whose structure is inspired by dinosaurs, on which the tail is used to help maintain balance during locomotion and during manipulation tasks that the robot performs with its neck. The tail is also used so that the robot can stand on it, making a stable support tripod. Hirose and Kato (1998) [15] propose using the TITAN-VIII quadruped robot in the task of landmine detection and removal. For this purpose it uses one of the robot legs as a manipulator arm, with the possibility of being equipped with a set of different end effectors.

Omata et al. (2002) [16] also propose the adoption of a quadruped robot for manipulation tasks, in which two of its legs are used for locomotion, while the body and remaining legs are used for object manipulation. Takahashi et al. (2000) [17] and Koyachi et al. (2002) [18] present similar solutions to the previous ones, but for hexapod robots. The solutions described have as advantages reduction in system weight and a corresponding increase in

energetic autonomy, because otherwise it would be necessary to mount arms on the locomotion system, these devoted only to manipulations tasks.

So far the structure, area of use and properties of the wheeled, tracked and legged robots are mentioned. To summarize, the majority of mobile robots are wheeled robots which are easier to design, construct, and control than legged robots. Wheeled robots are suitable for traversing level terrain. They need specially designed mechanisms for moving in outdoor environments. In general, legged robots have more complexity in design and control, but they are more practical in some applications than wheeled robots. Legged robots have their advantages and disadvantages compared with wheeled robots. Legged robots have many advantages over wheeled robots. In order to move effectively, a wheeled robot must have all wheels contacting the surface all the time, while a legged robot can travel by using some legs touching the ground at any given time. As a result, legged robots are more suitable for traversing on non-continuous surfaces especially the natural terrain and outdoor environments. In addition, they can step over small obstacles. Also they can walk up and down stairs or slopes. With well-designed leg mechanisms, they can step or even jump over wide abysses. They can travel over irregular terrain while maintaining smooth motion of their center of gravity by varying the vertical stride of each leg. Legged robots can also move on soft ground, such as sand, mud, and loose surfaces, where wheeled robots might slip. Legged robots disturb and do damage to the ground less than wheel robots. Furthermore, legged robots can maneuver around using a smaller area than wheeled robots. They can change direction by changing their foot placement. The average speed of legged robots is the same for all types of terrain, while the speed of wheeled robots decreases when they are moving on irregular surfaces. These advantages make legged robots appealing for natural terrain exploration. On the other hand, legged robots have some disadvantages as compared to wheeled robots. Legged robots have more mechanical complexity than wheeled robots because each leg has many links and joints. Consequently, complex electronic systems for

controlling and powering those joints are required as well as sensor systems for determining the status of each leg. Typically, the more complex the system is, the more expensive the total cost of the system is. Furthermore, the control algorithms for legged robots are more complex than wheeled robots. The movement of all joints must be synchronized and respond to sensory input from all legs. In addition, on level terrain, legged robots can not achieve the speed of wheeled robots [23]. Although legged robots have some disadvantages and may not be suitable for some applications, there are many advantages of them. Legged robots are by nature strongly non-linear, high-dimensional systems whose full complexity permits neither tractable mathematical analysis nor comprehensive numerical study [19].

1.3. Present Day Legged Robots

Today's legged locomotion vehicles are classified according to the number of the legs.

- Monopod
- Biped
- Quadruped
- Hexapod
- Multi-legged

1.3.1. Monopod Robots

In the case of one legged robots, locomotion is performed through hops. Therefore, these machines are also known as hopping robots. Although the most approximate natural example of hopping locomotion is the kangaroo, this model can also be applied to running bipeds, which alternate between one or no foot in contact with the ground. These machines keep an active balance as they move, achieving dynamic stability, allowing a better

understanding of the energy exchanges that occur during a locomotion cycle, and emphasizing the active and dynamic stability problems, without requiring leg coordination schemes.

Matsuoka was the first to build a machine according to these concepts, which means, with ballistic flight periods in which the feet lose contact with the ground. His objective was to model the cyclic jumps in human locomotion. In order to achieve this objective, Matsuoka formulated a model, consisting of a body and a weightless leg (to simplify the problem), and considered that the support phase duration was short when compared with the ballistic flight phase. This motion, in which almost the entire cycle is spent on the transfer phase, minimizes the inclination influence during the support phase [20].

To test the control system, Matsuoka built a planar one legged hopping machine. The machine stands over an inclined table (10° with the horizontal), rolling on ball bearings. An electrical solenoid gave a fast impulse to the foot, in such a way that the support period was small. The machine hopped in place with a period of 1 hop s^{-1} and could walk forward and backward over the table.

Raibert was another researcher working on dynamical locomotion systems and, in 1983, built at Carnegie Mellon University (CMU) a hopping robot. This system, formed by a body and a single leg, needed to hop continuously in order to maintain balance [21]. The body constituted the main structure, which transported the needed actuators and instrumentation for the machine operation. The leg could be extended, varying its width, and was equipped with springs along its axis. Several sensors measured the body inclination angle, the hip angle, the leg width, the spring leg stiffness and the ground contact. This first machine was limited to operate on a level surface and, therefore, could only move up and down, front and back, or rotate in the plane. A second hopping machine, named Pogostick (Figure 2), had an additional hip joint to allow the leg to move sideways, as well as forward and back.

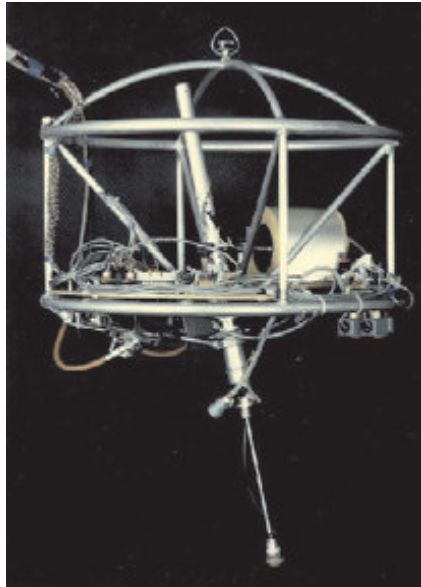


Figure 2 Raibert's Pogostick

During operation, this robot balanced itself while hopping; moving at a maximum speed of 2.2 m/s. A cable connected the machine to the electric power supply and to the control computer. For this machine, the running/hopping cycle presented two phases: support (the leg supports the body weight and the foot remains at a fixed location on the ground) and flight (the centre of gravity moves ballistically with the unloaded and free-to-move leg). Its control was implemented through a small set of simple algorithms.

ARL Monopod II (Figure 3), with two dof and electrical actuation, is a more recent example of this sort of machine. This robot presents two parts: the body that carries the sensors and actuators, and the leg that allows the displacement.

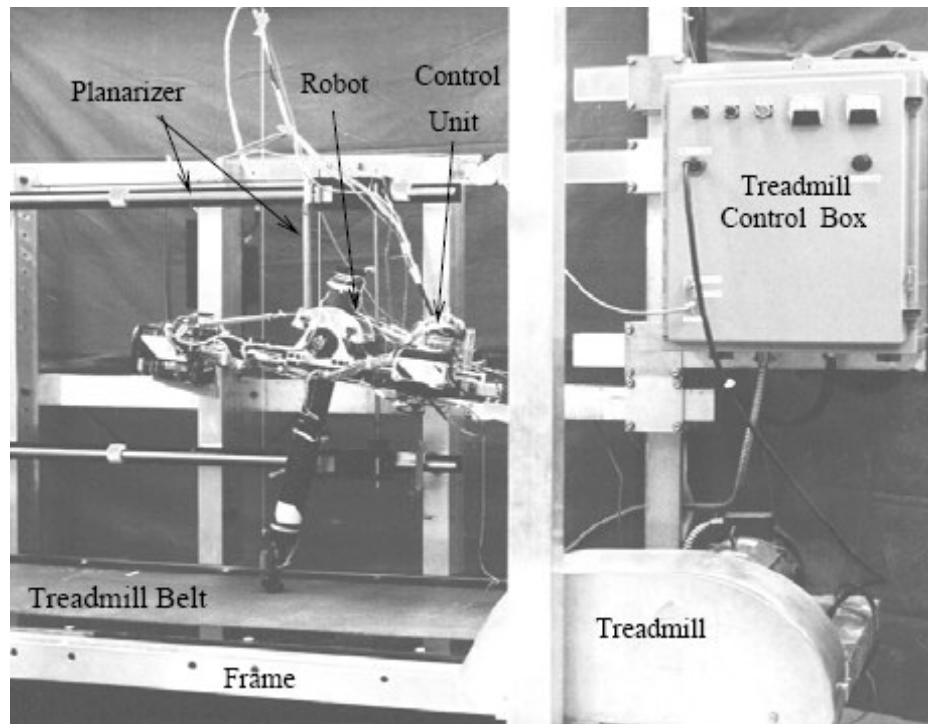


Figure 3 ARL Monopod II Experiment Setup

The ARL Monopod II possesses an electrical motor that actuates a lead screw, as well as a storage/recovery energy system through springs [22]. Different from the ARL Monopod II, that have a prismatic degree of freedom (DOF) in the leg, Schwind and Koditschek (1997) presented a monopod robot with two actuated rotational DOF in the leg. More recently, Hyon and Mita (2002) developed a hopping robot that has three rotational DOF in the leg, one of them being passive. The configuration adopted for the legs of these hopping machines presents a better approximation to an animal's legs, allowing the study of the leg biomechanics of living beings. Under development are also monopod robots that use the hopping principle for their locomotion, but adopting mechanisms that allow them to maintain balance when stopped, namely feet with a special geometry [23]. At first sight one may think that there are no practical applications for equipments with this configuration. However, the reality is quite different. These robots allow jumping over obstacles or positioning themselves in places where available places for feet placement exist, without worrying about the static stability.

1.3.2. Biped Robots

Bipeds, or two-legged robots, are mostly biologically inspired by human anatomy. Many research groups have developed humanoid robots but biped locomotion has complexity in balance and stability control so the research on biped locomotion, when compared with the multi-legged case, has advanced more slowly. Their movement requires considerable sensor information and dynamic control of the center of gravity motion.

It was the first example of the humanoid robot in the world, The Wabot-1, (Figure 4) developed at the Waseda University between 1970 and 1973. Considering this machine was born in the very early 70's, its announced abilities were impressive: the Wabot had a humanoid structure including working legs, gripping hands with tactile sensors, and "artificial intelligence" systems that made it comparable to a one-and-half-year-old child, as stated at the time.

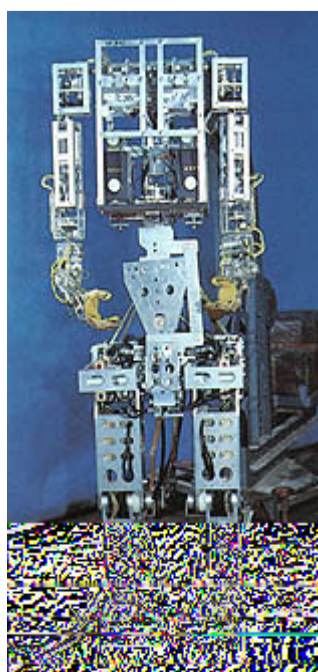


Figure 4 WABOT-1

Wabot-1 is able to achieve "static walking", that is, transferring its center of gravity from one leg to another and moving the leg/raising the feet accordingly. AI interaction systems included a communication system (speech synthesis, speech recognition) and a visual system. It was able to "communicate" in Japanese. The development that led to the Wabot-1 actually began in 1967 with the WL-1 "biped robot" project. The experiments at the Waseda University first focused on the developments of robotic legs. The WL-5 was used as the Wabot-1 lower limb, and development of the WL series lasted long after the Wabot-1 was introduced.

In 1984, Waseda University presented the Wabot-2 (Figure 5). This machine was the first attempt of specializing a robot for domestic use. The chosen activity was music, and the Wabot-2 got worldwide famous as the first robot in the world which played piano. Playing a keyboard instrument was set up as an intelligent task that the WABOT-2 aimed to accomplish, since an artistic activity such as playing a keyboard instrument would require human-like intelligence and ability. Therefore the WABOT-2 was defined as a "specialist robot" rather than a versatile robot like the WABOT-1.



Figure 5 WABOT-2

The robot musician WABOT-2 can talk with a person, read a normal musical score with his eye and play tunes of average difficulty on an electronic organ. The WABOT-2 is also able of accompanying a person while he listens to the person singing. The WABOT-2 was the first milestone in developing a "personal robot". The development of new robots researches continues at the Waseda University. Since 1985, new robots from the Waseda University are presented under the "Wabian" name.

Nowadays there is a large variety of biped robots presenting humanoid shape and having good locomotion capabilities.

One of the biped robots having good locomotion capabilities is the Honda Humanoid Robot (Figure 6). This robot project began in 1986 and the key ideas adopted for its development were "intelligence" and "mobility", since the robot should coexist and cooperate with human beings. The development of the Honda Humanoid Robot was based on data retrieved from human locomotion. Honda's idea was to create a robot that could be used in daily life, in contrast to a robot developed for a particular application, aiming its introduction in factories [24].

Honda also specified three functions that had to be fulfilled: the locomotion speed should correspond to that of a human being (approximately 3 km/h), the robot structure should be capable of supporting arms with hands, and should be able to climb up and down stairs. The latest version of this robot, so called ASIMO (Advanced Step in Innovative MObility) model, was concluded in 2000, having 1.2 m height and 43 kg weight. The ASIMO has 26 dof, is electrically actuated, and can hold 0.5 kg in each hand. It is a completely autonomous robot, in terms of processing capability and in terms of power (it carries on its back batteries that allow 15 minutes autonomy).



Figure 6 ASIMO (Advanced Step in Innovative MObility)

Sakagami present an evolved version of the ASIMO model, prepared to perform people attendance tasks and museum visit guiding, due to the integration of a vision and audition sensors set and a human gesture recognition system, allowing this humanoid to interact with human beings. [25]

1.3.3. Quadruped Robots

Quadrupeds, or four-legged robots, are similar to some reptiles and mammals [26]. Reptiles evolved their leg arrangement to be wide and stable which is appropriate to their environment. The disadvantages of reptilian motions are the twisting movement of the bodyline, and the hip has to support the body weight. Dissimilar to reptiles, the mammalian leg arrangement has no disadvantages except difficulty in stability control [27].

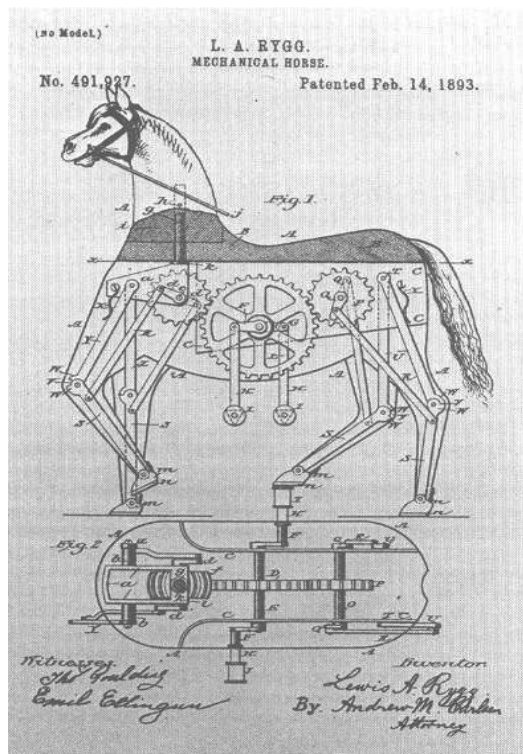


Figure 7 First Quadruped Machine

Figure 7 shows a drawing of the first quadruped machine, named The Mechanical Horse, proposed by L. A. Rygg. This machine was patented on 14 February 1893, but there is no evidence to prove that he actually built this machine [28]

One of the first vehicles that was able to adopt different gaits was the General Electric quadruped (Figure 8), developed by R. Moshier and finished in 1968 [29], [30]. This vehicle, with 3.3 m height, 3 m long and 1400 kg weight, presented four legs with three dof (one in the knee and two in the hip), each joint being actuated through a hydraulic cylinder, and powered by a 68 kW internal combustion engine. Machine control was dependent on a well trained operator in order to function properly. The operator controlled the four legs through four joysticks and pedals that were hydraulically connected to the robot legs, with force reflection. The vehicle control was demanding due to 12 dof system. Although it demonstrated an ability to overcome

obstacles and had good mobility in difficult terrain, it became clear that it needed a computer control system.

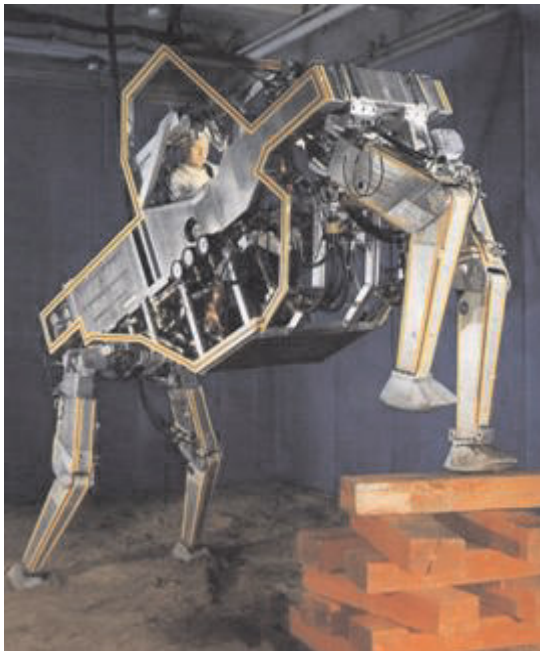


Figure 8 General Electric Quadraped

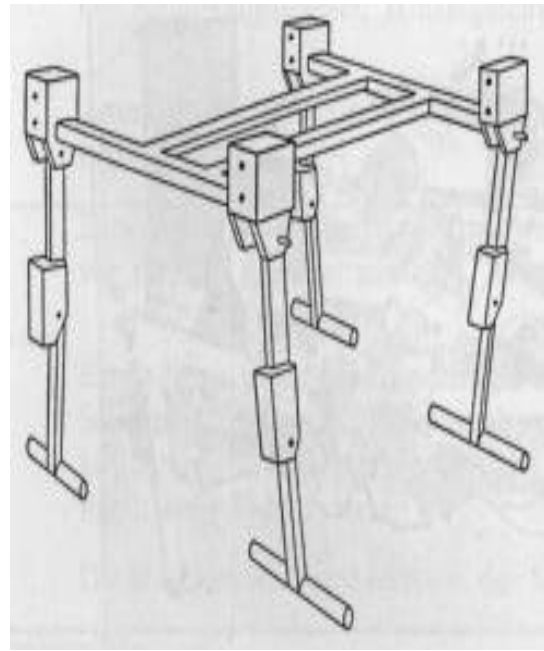


Figure 9 Phoney Poney

The Phoney Poney (Figure 9) was developed by McGhee and Frank around the same time [31], [32]. This quadruped, completed in 1966, was the first legged robot to move autonomously under computer control and with electrical actuation. Each leg had two dof, each of its joints being actuated through an electrical motor (with external power) and a speed reducer. The joint coordination was performed through simple digital logic and presented two different gaits. Its main limitation was the fact that it only moved in a straight line, not being able to turn.

Buehler proposed the SCOUT-I quadruped robot (Figure 10), with only one dof per leg (placed in the hip and actuated by a servomotor), that is able to move straight or on a curve, climb stairs and run under open loop control [33]. More recently, a new version of this robot, SCOUT-II, was developed with legs having a second dof [34]. This additional dof may be passive and prismatic [35] or rotational [36].



Figure 10 Scout I

1.3.4. Hexapod Robots

Hexapods, or six-legged robots, are biologically inspired by insects such as a cockroach [37]. More legs require more hardware and make the hexapods less agile than bipeds and quadrupeds [38]. The greatest benefit of hexapod structure is that they are more stable than the two biped and quadruped systems. Generally, the six-legged gait is a tripod gait. The front and back legs of one side and the middle leg of the other side form one tripod. One tripod is always touching the ground while the other is moving. Consequently, the tripod gait has both static and dynamic stability while one-leg-standing bipeds or two-leg-standing quadrupeds are only dynamically stable.

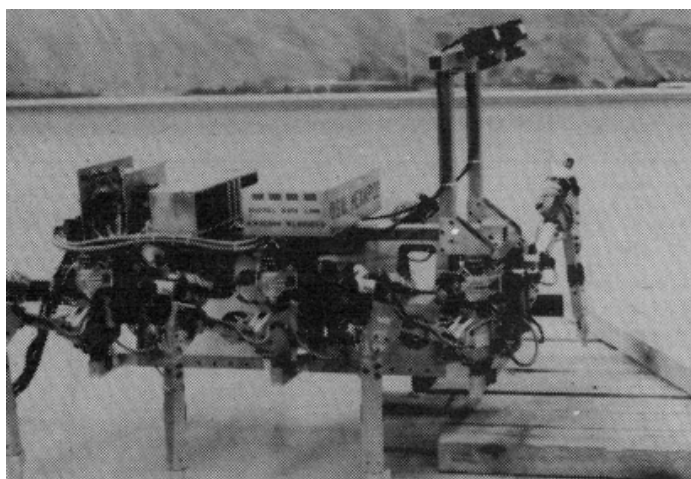


Figure 11 OSU Hexapod

R.B. McGhee built the Ohio State University (OSU) Hexapod in 1977 [39]. This hexapod is 1.3 m in length and 1.4 m in width. Its total weight is about 100 kg. Each leg has three degrees of freedom controlled by electric motors. A PDP-11 computer controlled all legs by connecting through a set of cables. It can move at a slow speed (a few inches per second). This robot has been used as a test bed for various purposes for instance walking with different gaits on a plain surface, stepping up stairs, using sensors, etc. Figure 11 shows the OSU hexapod with a vision system implemented in 1985 [40].

The Massachusetts Institute of Technology (MIT) has also developed biologically inspired robots. Boadicea (Figure 12) has aspects based on the *Blaberus Discoidalis* cockroach [41] and was one of the prototypes that were built. This hexapod presents three DOF in the hind and middle legs and two DOF in the fore legs. All legs possess a pantograph mechanism and the actuators are double effect pneumatic cylinders.

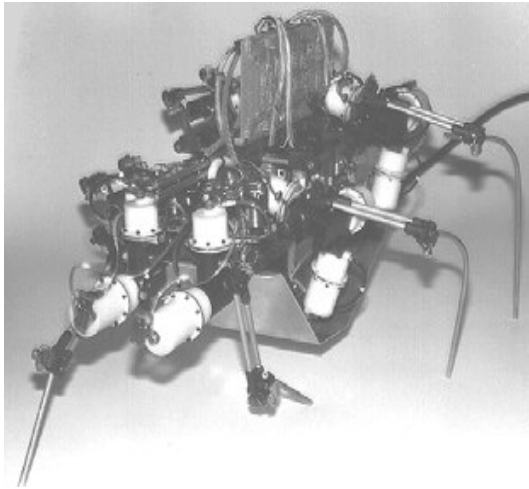


Figure 12 Boadicea

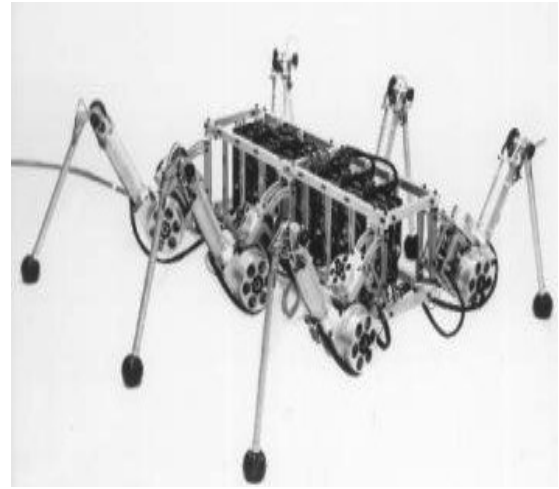


Figure 13 TUM Robot

Another example of a robot based on the stick-insect is the TUM robot developed at the Technical University of Munich (Figure 13). This hexapod robot adopts leg geometry and kinematics, gaits and control system based on the legs of the *Carausius Morosus* stick insect [42]. Each leg of this robot performs its trajectory planning in an almost autonomous way, using a hierarchical control structure based on three levels. Leg coordination is achieved through information exchange on the state of each of them.

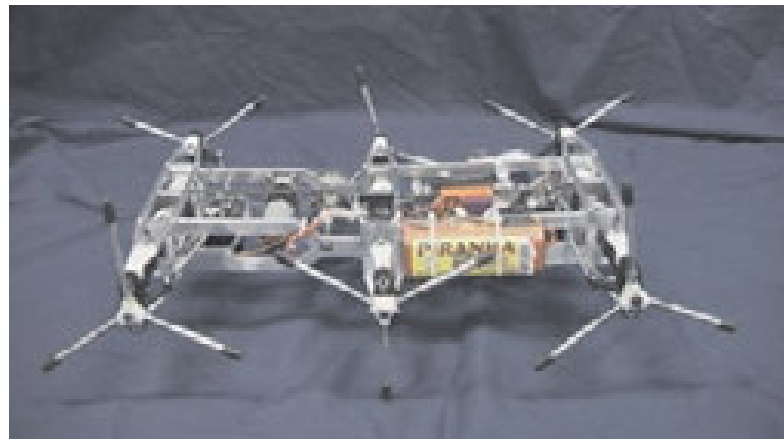


Figure 14 Whegs I

The Whegs I, developed by Quinn [43], makes use of a similar locomotion concept, although its implementation presents slightly different aspects (Figure 14). The machine has six appendices, named Whegs (word resulting

from the junction of the words wheel and legs), consisting of three equally spaced spokes.



Figure 15 Rhex - Compliant-Legged Hexapod Robot

RHex (Figure 15) is a hexapod robot that is capable of locomotion over terrain approaching the complexity of the natural landscape and breaks the speed record for power autonomous legged locomotion. RHex has only six actuators - one motor located at each hip - achieving mechanical simplicity that gives reliable and robust operation in real-world tasks. Stable and highly maneuverable locomotion arises from a very simple clock-driven, open-loop alternating tripod gait, with left front, right middle and left hind legs down together (L-tripod), followed by right front, left middle and right hind down together (R-tripod), each stance phase lasting 55-60% of a full stride cycle. RHex achieves fast and robust forward locomotion traveling at speeds up to one body length per second and traversing height variations well exceeding its body clearance. [44]

1.4. Flexible Multibody Dynamic Simulation

So far the history and improvement of the robots are mentioned. The first robots are machines that are designed for limited and repetitive jobs and do not have to perform more demanding functions. More complex designs

appear in the 15th century with Leonardo da Vinci. Finally today's robots arise which are complex enough to behave autonomously with the development in the computerized control systems. Today's robotic systems are classified, generically, into two major areas: manipulation robotics and mobile robotics. Mobile robots, that have the capability to move around in their environment and are not fixed to one physical location, can be classified according to the way that they use to move. Wheeled robots, Tracked robots and Legged robots. The advantages of each type of robots are discussed. The legged locomotion is the only choice when rough surfaces are considered. Monopod, biped, quadruped and hexapod robots are studied in this section. Hexapod robots have the advantage being statically stable because of the tripod gait. They are biologically inspired from insects. So the most realistic type of legged locomotion is the hexapods.

This thesis concerns the hexapod robot with compliant legs, RHex. The present design of RHex has been changed according to its known limitation. RHex achieves fast and robust forward locomotion traveling at speeds up to several body lengths per second and traversing height variations well exceeding its body clearance. The actuators and the body dimensions are the handicaps that RHex could run faster and traverse higher barriers.

The study is mostly focused on the flexible multi-body dynamic modeling of the RHex. The most important property of this work is using of a finite element and dynamic simulation program together. There are previous examples of this kind of implementation.

ANSYS is a software product for solving physical problems through the Finite Element Method (FEM). ADAMS is also a software product, applied among others for static, kinematic and dynamic analysis of mechanisms, usually with rigid members, but it also enables to calculate generally with non-rigid links between the members or between a mechanism and its surroundings. However, with ADAMS/FLEX module, the system ADAMS makes possible to

find solutions of mechanisms with flexible members by means of a method of modal synthesis. The condition is, though, that flexibility of such bodies in the data files communicating with the ADAMS environment was presented in a previously prepared form, "Modal neutral file" ("MNF") has been chosen as such a form, which results from several previously realized analyses in FEM and contains information about geometry, weight characteristics and modal shapes of a flexible body. When using ANSYS, "MNF" is generated directly, after the analyses in the following order: modal analysis, reduction of FEM object to a super-element and spectral analysis. However, flexibility of the corresponding object/member of the mechanism has to be considered in the frequency range, i.e. the user has to be aware of what frequency range the system/mechanism should operate.

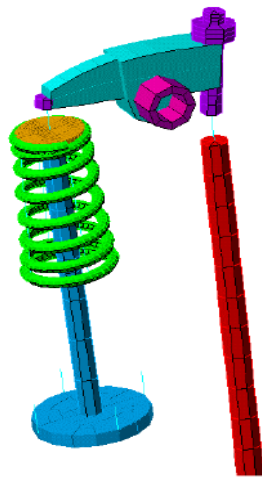


Figure 16 ADAMS Model

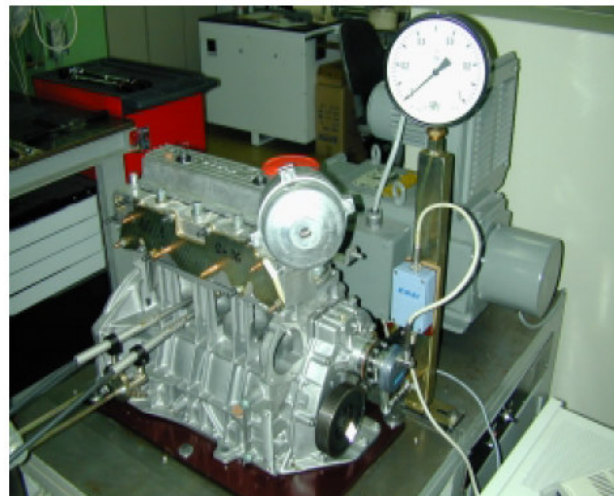


Figure 17 Experimental Setup

Using this phenomenon the behavior of distribution systems OHV and OHC are studied by Antonin Potesil and Vaclav Hanzlik. [45] By means of the FEM and ADAMS models (Figure 16);

- kinematic quantities could be predicted,

- loading and stresses of individual parts of the system could be identified,
- the weight, dimension and the strength characteristic of the parts could be optimized,
- a cheaper and faster test method is used compared to running the real experiment (Figure 17).

In the past Finite Element Analysis (FEA) and Multibody System Simulation (MBS) were two isolated approaches in the field of mechanical system simulation. While multibody analysis codes focused on the nonlinear dynamics of entire systems of interconnected rigid bodies, FEA solvers were used to investigate the elastic/plastic behavior of single deformable components. In recent years different software products e.g. ADAMS/Flex have come into the market that utilize sub-structuring techniques to combine the benefits of both FEA and MBS. In the field of multibody system simulation the intention is the realistic representation of component level flexibility. For FEA purposes this method can be used to derive complex dynamic loading conditions for these flexible components, which cannot be done manually in general. Particularly in the field of finite element based structural optimization, the formulation of realistic boundary and loading conditions is of vital interest as these significantly influence the final design. Since structural optimization implies a change of the components shape (i.e. the mass distribution) during each iterations, the dynamic inertia loads and the components' dynamical properties will change accordingly. In traditional structural optimization, usually constant loads and boundary conditions are used. A coupled MBS-FEA optimization approach opens up the possibility to take these iteration dependent load changes into account while optimizing the component. This leads to an improved design of the considered component and shorter product development time. Another study was performed by Albers, A. [46] about shape optimization of a simple crank drive mechanism (Figure 18) using this FEM-MBS optimization approach. In this study, the structural optimization of dynamically loaded finite element flexible

components embedded in a multibody system by means of an automated coupling of MSC.ADAMS with MSC.NASTRAN Sol200 as optimizer is described.

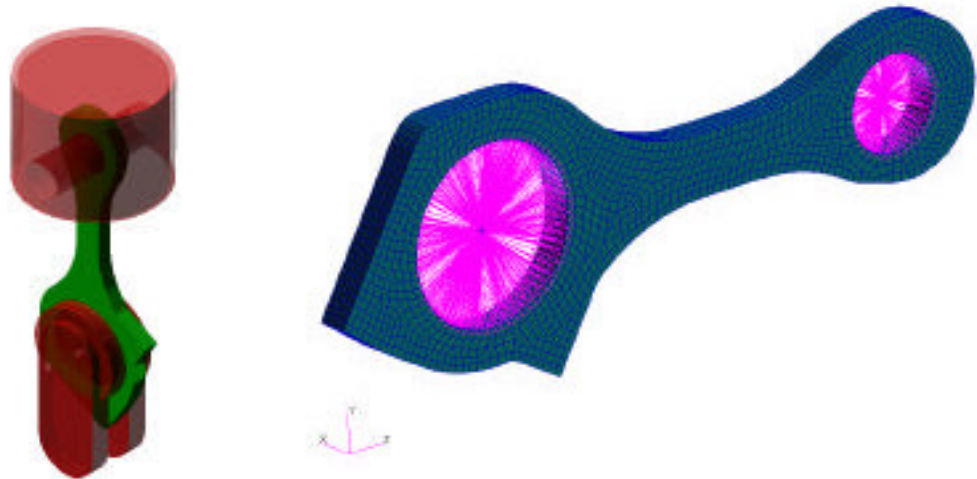


Figure 18 Optimization of Crank Driver Mechanism Part

P. Fischer and W. Witteveen have performed a durability analysis of a truck frame components. There is a spare-wheel carrier attached to the truck frame and the durability of this attachment is simulated using Multibody Dynamic Simulation (MBS) and Finite Element Analysis (FE) methods implementation (Figure 19).

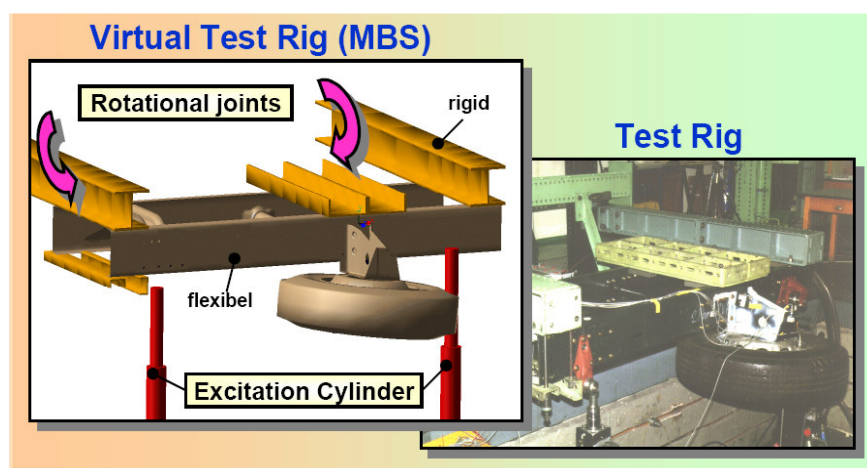


Figure 19 Durability Analysis of Spare-wheel Carrier

The idea is the same. First the finite element analysis is performed and the deformations are calculated to the corresponding loads. Then the shapes and positions of the parts are updated in the multibody simulation according to the FE analysis. After performing the dynamic simulation with the updated information the new calculated loads are transferred to the FE analysis. Same procedure repeats itself until a failure is detected.

Although in the past MBS and FE analysis were different approaches, nowadays they are used together to perform studies about flexible multibody dynamic systems. The focus of this thesis is to build a virtual prototype of RHex which is a multibody system with six compliant legs. MSC ADAMS software is used for dynamic simulation of the robot, the finite element model of the flexible legs is created with MSC Patran and the useful MNF file is built with MSC Nastran. The details of this study and implementation of these programs are discussed in the following section.

CHAPTER 2

2. MECHANICAL DESIGN OF RHEX

RHex is primarily a research platform that is based on over five years of previous research. The purpose of the present task is to design the next iteration of the successful RHex hexapod mobile robot platform. Previous versions of RHex successively completed the primary mission which is to operate on rugged, fractured terrain through statically and dynamically stable gaits while stability of locomotion is preserved. Although RHex meets the basic requirements to accomplish the primary task, there are lots of known limitations or points that could be improved. Modularity of the design is of utmost importance in order to give the ability to experiment with design choices concerning electrical system, sensors, actuators, computational hardware as well as body mechanical design features. Therefore mechanical parts are designed such that the components could be easily detached and changed or at least reachable without demounting another part. This valuable information illuminate the way for the next mechanical design iteration. In the following section, mechanical design optimizations of RHex are discussed.

2.1 Overall Description of the Design

The platform RHex consist of base frame, crash frame, motor mounting parts, interior mounting parts, legs and leg mounting parts. The base and crash frame form the main body of RHex (Figure 20) with the base frame being the main carrier of critical drive-train components. The six motors and gearboxes are mounted hence to the base frame. This frame has three cross members each carrying a pair of motor and gear box combination. Motor mounting parts consist of two parts, a ball bearing and a shaft collar. This sub-assembly is held together by four screws to the motor body and is

mounted with two M3 screws to the end of the cross members of the base frame.

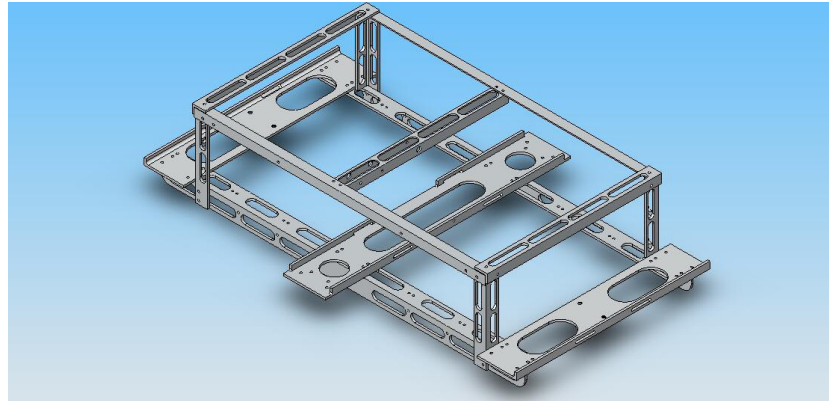


Figure 20 The base and crash frame assembly

In addition to the motors and gearboxes battery packs are also carried by the base frame. For the time being three battery packs are used and each are mounted below the cross member. Figure 21 shows clearly the produced motor assemblies under which the batteries will be carried.

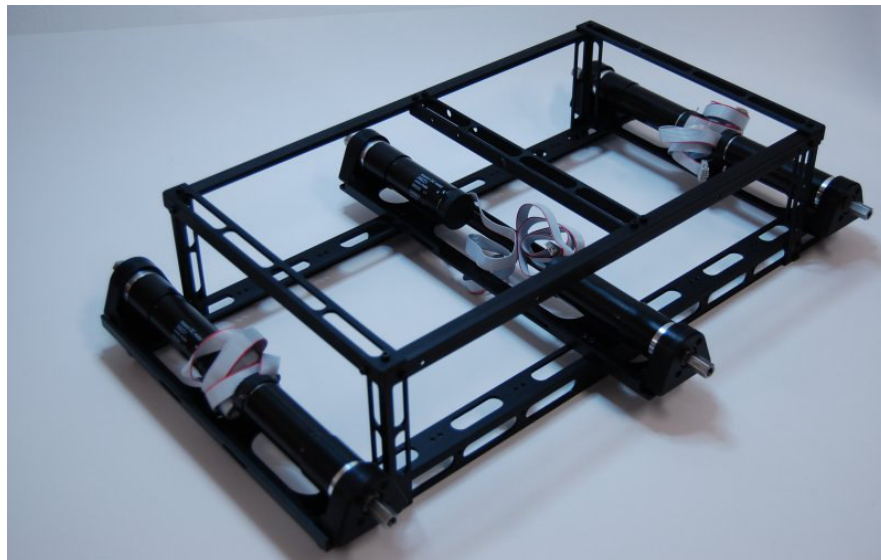


Figure 21 The photograph of the main body of Rhex (base and crash frame) with motor and gearbox assemblies.

2.2. Crash Frame

The crash frame, as the name implies, is protecting the interior electronic parts. The experimental results with the previous version of RHex showed that crash frame could be damaged or even broken when the robot rolls over. Therefore this frame should be both structurally protective and modular. In case of a crash, parts should be easily exchangeable. The crash frame consists of nine parts as could be seen from the Figure 22.

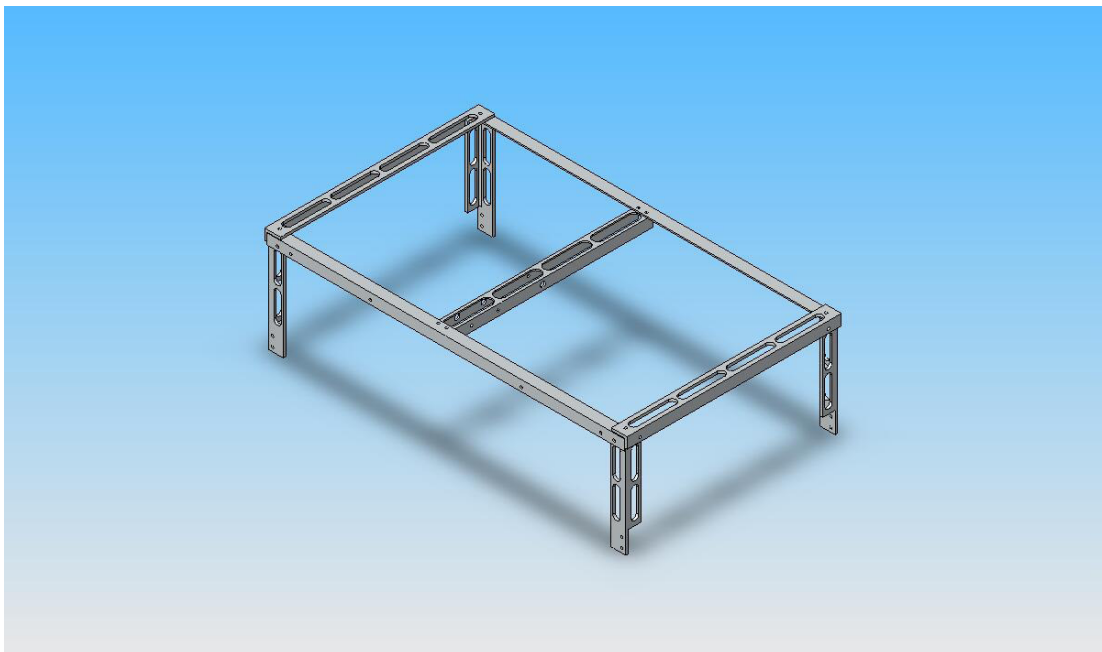


Figure 22 The crash frame of RHex

The design is updated such that the whole mechanical system is modular. One mechanical part or an electronics component should be reachable and could be detached without demounting any other component. Keeping this principle in mind, all the mechanical parts are reviewed and subjected to slight changes to accomplish this criterion. The previous experimental data and outdoor run results are used to perform this study. One of the examples of this design modification is with the motor mounting parts. The mounting holes of this sub-assembly used to attach it to the base frame could not be

reached after installation of motor and gearbox couple. Those mounting holes are moved close to the edges of the part (Figure 23). This change enables one to detach motor mounting sub-assembly without demounting motor and gearbox. This design change required a small modification in the size and shape of the mounting sub-assembly but did not result in a noticeable weight change.

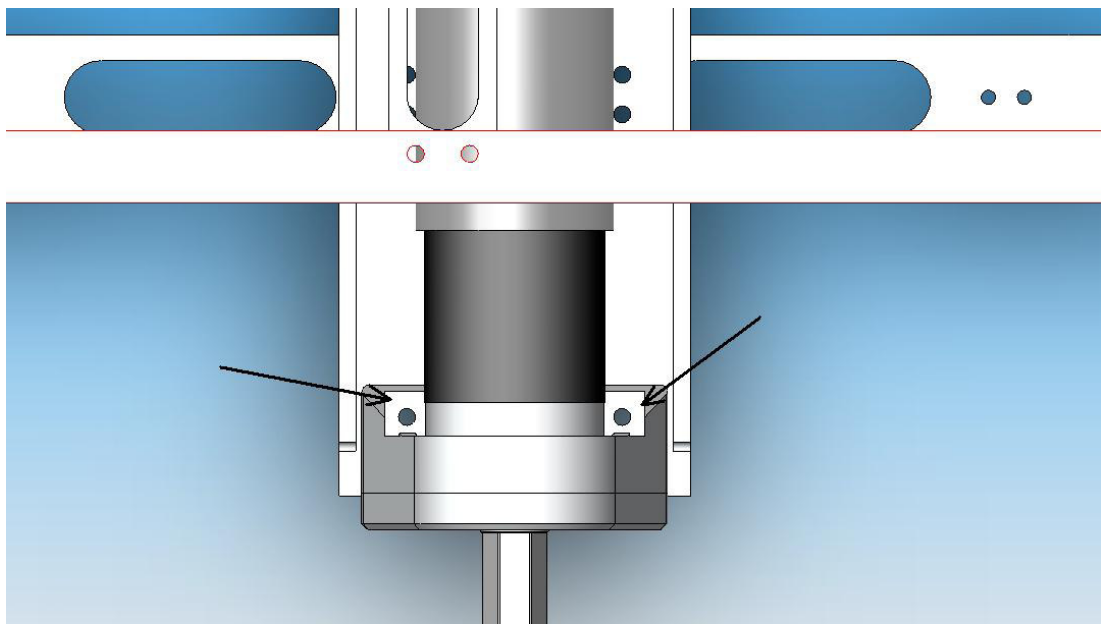


Figure 23 The new motor mounting part.

Mechanical design of RHex is made in Solid Works 2006. The drawings of the previous version of RHex were also in this environment. All the modifications are made with this program and the assemblies are updated according to these changes.

2.3. Base Frame

The base frame consists of three cross member and two longitudinal parts which are mounted as in the Figure 24. Motor and gearbox couple of RHex is upgraded because of the velocity limitation in the previous version of RHex. A scientific analysis of the motion requirements of RHex is performed and a new motor/gearbox pair is selected. The new combination of the motor and

gearbox made our robot faster and more powerful. So there was an opportunity to slightly enlarge the size of the robot, resulting in better payload (sensors) capability. The parts forming the base frame are extended preserving the length over width ratio of the robot. The overall change in the length and width of the robot is approximately 10%.

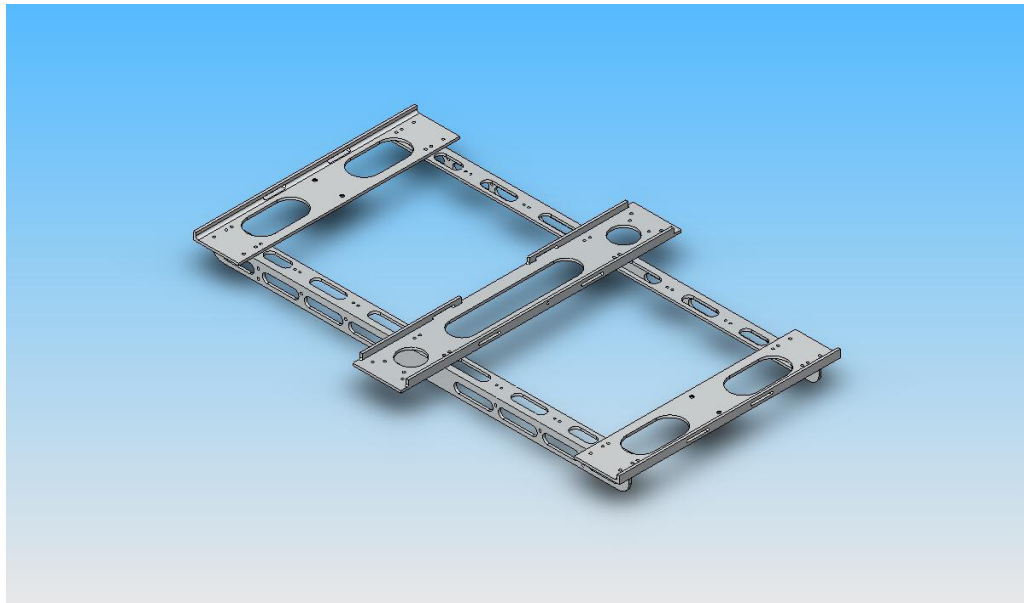


Figure 24 The base frame

The parts that form the crash frame are slightly changed in dimension. They are redesigned and made some modifications in order to be manufactured out of stock parts which are available in the market. This change results in manufacturing “frame left rail” and “frame right rail” (Figure 25) from 25x25 L profile aluminum.

The width of the cross members (Figure 26 and Figure 27) is increased because of the changes in the motor mounting parts. Therefore the weight is increased. In order to keep the weight of the main body same, the slots and holes, which are used for weight reduction, are made bigger. Due to higher grade aluminum selection, using 7000 series of aluminum instead of 6000 series, the strength of these parts is preserved.

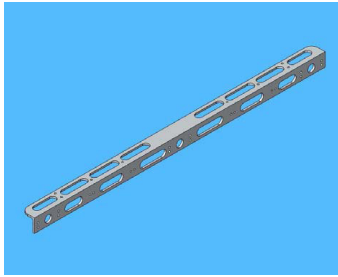


Figure 25 Frame Left
Rail

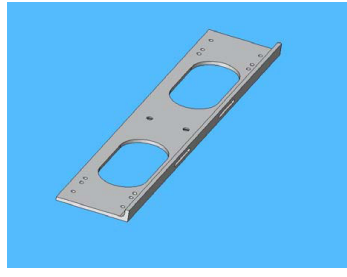


Figure 26 Frame end
angle

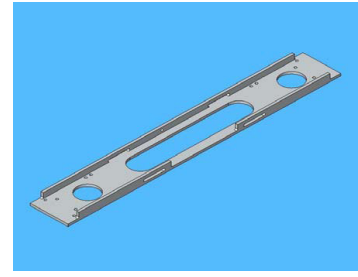


Figure 27 Frame
middle angle

The crash frame is a nine parts assembly. The dimension of the frame is approximately 250x430x100mm. This is a 10.75 dm³ volume. The control units, motor drive boards, gyro, camera and sensors will be installed within the volume of this frame, being protected from outside impacts. As the dimensions of the base frame are changed, the volume of this frame is also increased when compared with the previous version. Modularity is a very important criterion for RHex. Therefore the volume increase is an advantage while installing electronic parts (Figure 28). The parts forming crash frame are redesigned and the dimension of the parts are changed such that all the members could be manufactured out of stock parts. The cross member which is named “crash frame handle” in the design is manufactured from an available “U” profile aluminum different from the other members of the frame.

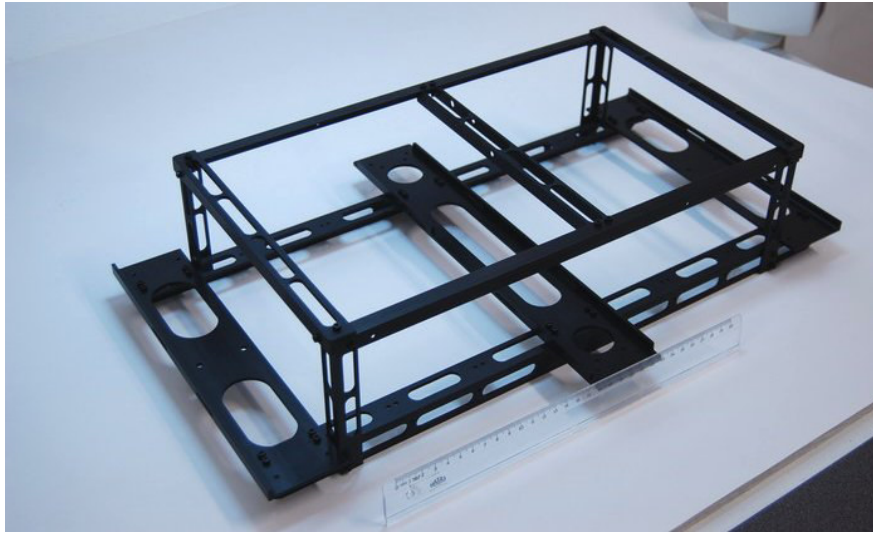


Figure 28 Frame assembly

2.4. Motor mounting parts

Two main parts; “hip bearing seat” and “hip bearing spacer”, are used to mount motor and gearbox couple to the base frame (Figure 29). There are two main modifications on these parts. The height and width of these parts are increased. The reason to increase the height is because of the motor change. The diameter of the previous motor, RE-25 Maxon motor, is 25mm. In RHex v2.0 RE-30 Maxon motors will be used which are 30mm in diameter. The height is increased such that a future RE-35 motor, if required, could be installed without any further modifications or any interference with the present design. The second change in these parts is that they are widened. After installing motor and gearbox, the motor mounting assembly could not be detached from the base frame because the mounting holes are not reachable. This problem is fixed with a design improvement in the present version.



Figure 29 Hip bearing seat and Hip bearing spacer

An exploded view of the motor mounting assembly is given below in Figure 30. There are two additional parts used in this assembly besides hip bearing seat and spacer. These are MOS 61800 2RS ball bearing and the shaft collar part. The ball bearing is inserted to its housing in the hip bearing seat. Then the hip bearing spacer part will be attached to hip bearing seat. After inserting motor and gearbox assembly these four parts are fixed with four M3 screws. The shaft collar part could be installed afterward. This part is used for transferring the rotation to the legs. The main purpose of this assembly is to transfer the load of the legs from the motor shaft to the ball bearing, hence preventing wear on the motor bearings and bending on the motor shaft.

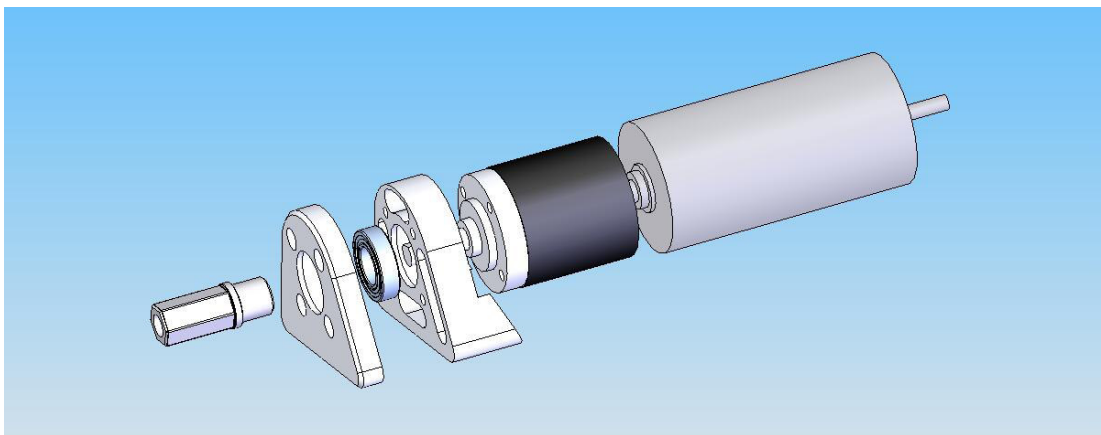


Figure 30 Exploded view of the motor mounting assembly

2.5. The Flexible Legs

The most important mechanical part of the robot is the legs (Figure 31). They are manufactured from fiberglass with a special manufacturing process. The fiberglass is chosen to be with a %50-%50 distribution of fibers in the 0-90 degrees orientation. The matrix which is made from multi layer fiberglass with different orientations is then pre-impregnated in epoxy resin.

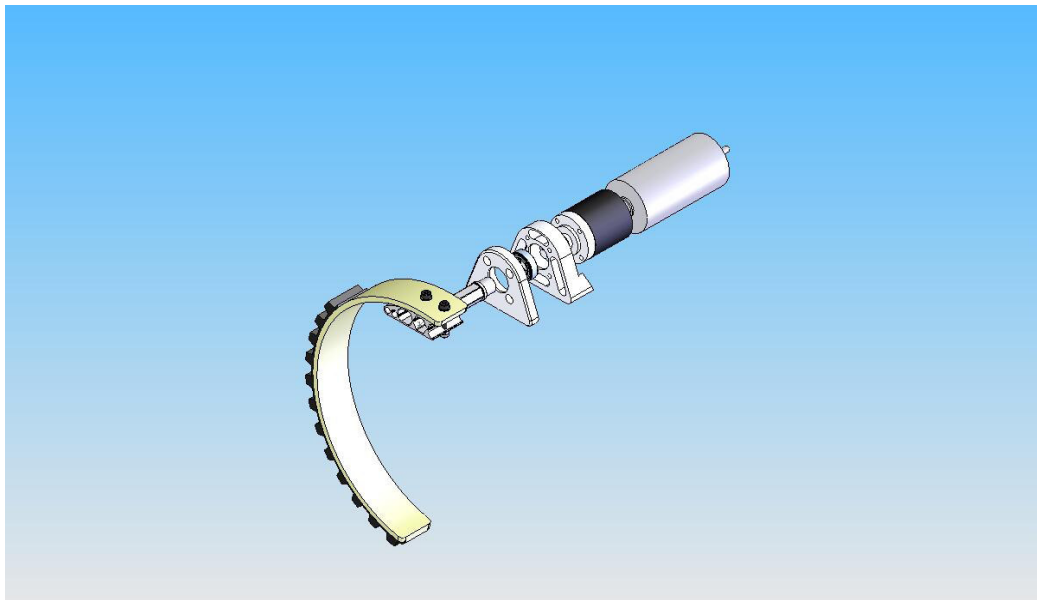


Figure 31 Leg mounted to the motor mounting assembly

The number and the orientation of the fiberglass are shown in Figure 32. The legs contain 13 layers which are alternated in order to maximize lateral stiffness. The stiffness is very low if all the layers are oriented at 0 degree. The maximum strength of the fibers is only attained in one particular direction, so, by alternating the orientation of the layers, the torsional and longitudinal stiffness of the legs are optimized.

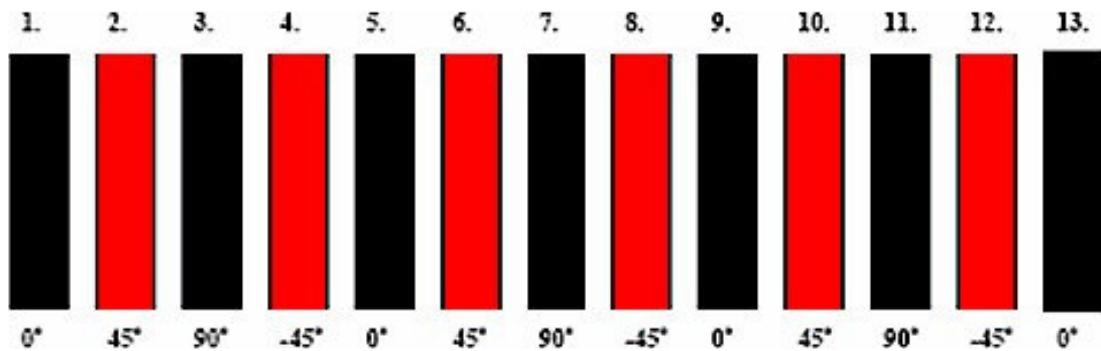


Figure 32 The orientation of the multilayer fiberglass

The fiberglass sheets have been rolled tightly onto the mold, which is a cylinder in shape. After applying the resin to this matrix the composition is cooked in a vacuum bag in order to obtain a compression of slightly less than 1 atm. on the part. The heating process first allows the resin to flow then increasing the temperature curing occurs. Finally the composite material is brought to the room temperature and the vacuum is released.

2.6. Inner Mounting Parts

Base frame as the name implies is the carrier of the robot. Six motors and legs are directly mounted to the base frame. The crash frame is the upper protective part of the assembly. This frame is sacrificing itself in case of a roll over, protecting the inner electronic components. Although all the dimensions and types of these components are not determined, motor drive boards and the computer (PC 104 stack) are ready to mount. The mounting parts of these boards and computer are designed such that the settlement of these components is modular.

2.6.1. Motor Driver Board Holder

Each motor has a driver board. After determining the dimensions of the board a fixture is designed such that the boards are mounted on top of the motors (Figure 33). Since the holder is attached directly to the motor the vibration is very important. Each time legs touch the ground there will be a high impact force acting on the motors. The only contact of the motor and leg assembly is the motor mounting part. Therefore each impact results in vibration of the whole assembly. The use of shock absorbers is essential to protect the motor driver board and connectors.

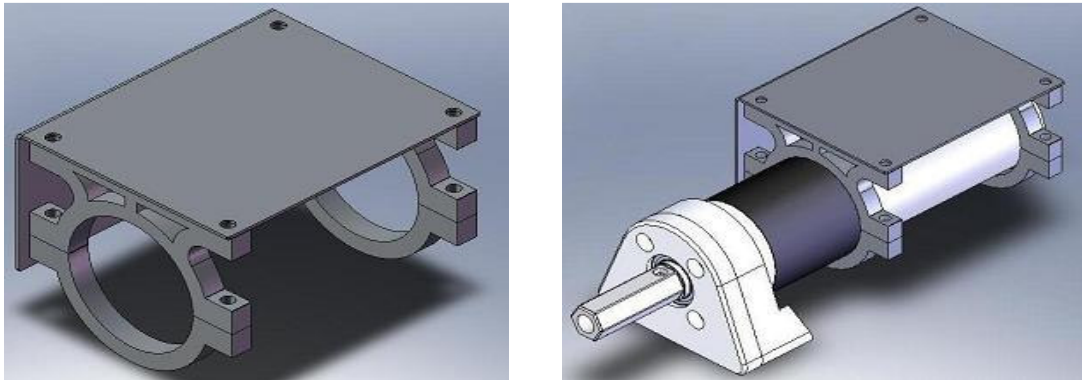


Figure 33 Motor driver board holder

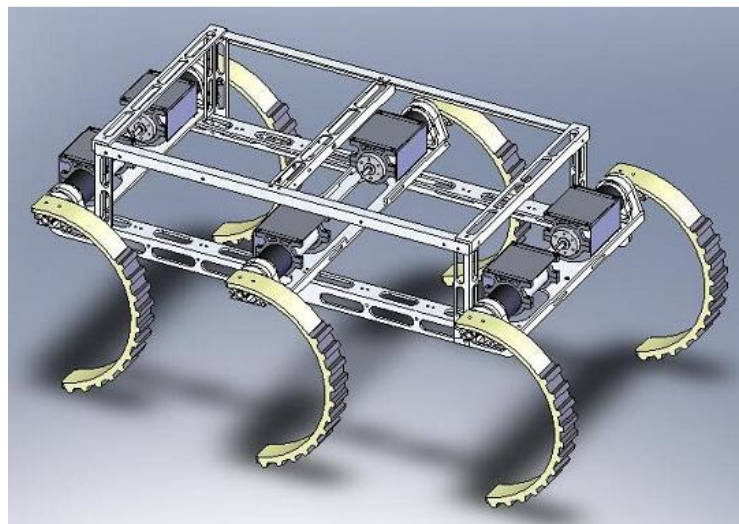


Figure 34 The final assembly of the robot

The final assembly of RHex is shown in Figure 34.

2.6.2 Side Supports

The crash frame provides a volume to locate all the electronic parts. According to the arrangement of these components the supporting and mounting parts are designed. One of the most important supports is the side support which is made from Plexiglas (Figure 35). Since the inside of the crash frame is empty and the components could be fixed by use of a side support part. Another function of this support is to protect the inner components. The final assembly of RHex is planned as a closed box.

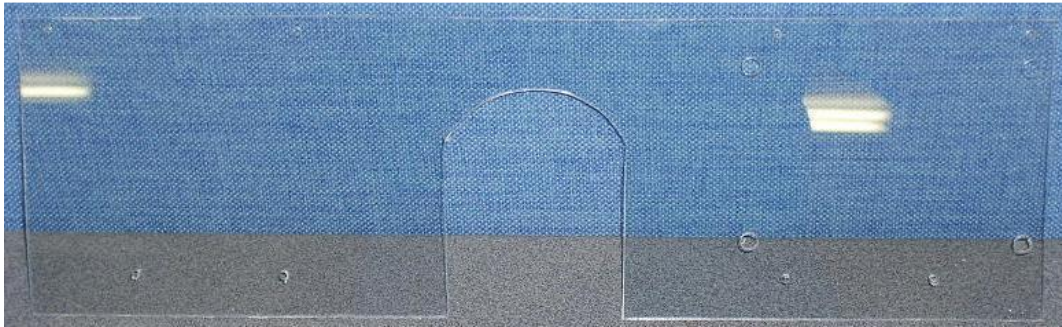


Figure 35 Side support

2.6.3 PC104 Housing

PC 104 stack is the main computer of RHex and occupies the biggest volume compared to any other electronic component.

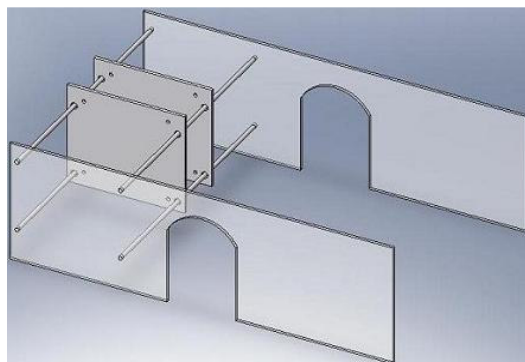


Figure 36 Side supports and PC104 housing assembly

This computer is a multi board assembly. Every board is mounted between two aluminum sheets (Figure 36). Vibration is also a major problem as in the case of motor driver board. Therefore shock absorber should be used between every sheet and board.



Figure 37 Final assembly of the manufactured parts

An important property of this designed structure is, in order to replace PC 104 computer on the robot, the whole assembly of the structure is not needed to be repeated.

CHAPTER 3

FLEXIBLE MULTIBODY DYNAMIC SIMULATION

3.1. Motivation

Multibody Dynamics is an exciting area of Computational Mechanics, which merges and blends various disciplines such as structural dynamics, multi-physic mechanics, computational mathematics, control theory and computer science in order to deliver methods and tools for the virtual prototyping of complex mechanical systems. Multibody dynamics plays today a central role in the modeling, analysis, simulation and optimization of mechanical systems in a variety of fields and for a wide range of industrial applications.

The focus of interest in this study is the Rhex robot, which is an autonomous hexapod robot with compliant legs. It consists of different rigid bodies assembled together to build base frame and crash frame for the first part. For the second part six compliant (currently half-circular and made from composite material) legs are attached to the base frame with a rotating hip mechanism and are actuated by one motor per leg. The half circular and flexible legs contribute to the dynamic stability of the robot and act as a suspension system. So Rhex, being a complex mechanical system, is modeled in ADAMS software to be able to analyze and optimize the design.

3.2. ADAMS Software

When designing a mechanical system, designers need to understand how various components such as motors, rigid and flexible bodies interact as well as what forces those components generate during operation. ADAMS is a dynamic motion simulation solution for analyzing the complex behavior of mechanical assemblies. ADAMS allows one to test virtual prototypes and optimize designs for performance, speed, and durability without having to build and test numerous physical prototypes.

ADAMS is a family of interactive motion simulation software modules, which allows one to import geometry from CAD systems. There is also an opportunity to build a solid model from scratch. After defining the joints, constraints, motions etc. the dynamic model is completed. Then ADAMS offers wide variety of simulations and graphical representation of the results. The most important part is one can export these data in a desired type. There is also an option to save the animation and visually inspect the simulation. Another property of this software is the ability of communicating with finite element analysis programs. This feature is used for RHex in order to build a virtual prototype.

Several modules that are part of ADAMS can be used to accomplish specialized tasks. For example, ADAMS/Flex can be used to examine the effect of flexible links on a mechanism and ADAMS/Controls can be used to model control systems such as hydraulics, pneumatics, electronics and more. ADAMS also offers a range of modules tailored to industry specific applications. Several CAD interface modules allow you to explore the motion of CAD designs without having to leave a familiar CAD interface or transfer data into ADAMS.

The benefits of the ADAMS software could be listed as below:

- Work in a secure virtual environment, without the fear of losing critical data due to instrument failure or of falling behind schedule due to poor weather conditions, common elements that accompany real-world testing.
- Reduce risk by getting better design information at every stage of the development process.
- Analyze design changes much faster and at a lower cost than physical prototype testing requires.
- Improve product quality by exploring numerous design variations in order to optimize full-system performance.
- Explore system variations without having to modify physical instrumentation, test fixtures, and test procedures.

3.3. Modeling RHex

To start with modeling RHex it would be easy and simple to model Rhex as a rectangular box and six flexible legs attached to this box (Figure 38). However ADAMS allows one to import geometry from a CAD environment. As the robot is modeled in SOLIDWORKS and an assembly is present, the geometry is imported into the ADAMS environment (Figure 39). Although the importing mechanism works well, it is useful to import the geometry to PATRAN before importing it to directly ADAMS. PATRAN allows one to easily manage the imported geometry. As previously mentioned, Rhex is built from different bodies, assembled together to form base frame and crash frame. So these different bodies are attached together in PATRAN.

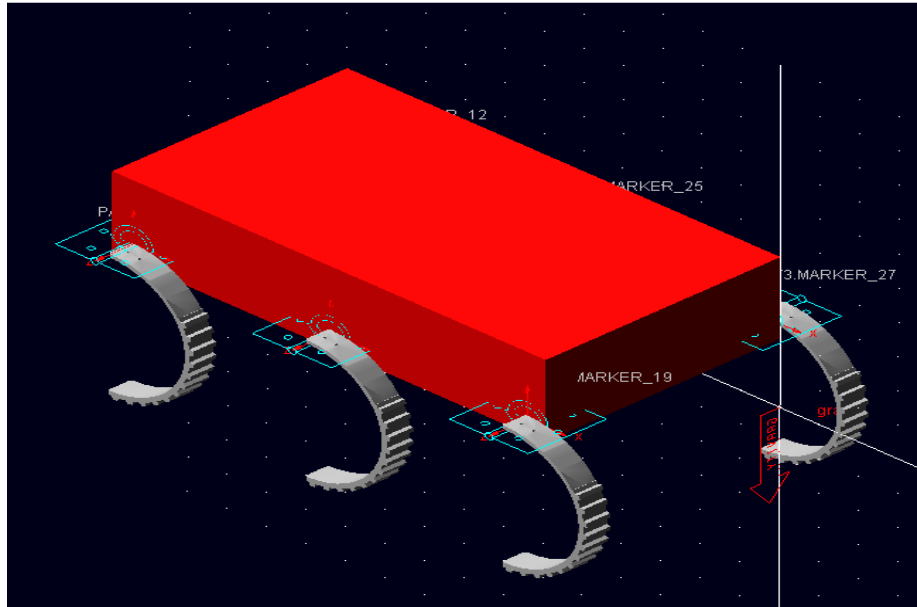


Figure 38 Box model

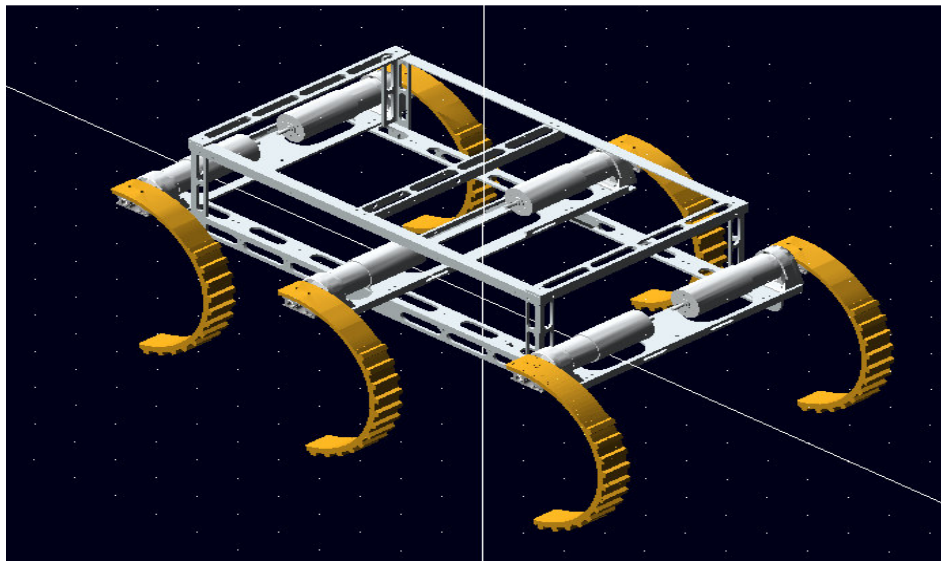


Figure 39 CAD import from Patran

Finally there are very few independent bodies to preserve the simplicity of the model. If the model is imported directly to ADAMS every part would be treated as an independent body. These different bodies should be fixed by joints at every assembly point, resulting in enormous matrices and calculation time.

ADAMS allows importing files from CAD environment with extension “Parasolid (x_t), Step (stp), IGES (igs), DXF (dxf), DWG (dwg)”. In this study the 3D model of RHex is saved as a parasolid file in SOLIDWORKS and then it is edited in PATRAN. The final state of the model is imported to the ADAMS easily choosing import option in the “file menu” and then selecting the parasolid file type (Figure 40).

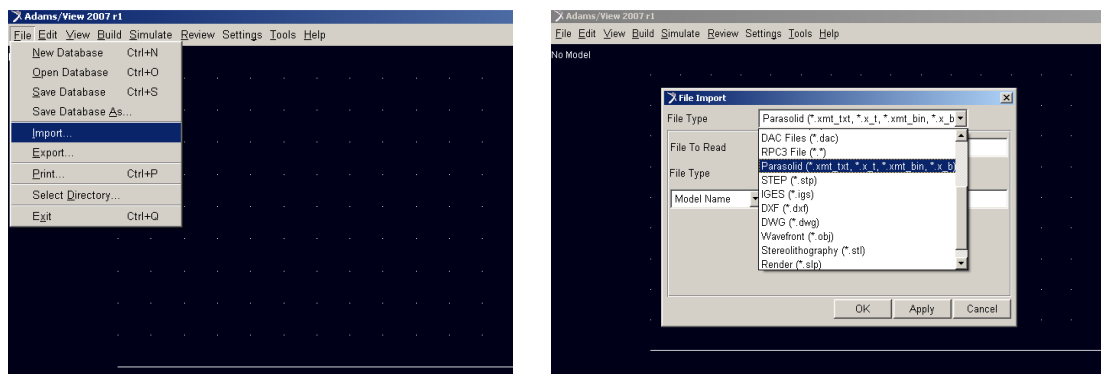


Figure 40 Import menu in ADAMS software

The first modeling attempt does not include flexible legs. The geometry was imported directly from the CAD model. Then joints and rotations are defined. After numerous trials with this model, the flexible legs are introduced. ADAMS software offers a module, which translates the rigid bodies to flexible one. This module is called ADAMS / Flex. There is an “Autoflex” option of this module, which is a simple and automatic way to convert rigid bodies to flexible bodies. Despite of the simplicity, this option does not offer wide variety of property selection. In order to fully define flexible leg properties MSC PATRAN and MSC NASTRAN Finite Element Analysis softwares are used.

MSC PATRAN has a graphical interface to select and define the properties of the flexible legs. There exists a 3D model of RHex, so legs parasolid file is directly imported to MSC PATRAN program. The procedure is the same as importing RHex body model to the ADAMS software (Figure 41).

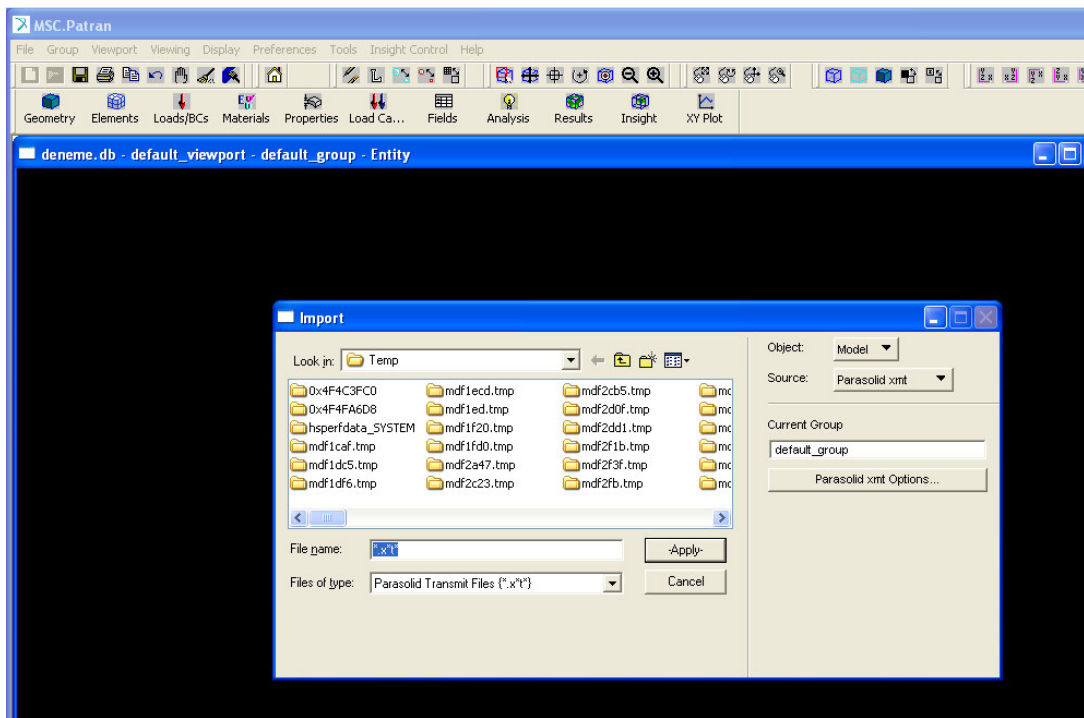


Figure 41 Import Menu in MSC PATRAN

The solid model of the leg is imported to PATRAN. The aim is to define properties of the flexible legs. First definition is the most important one, which is the mesh property. This property is very important because it directly affect the calculation time of Finite Element Analysis.

Finite element model needs the solid to be meshed in order to calculate the resulting deformation. A short literature search is made to determine the “Element Shape” [47]. If the surface of solid which is to be meshed is smooth and the shape is uniform “tetrahedron” element type is appropriate. The meshing properties are defined as in Figure 42.

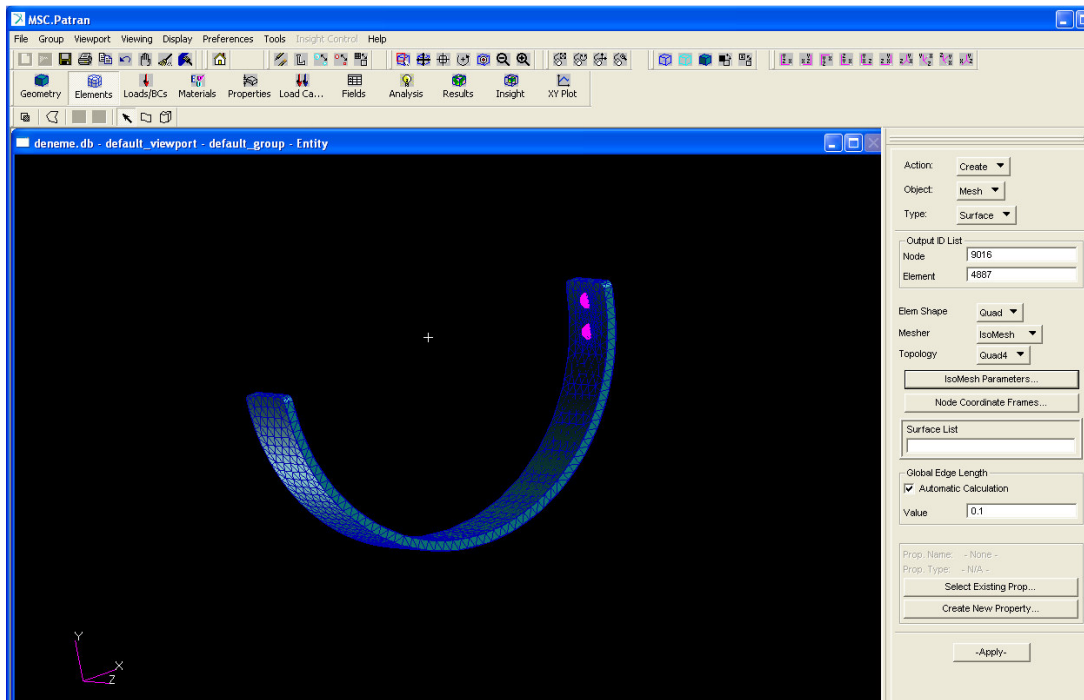


Figure 42 Mesh properties definition

MSC Patran software allows choosing automated meshing option with optimum parameters. Global edge length is an important parameter which determines the number of element used for meshing the geometry. In automatic calculation mode this value is determined in order to have an optimum element number. In this case automatic calculated value is 0.00854 (Figure 43). For that value there is one row element along the thickness of the leg. The number of rows could be increased by choosing the global edge length value less than 0.00854. For 0.0022 global edge length the number of elements increases to 35811 (Figure 44). In the automatic calculation mode the element number is 1899. So in order to have 3 or 4 rows element along the thickness, the number of elements increases dramatically.

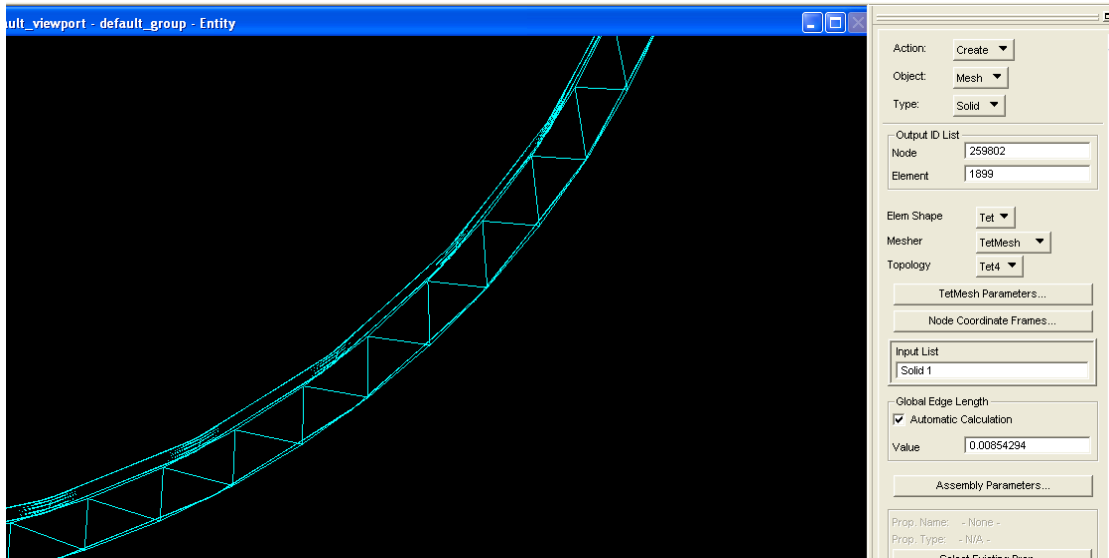


Figure 43 Tetrahedron element meshing with 1899 elements

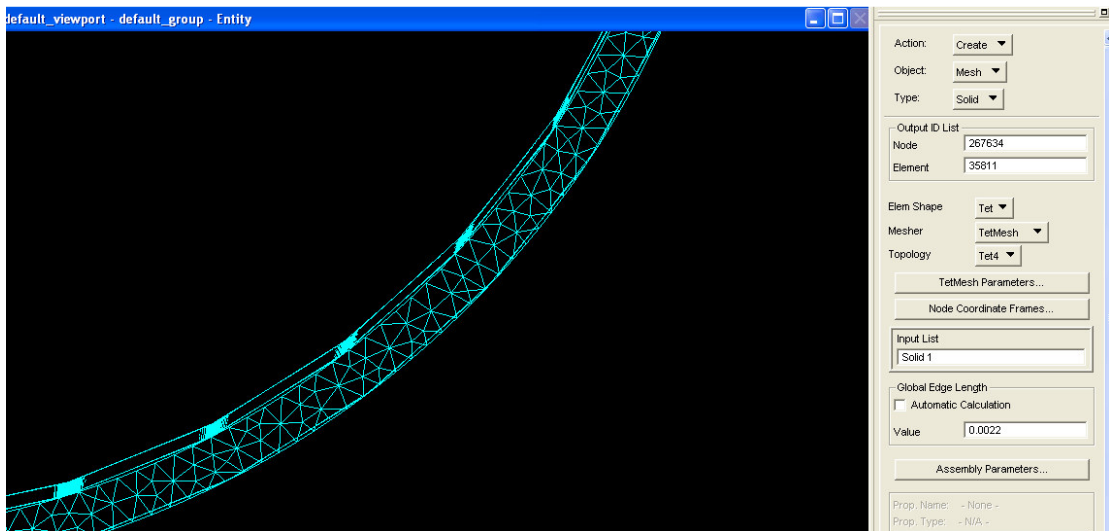


Figure 44 Tetrahedron element meshing with 35811 elements

Two different finite element solutions are performed to see the difference and the effect of the element number. The solution takes place approximately 2-3 minutes when the element number is 1899. As expected, the calculation time increases to 2 hours, when the element number is 35811. The effect of the total element number to the “mnf” file is the same, increasing the element number results in bigger “mnf” file. The total simulation time in ADAMS is also affected by the element number. There has been a trial made to see the

effect of the increased element number. The simulation time increased such that it could not be finished in one day.

The result is that the automatic calculation mode is used, because this mode includes curvature checks with automatic density control. The used advanced algorithm ensures that elements with the best shape and size are created at the boundaries.

After meshing is completed, the connection points which are called “nodes” are defined. The nodes are shown as purple points in Figure 42. These nodes are the connection points to the hip element and obviously the force is applied to these nodes. Figure 45 shows how to create a node in arc center. Actually the whole body is consists of elements with nodes. Two new nodes are introduced in order to fix the legs to the hip assembly. As these two nodes are arbitrarily defined, they should be connected to the other elements or nodes. Figure 46 shows the connection procedure of the nodes to the neighborhood nodes.

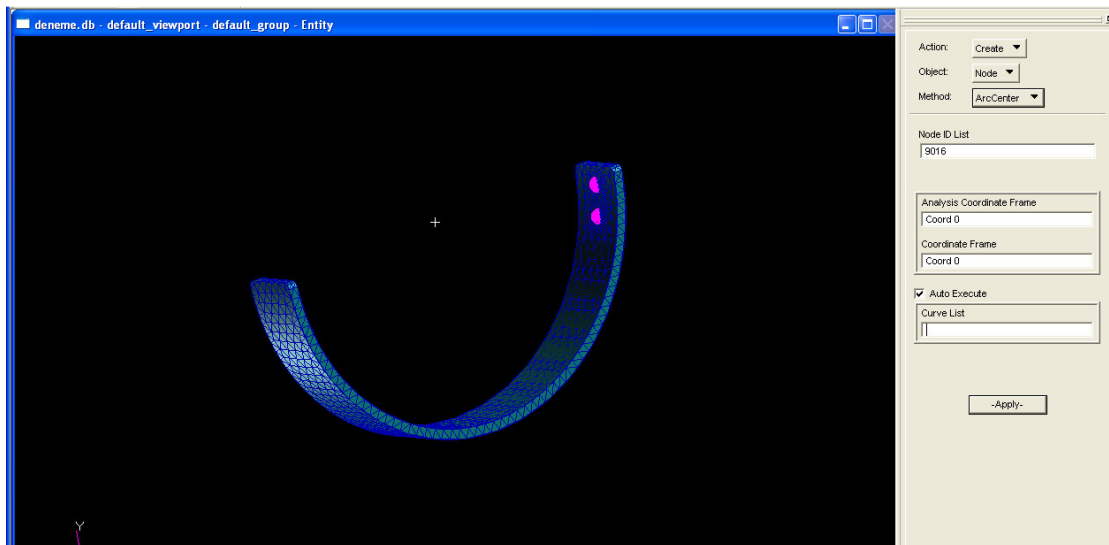


Figure 45 Create Node – The connection point

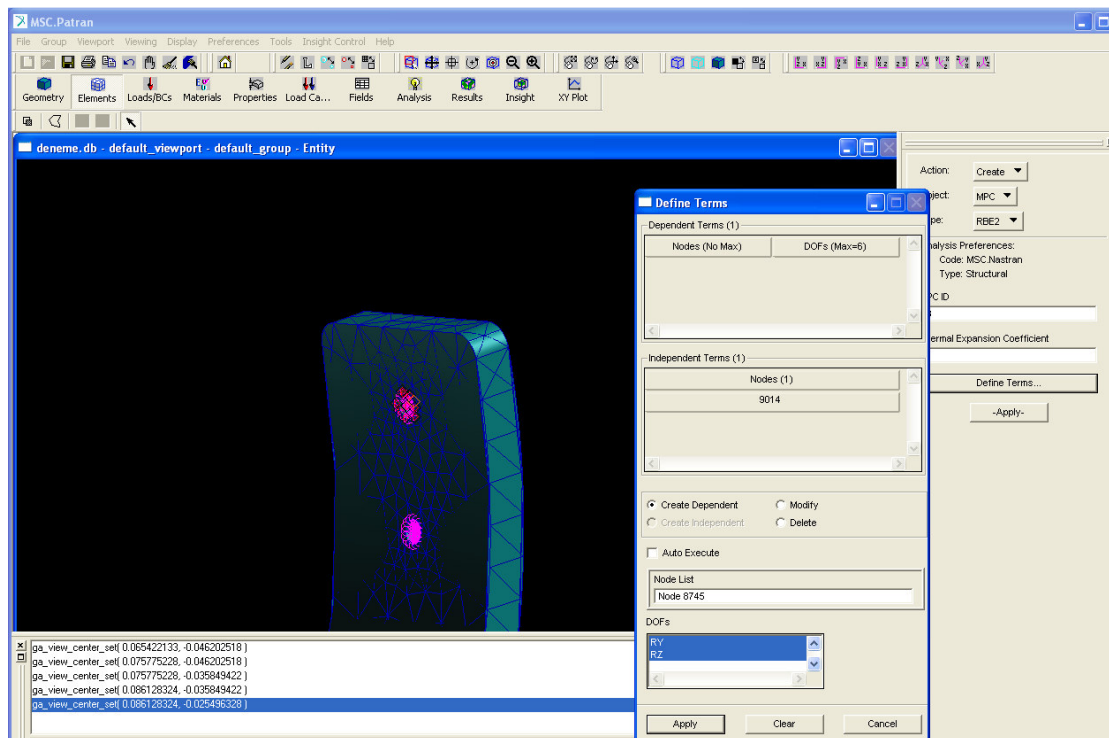


Figure 46 Node definition and connection

The next step is to define the material properties of the legs. The flexible legs are produced from carbon fibers. These fibers are oriented in 0, -45, 45 and 90 degrees and these different oriented layers are glued with a special resin. Therefore there is not an opportunity to directly select the material and its properties in PATRAN. The technical report that tells how to produce the legs includes also the mechanical property of the legs. So a new material is created in the material sub menu. Elastic modulus, poisson ratio, shear modulus, density, thermal expansion coefficient, structural damping coefficient and reference temperature could be defined as being the properties of the created new material (Figure 47). Tests are performed on the manufactured robot legs treating them as an isotropic solids and elastic modulus of the legs are found to be 10 Gpa. Poisson ratio is assumed as 0.41. The density of the leg is 1400 kg/m³. Finally structural damping coefficient is taken as 0.1 (an educated guess).

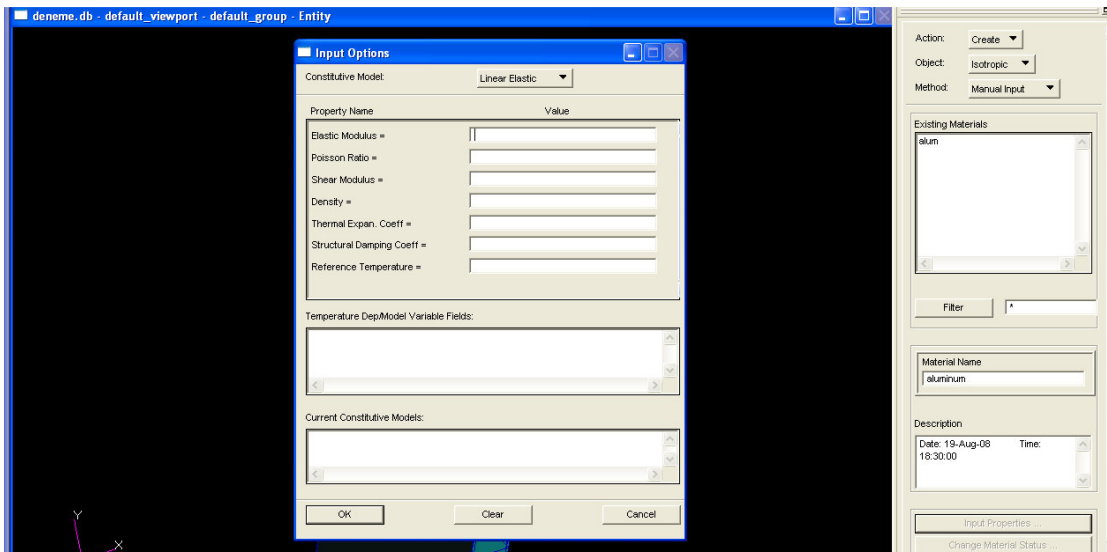


Figure 47 Material creation and property definition

So far a new material is defined in PATRAN. At this stage, it is possible to select this material for any of the solid model. Figure 48 shows how to assign the created material as being the material of the leg.

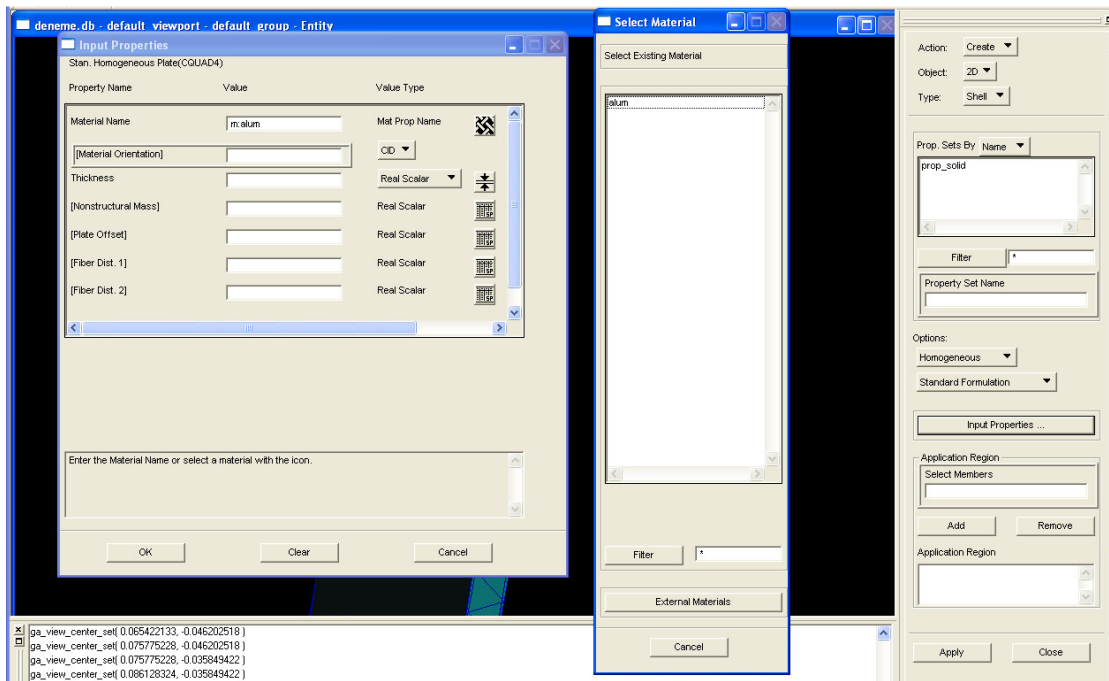


Figure 48 Material assigning

Up to this point mesh element properties are defined and the material selection procedure is completed. The finite element model of the legs is ready. The final step is to set the analysis parameters. Figure 49 and Figure 50 show these parameters. The solution type is selected. Then the connection points which are created arbitrarily after defining the mesh properties are assigned in the DOF list. The output requests are also defined in this section.

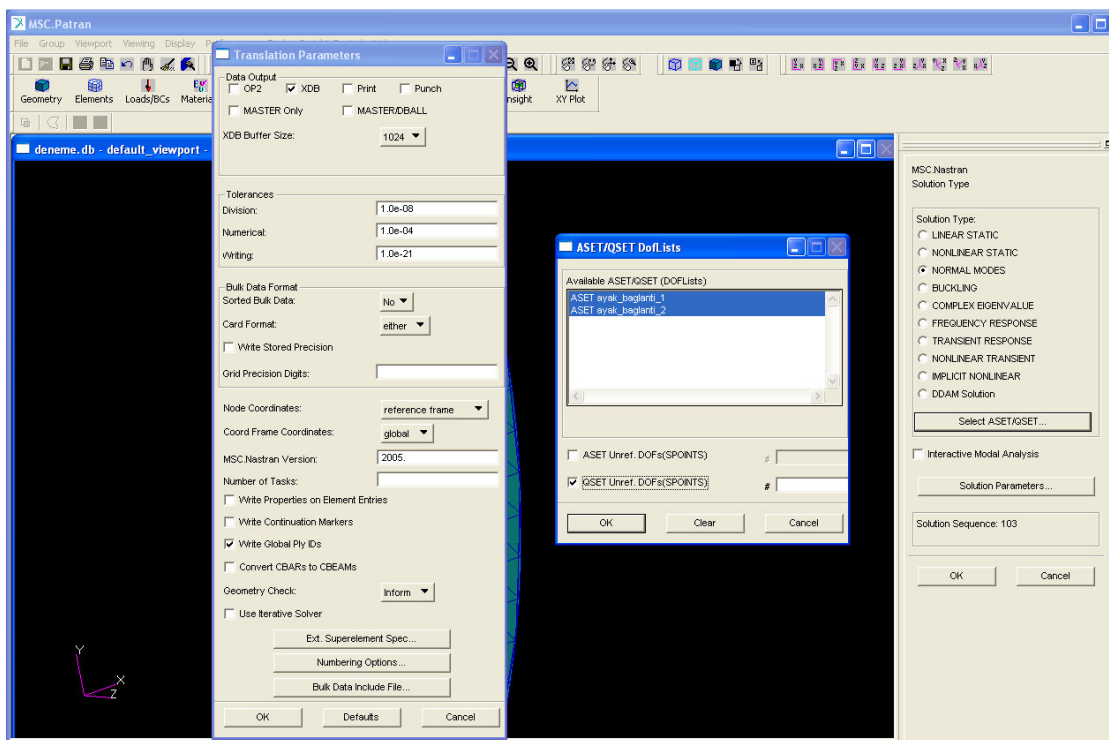


Figure 49 Analysis settings-1

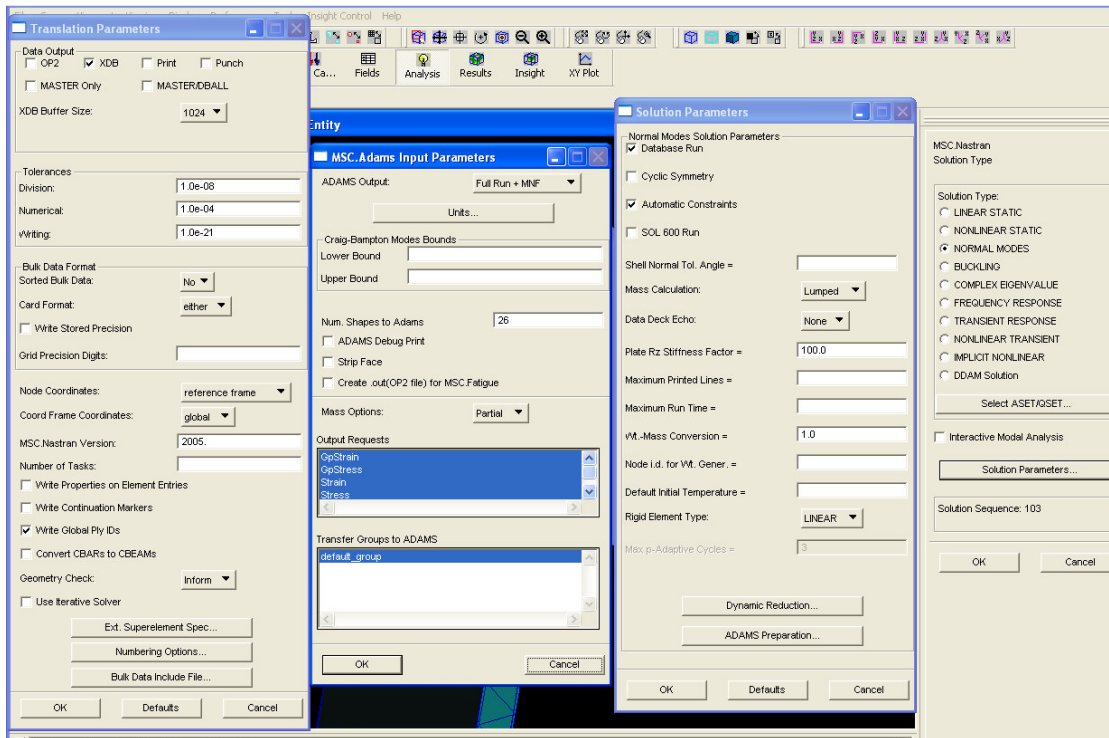


Figure 50 Analysis settings -2

Figure 51 shows the final step of the analysis parameter settings. In this sub window the output units are selected. This selection is very important for the rest of the modeling.

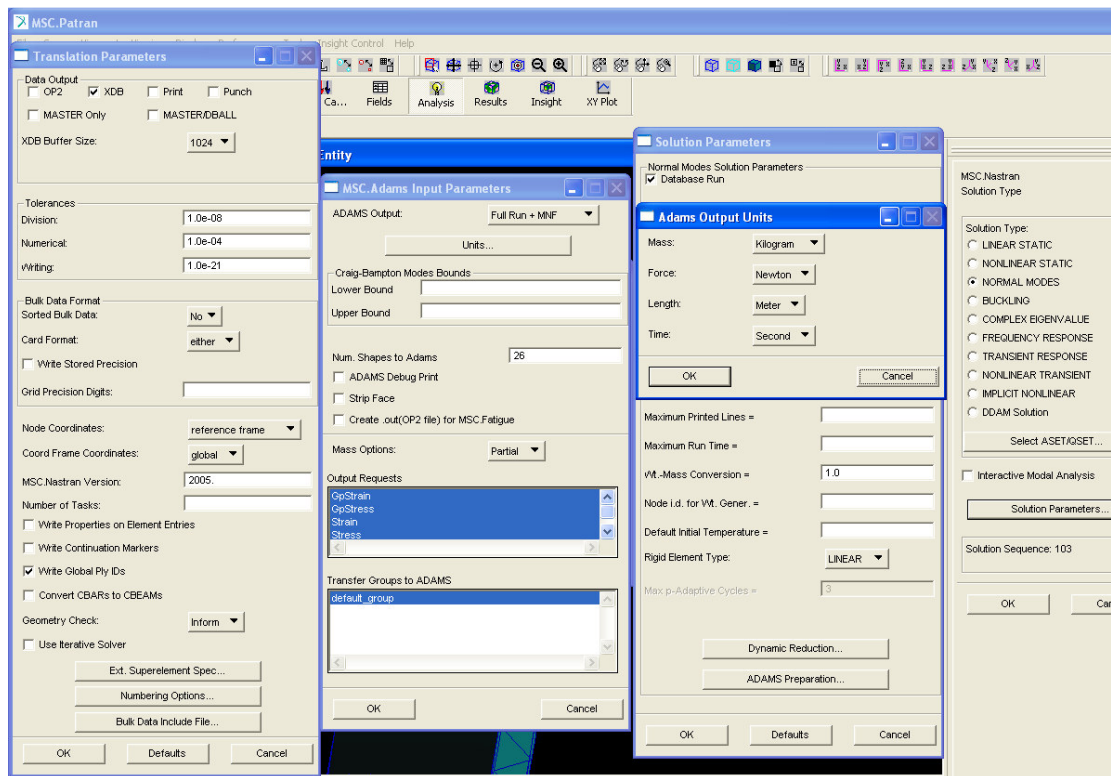


Figure 51 Analysis settings-3

The finite element model is completed and the analysis parameters are set. Hitting apply button a new job is started and after finishing this job a “bdf” file is created. This file is opened in MSC NASTRAN software. After compiling, Material Neutral File (MNF), which corresponds the flexible leg model including all the set properties, is created. This file is included in Rhex’s dynamic model in ADAMS by the help of the ADAMS/Flex Module. Now the dynamic model fully simulates the real case. The body of the Rhex is directly imported from 3D model and the flexible legs are fully defined as a finite element model and included in the dynamic model.

At this stage, the dynamic model is ready for simulation. The very simple motion of RHex is the tripod walking mode. So the rotations of the legs are defined such that RHex could perform a successful tripod walking. ADAMS offers wide variety of functions to impose a motion to a revolute joint.

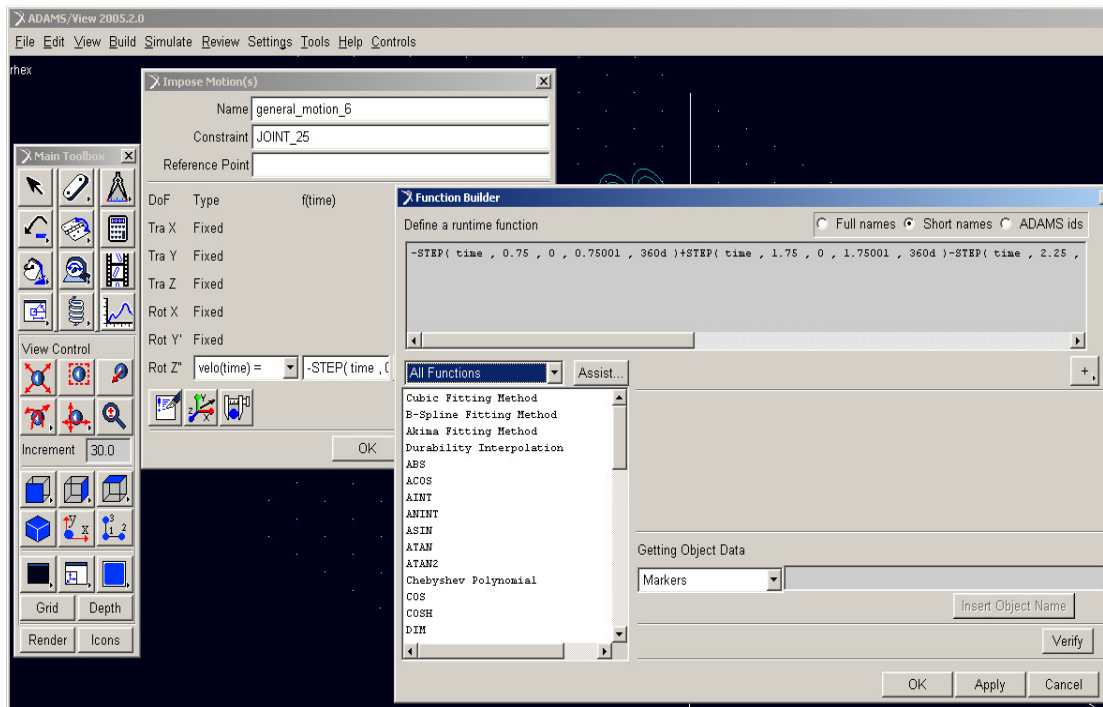


Figure 52 Function Builder Menu

As seen from the “Impose Motion” menu the rotational motion about “z” axis can be chosen as displacement, velocity, acceleration and free. Function builder is a submenu, where the motion can be defined using previously set functions (Figure 52). For example the motion of the legs is defined in terms of angular velocity in the form of a step function. The motion is set such that the robot will perform a tripod walking scheme. In order to start tripod walking, when the robot is standing, three of the legs, front-right leg, rear-right leg and middle-left leg, rotates synchronously while the others stay still. Then the standing legs, the other tripod, start to rotate while the rotating legs have not completed a full circle. Afterwards left and right tripods rotate continuously. The two functions and their graphical representation are given below (Figure 53).

FUNCTION 1: $-\text{STEP}(\text{time}, 0.75, 0, 0.75001, 360d) + \text{STEP}(\text{time}, 1.75, 0, 1.75001, 360d) - \text{STEP}(\text{time}, 2.25, 0, 2.25001, 360d) + \text{STEP}(\text{time}, 3.25, 0, 3.25001, 360d) - \text{STEP}(\text{time}, 3.75, 0, 3.75001, 360d) + \text{STEP}(\text{time}, 4.75, 0, 4.75001, 360d)$

FUNCTION 2: -STEP(time,1,360d,1.001,0)-STEP(time,1.5,0,1.5001,360d) +
STEP(time,2.5,0,2.5001,360d)-STEP(time,3,0,3.001,360d)+STEP(time,4,0,
4.001,360d)-STEP(time,4.5,0,4.5001,360d)

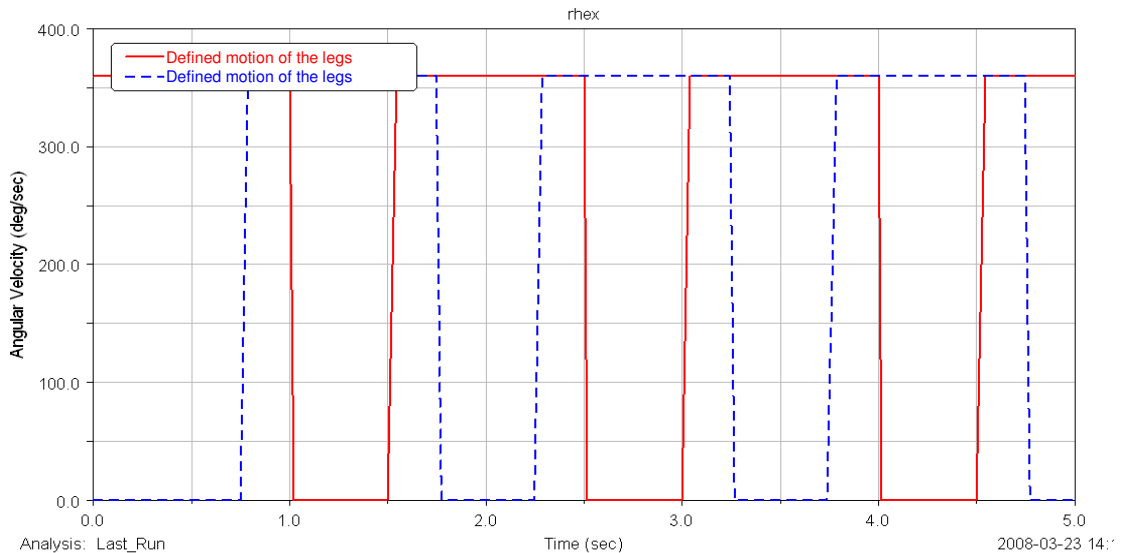


Figure 53 Defined motions of the legs

In this case velocity is the given input to the system. The velocity profile acting to the legs is exactly followed. The corresponding torque graph of the legs has some peaks which are very high and in actual case motors can not afford these high values of torque need. Since this is a first trail of the tripod walking this situation is omitted.

In real case the input of the system is the torque value of each of the motors. Actually the motors are driven by torque input and the positions of the legs are monitored. A closed loop control procedure is applied between the torque input and the angular position output. Therefore in order to have a virtual prototype of RHex which closely represents the real system, the model should be controlled by a closed loop system. The next step is to discover the control ability of the ADAMS/View platform. There is another module to cope with this type of situations. The interaction of ADAMS/View and ADAMS/Control module is investigated in the following section.

3.4. ADAMS/Control Module

The inputs which are given to the legs have such a pattern that the tripod walking is stable without having closed loop control. In this mode the position of the legs are not sensed in order to control the torque value of the legs. It means the input of the system does not change during motion.

However RHex is an autonomous robot which uses feedback to make decisions about changes to the control signal that drives the robot. By contrast, the first attempt was an open-loop control that does not have or does not use feedback. In order to have a complete virtual prototype of RHex to make analysis, simulation and optimization the system inputs can be changed according to the feedbacks.

“ADAMS Control” is a module of ADAMS, which enables defining a control plant of the system. A system representative “m-file” which will be explained later is to be created. The inputs and the outputs of the control plant, actually the actuators and the sensors of RHex, could be controlled by means of the “m-file” with MATLAB. This part of the study is considered for future implementation on RHex, but to be able to understand the process before the complications of the Rhex model are introduced the first trial was made with a simple pendulum model shown below (Figure 54).

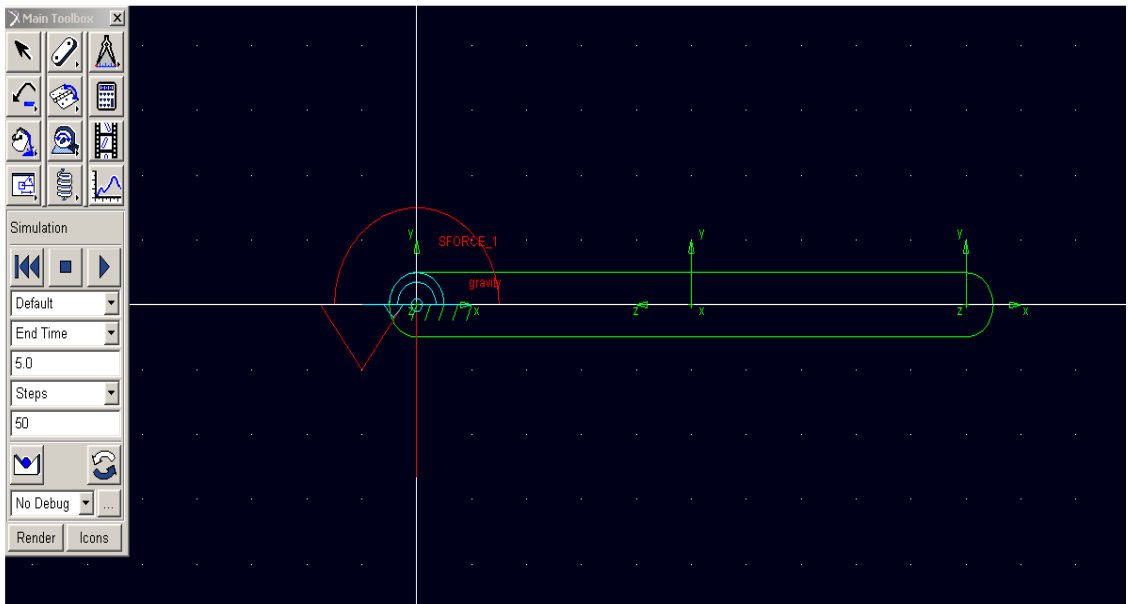


Figure 54 Simple Pendulum Model

The aim of creating such a simple pendulum model is that build a control system which has inputs and outputs. This system would be able to change the inputs according to the feedbacks. In this system a simple beam is created vertically and a torque, whose value is initially set to zero, is applied on the revolute joint shown in the figure. The position of the beam will be controlled with the torque input value.

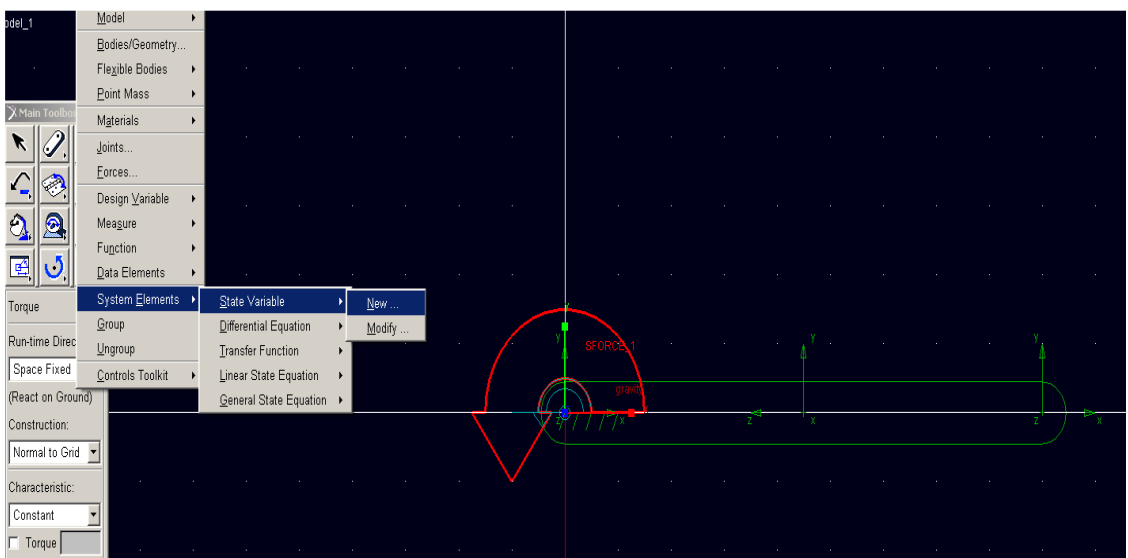


Figure 55 Assigning variables

Then two variables are assigned (Figure 55). The first one is a torque, the input variable and the second one, which will be the output, is the angular position of the beam.

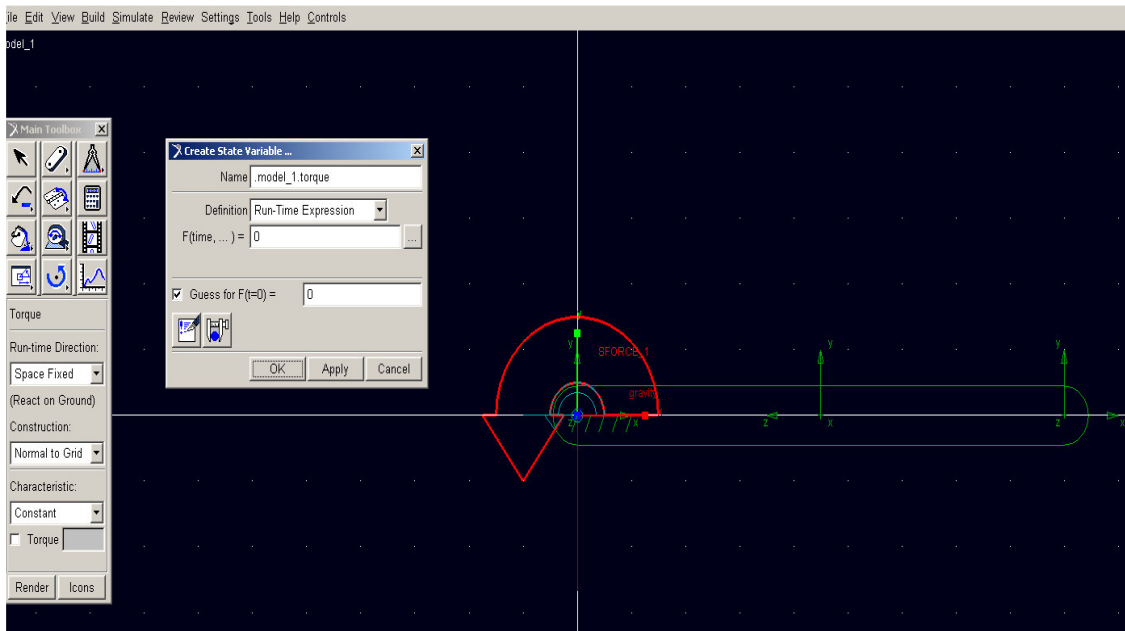


Figure 56 Torque variable

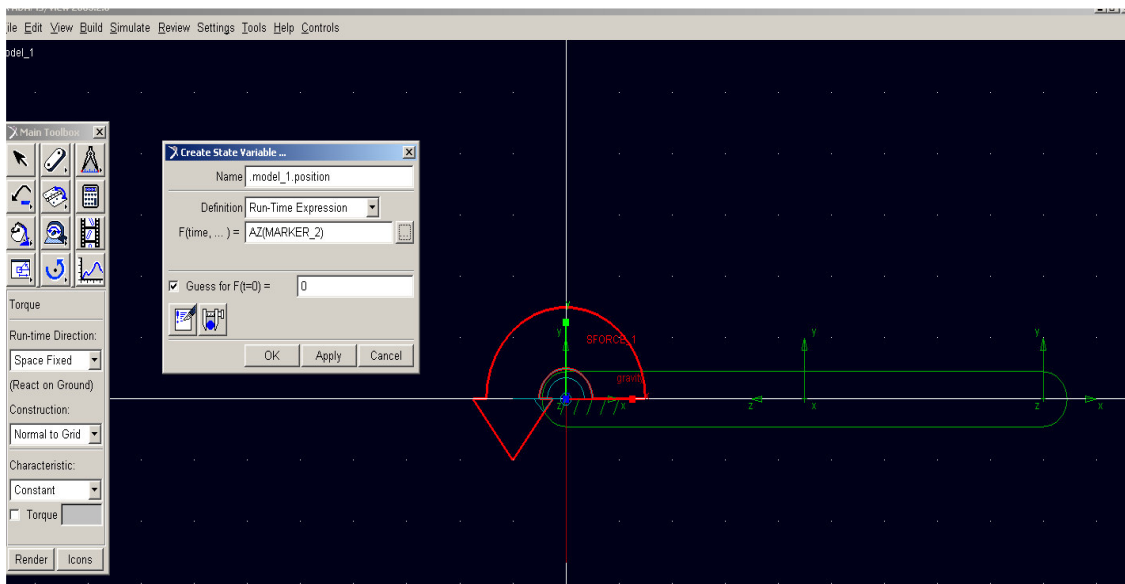


Figure 57 Position variable

The value of the torque variable is initially set to zero (Figure 56). Since this variable will be the input of the system and its value will change during the

simulation according to the feedback, the output angular position in this case. The output function is set to “AZ(MARKER_2). This means the angular displacement about z axis of the MARKER_2 which is the end point of the beam (Figure 57).

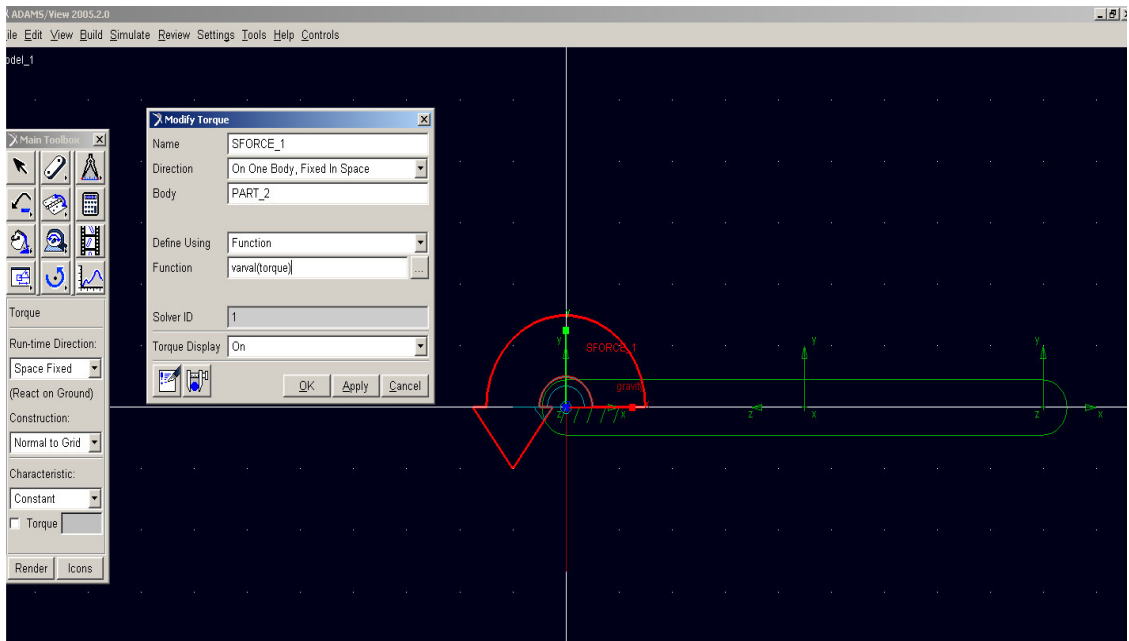


Figure 58 Assigning torque variable to the applied torque

The torque applied on the revolute joint will control the position of the beam. So its value which is initially set to zero will be changed to VARVAL (TORQUE). The torque variable, the input of the system, will be equal to the torque applied on the beam (Figure 58).

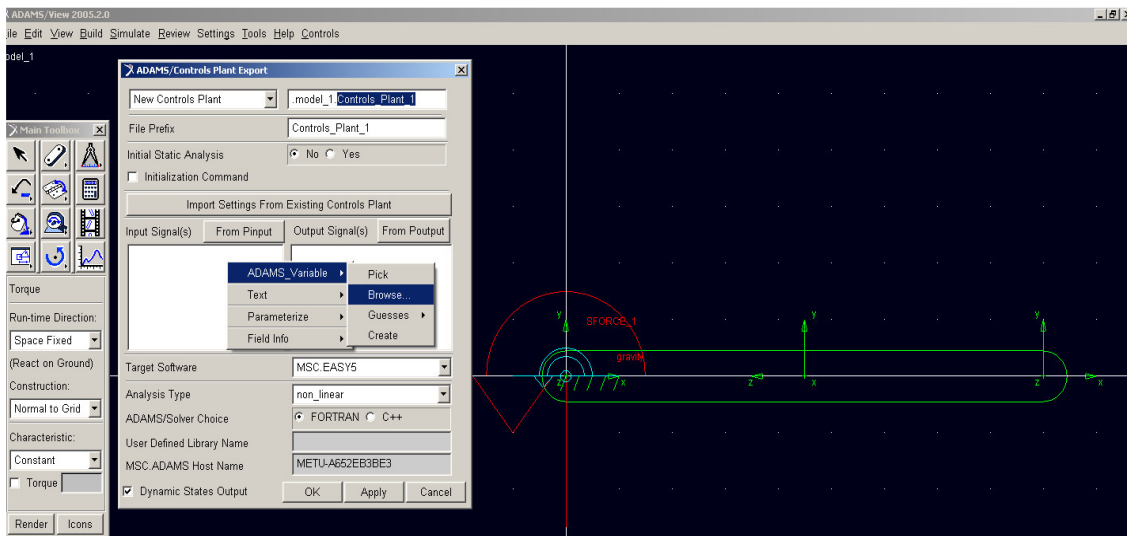


Figure 59 Defining control plant

The final step is to build and define the control plant (Figure 59). In this submenu the name of the control plant, inputs, outputs, target software and ADAMS/Solver choice can be defined. Obviously in the simple pendulum system the torque applied on the revolute joint is the input of the system and the angular position of the pendulum is the output system. After closing this menu the control plant and corresponding to the system an “m” file is created.

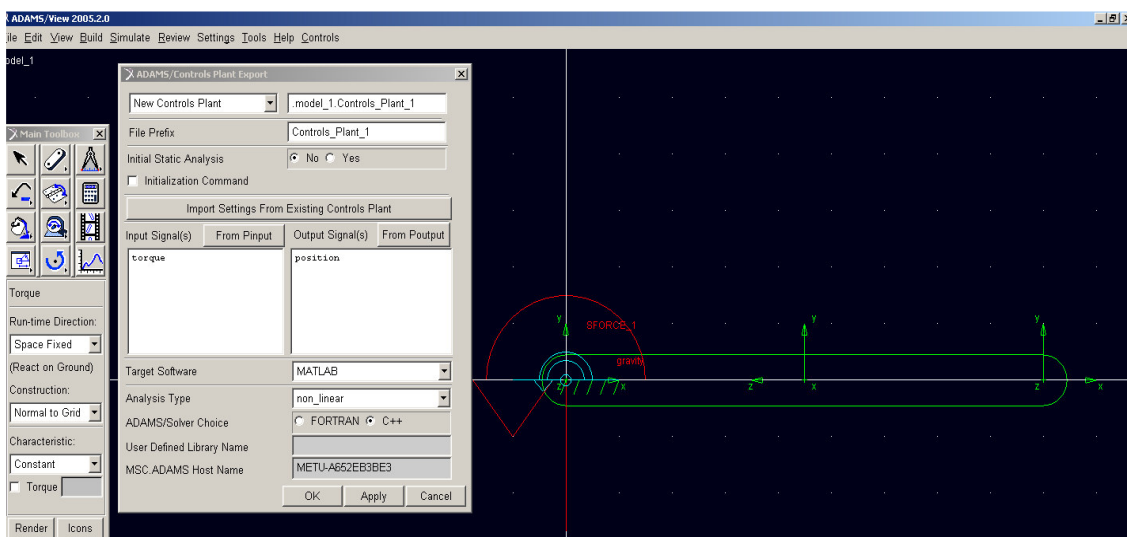


Figure 60 The final state of the control plant submenu

The generated “m-file” is a code which represents the simple pendulum system in MATLAB. This file contains an “adams_sub” block with an output named “position”. MATLAB lists the inputs and outputs when the m-file is called. Adams plant actuator name is `Torque`, and adams plant sensor name is `Position`. As a result, an “Adams_Sub” block is created which corresponds to our system and the system is actuated by an input called torque (Figure 61). The system acquires the position which is actually the output of the dynamic system.

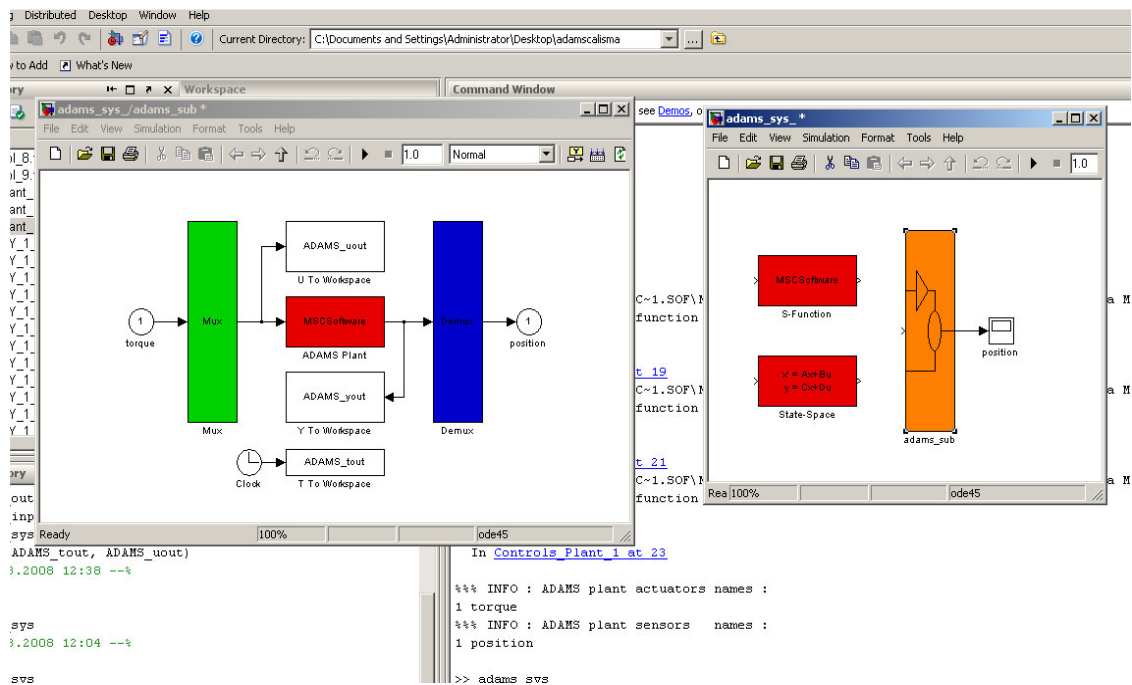


Figure 61 “Adams_sub” block, represents the simple pendulum system

A simple close loop scenario is tested. The discrete mode is chosen for ADAMS to solve the equation of motion from the Adams Sub-block menu and variable step ode45 solver type is selected in MATLAB in order to manage the control structure. In this scenario PID controller is used to control the position of the pendulum. There will be no torque initially applied to the pendulum. However the position of the pendulum is desired to be -60 degrees as measured from the vertical axis. PID controller reads the value from output and compares it with the desired value. In order to hold the

pendulum at -60 degree it calculates the applied torque based on the controller parameters. In the picture below the angular position of the pendulum vs. time is plotted. After the simulation is started, it takes approximately two seconds to reach the pendulum to the desired angular position (Figure 62). Although the response time not fast enough this trial shows that ADAMS – MATLAB interaction is possible and works fine.

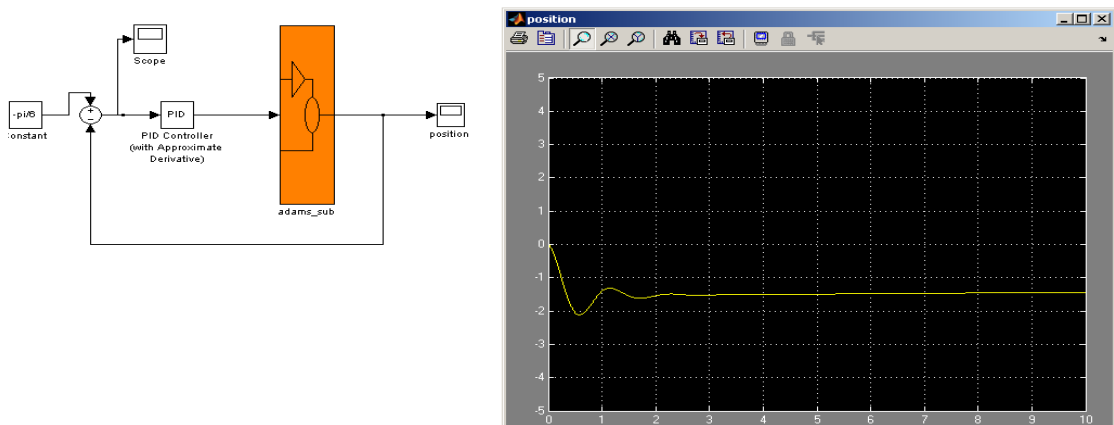


Figure 62 Closed loop control of the angular position

So far it is shown that a dynamic multi-body model, built in ADAMS, could be controlled from within MATLAB. This example shows that a complete representation of the ADAMS model could be successfully communicated with MATLAB. Then the control of the model could be easily done using the significant control capabilities of MATLAB software.

In the dynamic simulation model, RHex has six motors, each of which actuates a leg. This means there will be six inputs in the system. The inputs might be in the form of the angular displacement, angular velocity or angular acceleration of the leg. There is also other possibility one of which is to apply a torque at the revolute joint on the legs. The angular position of the legs could be controlled adjusting the applied torques and a feedback controller may also be designed for this purpose in MATLAB which is better representation of the Rhex in a more accurate way.

3.5. The complete and fully controllable model

RHex is an autonomous robot. There will be lots of sensors to determine what to do in any circumstances RHex run into. As the aim is to simulate the real system, the virtual prototype could be controlled by a control plant. The capability of the MATLAB-ADAMS interaction is proven by controlling the simple pendulum system. The next step is to create a fully controllable flexible multibody dynamic model of RHex.

In the first simple model, the input is given as a velocity profile. The simulation runs as if the torque source is unlimited and therefore could exactly follow this profile. Actually, motors have a speed torque chart that means the torque source is dependent to the rotational speed. Since the torque source is not unlimited this simple model does not correspond the real case.

The model of RHex is modified such that the given input to the legs will be the torque value. The compliant legs are attached to the motors with revolute joints. So a single component torque is applied to each of this joint. In the “Main Toolbox” “Applied Force: Torque (Single Component)” is selected to define torque values (Figure 63).

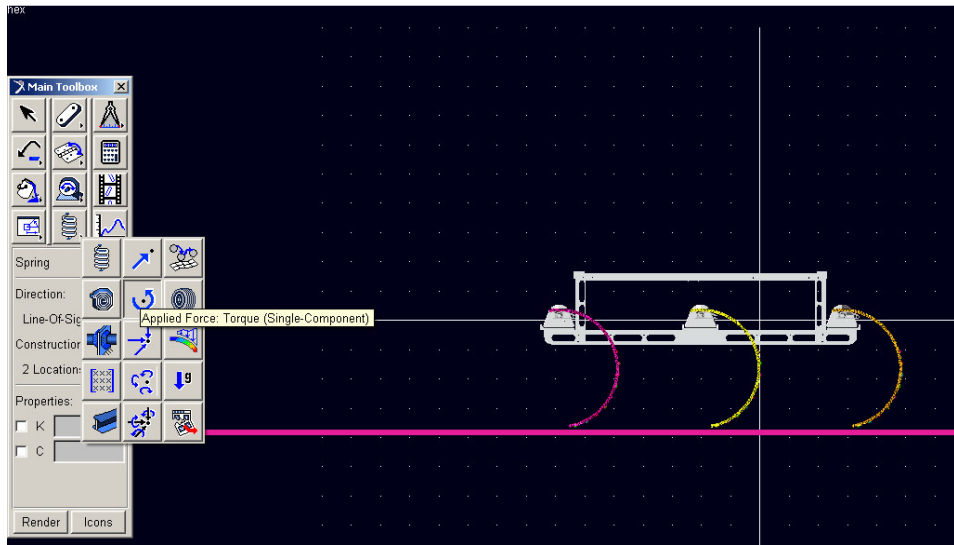


Figure 63 Torque input to the legs

In the previous section variable assigning and inputs and outputs definition are mentioned. For the time being there are six inputs which are the torque values given to the flexible legs and six outputs being the angular position of the each leg (Figure 64).

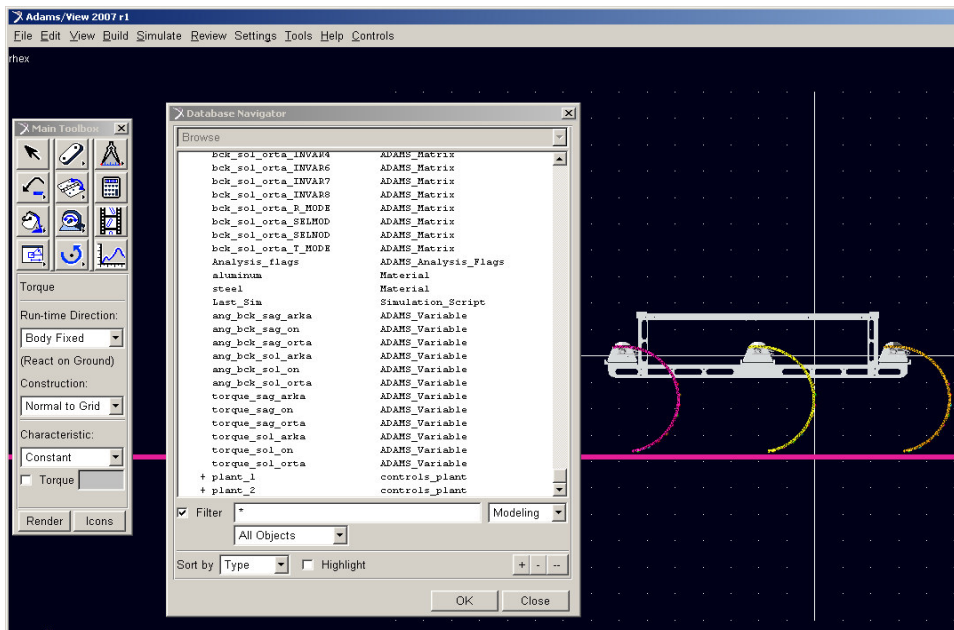


Figure 64 Definition of the inputs and outputs as a variable

After defining the twelve variables six of them are assigned as the torque value of each leg (Figure 65).

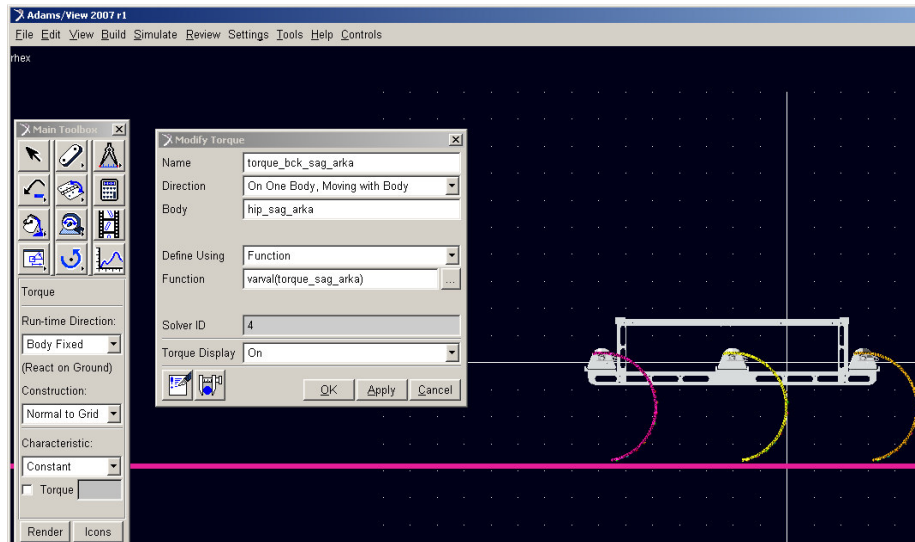


Figure 65 Torque variable assignment

The other six variables, which are the outputs of the system, are actually sensors attached to the marker on the compliant legs. They monitor the angular position of the legs (Figure 66).

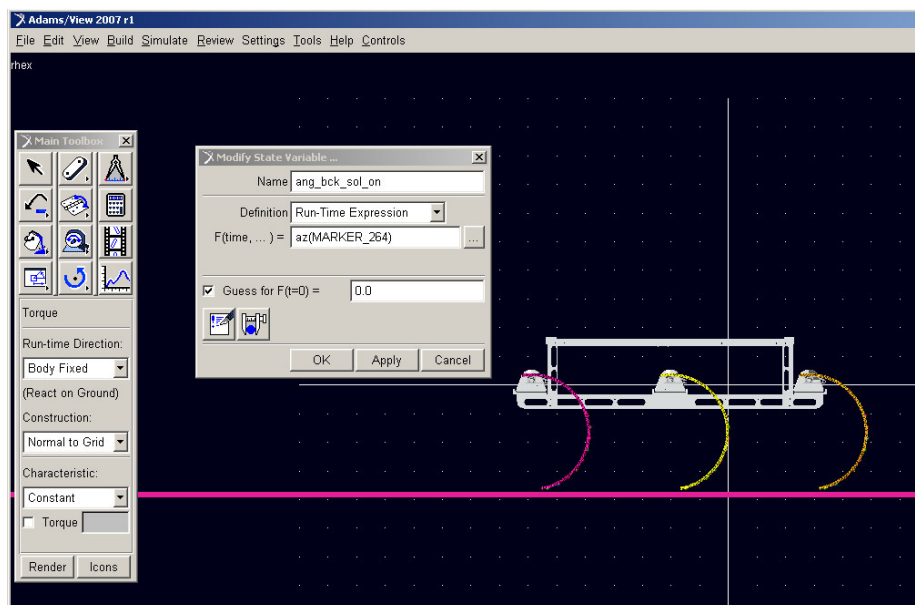


Figure 66 Angular Position of the Legs

The final step is to build a control plant which has six inputs, torque values, and six outputs, angular position of the legs.

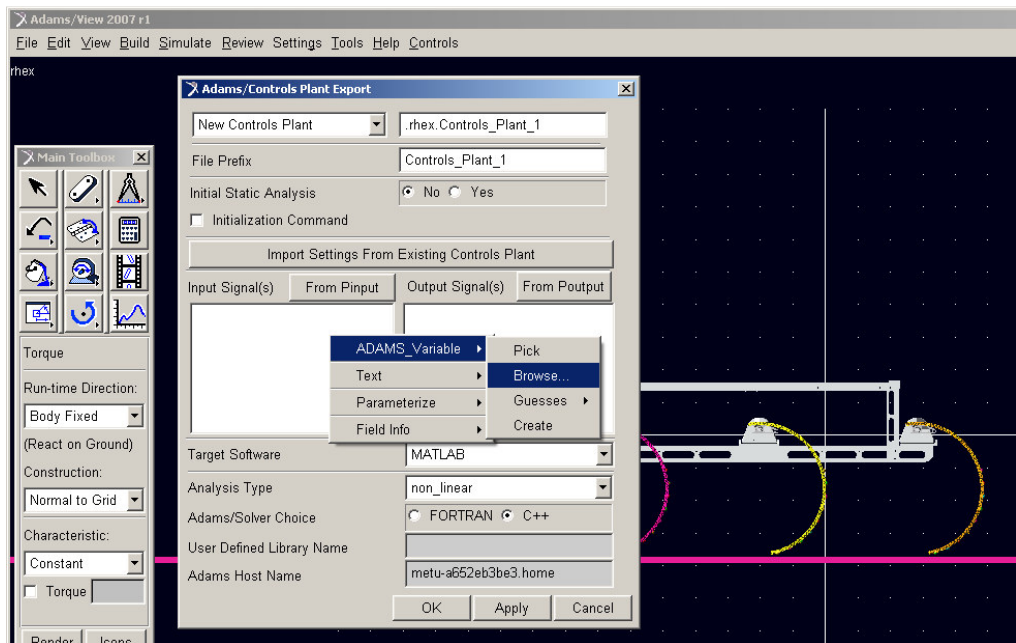


Figure 67 Control Plant Definition

In the upper menu “Controls” tab is selected to define a new control plant. The submenu contains the input and output signals list. Also the interacting control software “MATLAB” and the solver choice could be selected in this submenu (Figure 67). The final view of the control plant build menu looks like as in Figure 68. This procedure is followed to build an “m-file” which represents the simulation model in MATLAB with six inputs and six outputs.

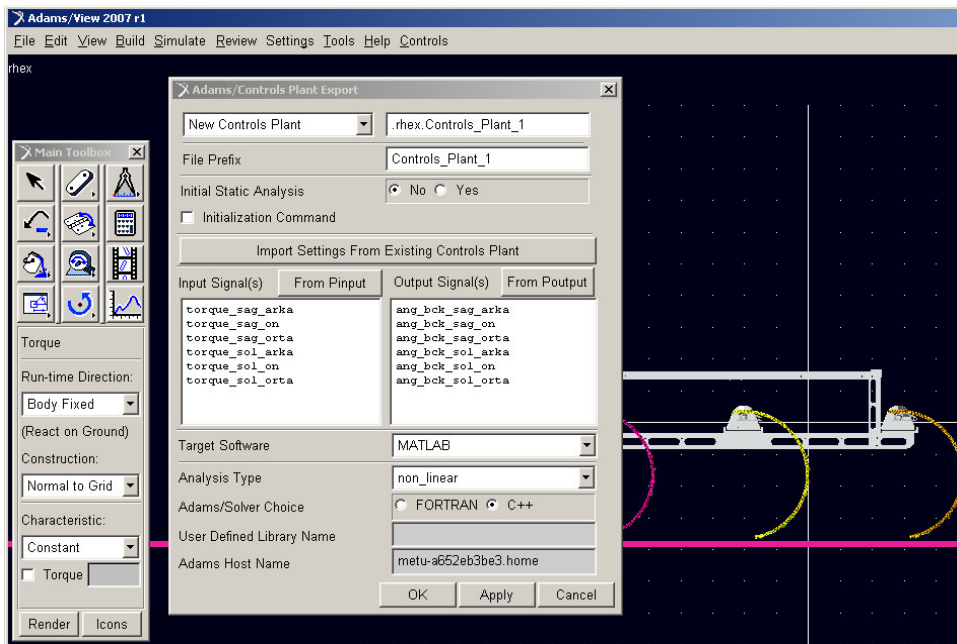


Figure 68 Final view of the Control Plant build menu

The m-file, which corresponds the simulation model, is copied in the current directory of MATLAB. The file is called from this menu and the inputs and the sensors are listed (Figure 69).

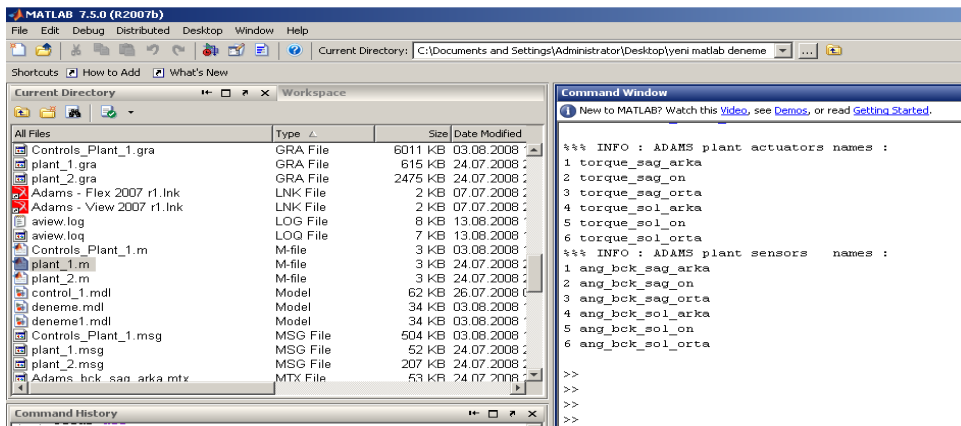


Figure 69 Calling m-file from MATLAB

The aim is to build a complete fully controllable simulation model of RHex. Up to this point, the complete and detailed flexible multibody dynamic model is completed in ADAMS environment. The ADAMS/Control module enables this model to communicate with the control software (MATLAB). Actually the m-

file represents this flexible multibody dynamic model in MATLAB. It transforms every information to this environment. Using “Simulink” module any kind of control algorithm could be implemented. In Figure 70 there is an example of a closed loop control algorithm including the motor parameters and the back emf effect. This PID controller checks the actual position of the legs with the given reference position. This position profile is the same with the first simple tripod walking trial. Although the real case is different, in that study the angular positions of the legs are the input. Now resembling the real case more accurately, the inputs are the torque values which are adjusted according to the comparison of the real and reference angular positions of the legs by the PID controller.

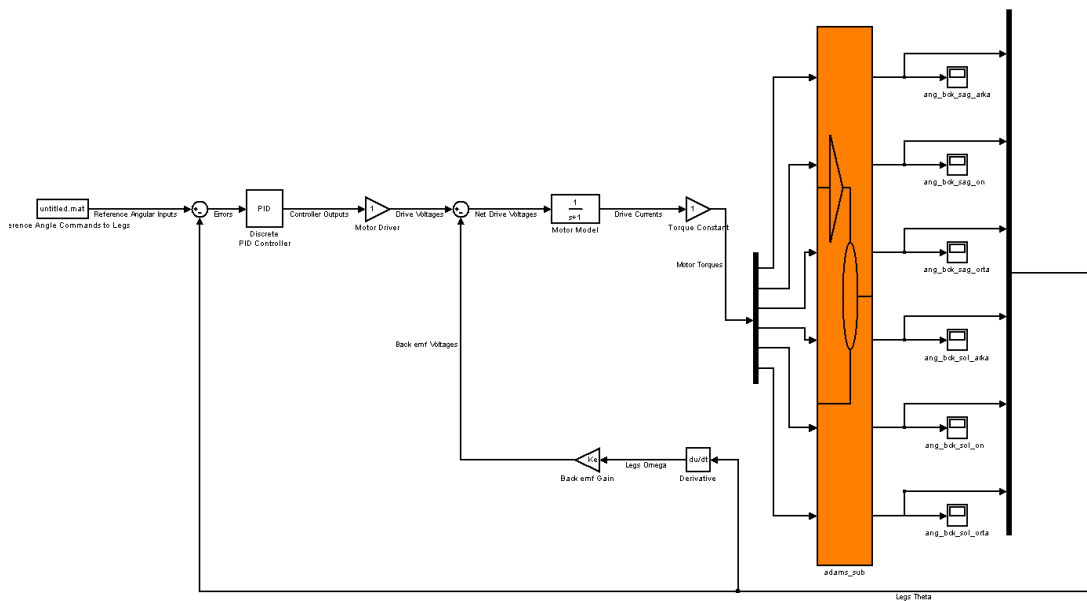


Figure 70 A closed loop PID controller

The reference position which is given to the system as an input would be followed by each leg. This reference position is defined by four parameters [43]. These parameters are t_c , t_s , Φ_s , Φ_0 . The time to complete one cycle is defined as t_c . This cycle include two different phases. One is slow and the other one is fast swing phase. The corresponding time value of the slow swing phase is t_s . Φ_s is the swept angle by the slow swing phase. Finally

the Φ_0 parameter offsets the motion profile with respect to the vertical (Figure 71).

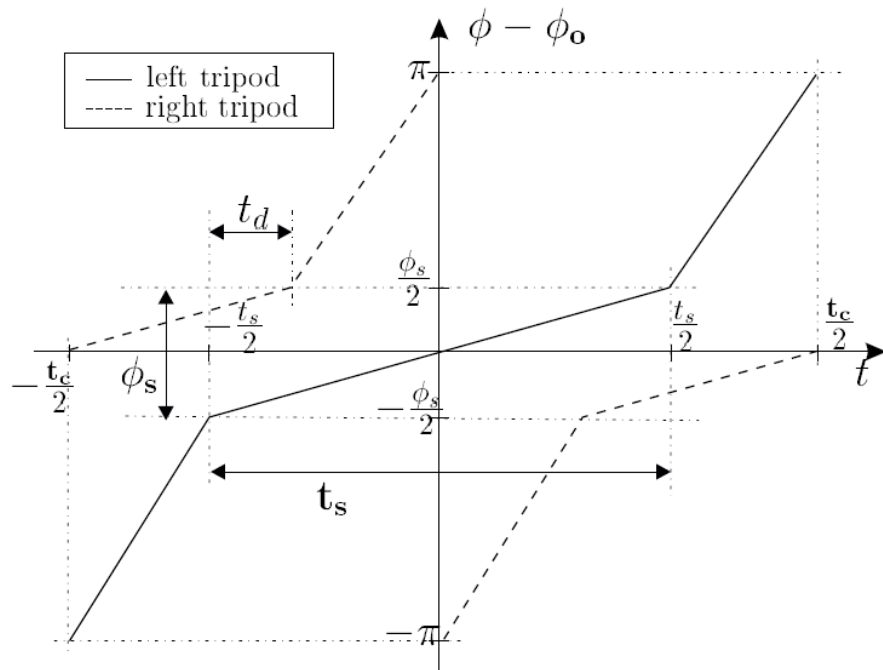


Figure 71 Reference position presentation [44]

CHAPTER 4

CASE STUDIES

The scope of this thesis is to build a virtual prototype of RHex, which is a hexapod robot with half circular flexible legs. The first step is to create a 3D model of RHex. This model could be imported to ADAMS software, which is a dynamic simulation modeling program. After importing the body of RHex, the second step is to define flexible legs properties by creating a “MNF” file. This model of the flexible legs is modeled in MSC PATRAN. Then using ADAMS/Flex module the mnf file is imported to ADAMS and added to the dynamic model. Finally the model represents the real case. The last step was to interact ADAMS with a control software, MATLAB, in order to add close loop control mechanism to simulate autonomous RHex.

4.1. Simulation study with parameters in literature

The first simulation trial is done in MSC ADAMS by giving angular velocity step input command to the legs. This input is actually the corresponding velocity value of the reference angular position profile, which is desired to be followed by the legs. As mentioned in chapter three reference angular position profile is defined by four parameters.

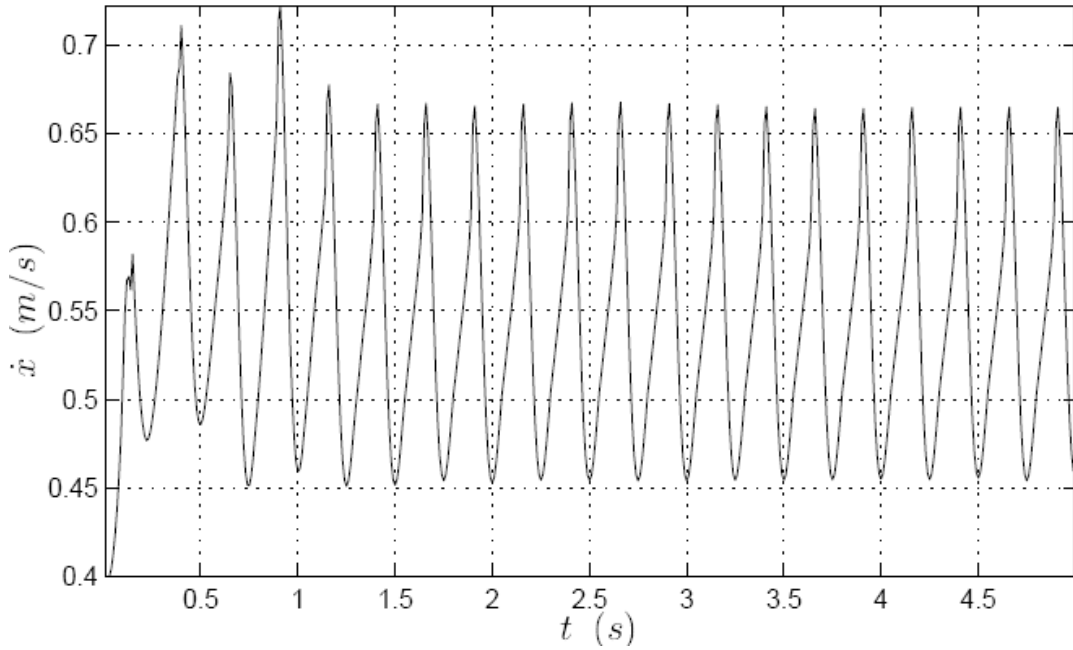


Figure 72 Forward body velocity for a simulation run with $t_c = 0.5s$, $\Phi_s = 0.7rad$, $t_s = 0.3s$ and $\Phi_0 = 0.03rad$. [44]

The forward body velocity profile for a simulation run with $t_c = 0.5s$, $\Phi_s = 0.7rad$, $t_s = 0.3s$ and $\Phi_0 = 0.03rad$. is given in Figure 72 [44]. Using the same parameter, the reference angular position profile is plotted and the corresponding velocity term is gathered for five seconds, which is the total simulation time.

$\Phi_s: 0.7$	$t_c: 0.5$	$t_{ratio}: 1.5$	$t_f: 0.2$
$t_s: 0.3$	$\Phi_0: 0.03$	$t_0: 0.0128571$	

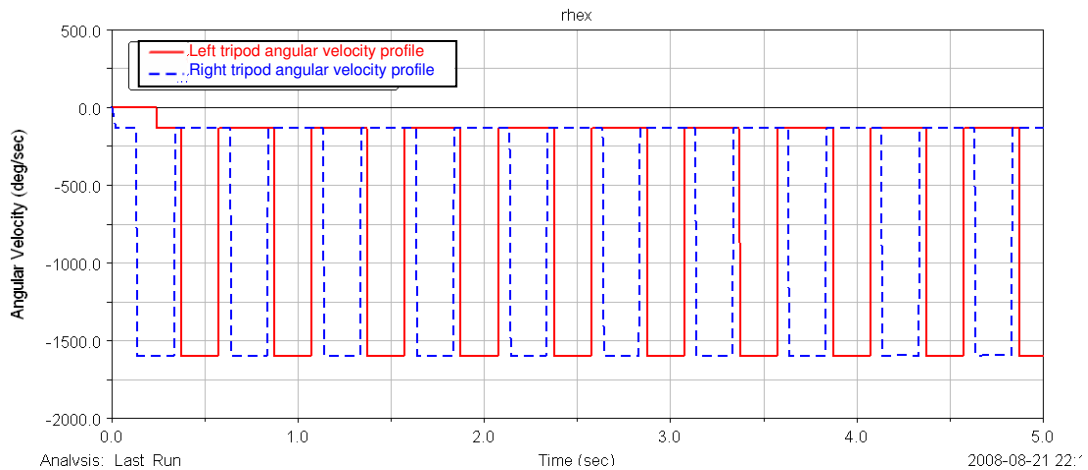


Figure 73 Left and right tripod angular velocity profile

Figure 73 shows the angular velocity of the left tripod and right tripod. The above function, which is in the form of STEP function (Appendix A), represents the desired velocity profile of the given four parameters. The six legs are attached to the hip assembly with a revolute joint. In Figure 52 how to define rotational motion to these joints is shown. After setting the motions the simulation is carried for five seconds.

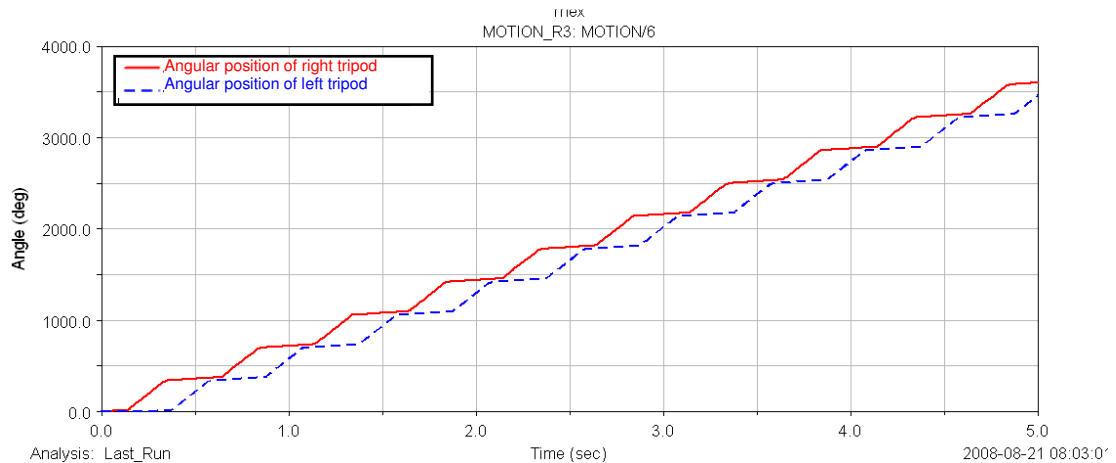


Figure 74 Angular position of left and right tripod

Figure 74 shows the angular positions of the right and left tripods. The profile is the same with the profile in Figure 71 which is published in literature [44].

The simulation results are shown in Figure 75. This graph represents the position and velocity of the body in x direction. The simulation starts from a stationary position. Therefore after 0.5 seconds the motion assumes a periodic profile.

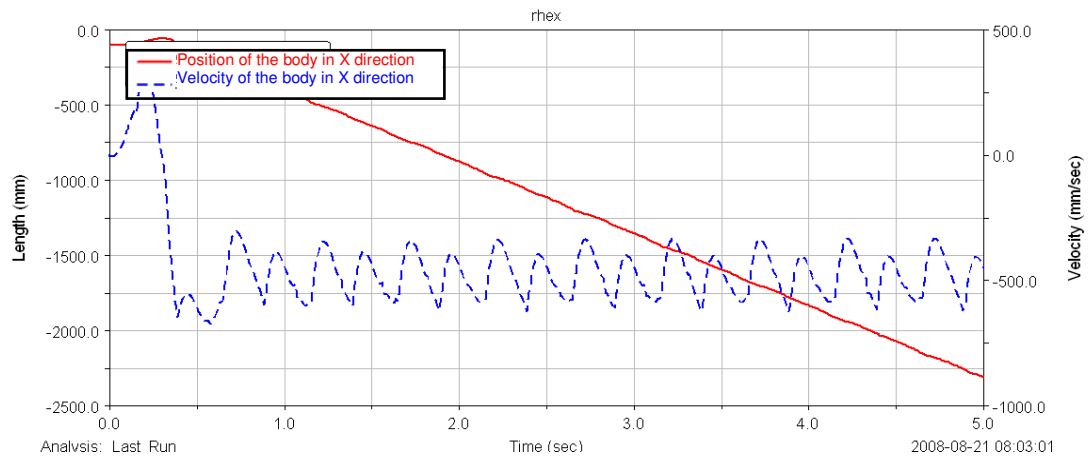


Figure 75 Position and Velocity of the body in X direction

The maximum velocity is approximately 630 mm/s and minimum velocity is 335mm/s. In five seconds the robot travels 2300 mm. in the x direction. The average velocity between first and fifth seconds is 480 mm/s. Comparing the simulation results with the results in literature, the average velocity was 550 mm/s which is 15% more than the velocity value get from the ADAMS simulation. The fluctuation of the velocity profile is the same with the previous result in literature, which is for the previous version of RHex.

In chapter two, the design changes were mentioned. The previous version of RHex is smaller in dimension. On the other hand the weight of the robot is increased. Another major difference is that the legs stiffness property is changed considering the weight and dimension increase. Although the modifications are applied in the same percentage to length and width of the body, there might be slight changes in simulation results.

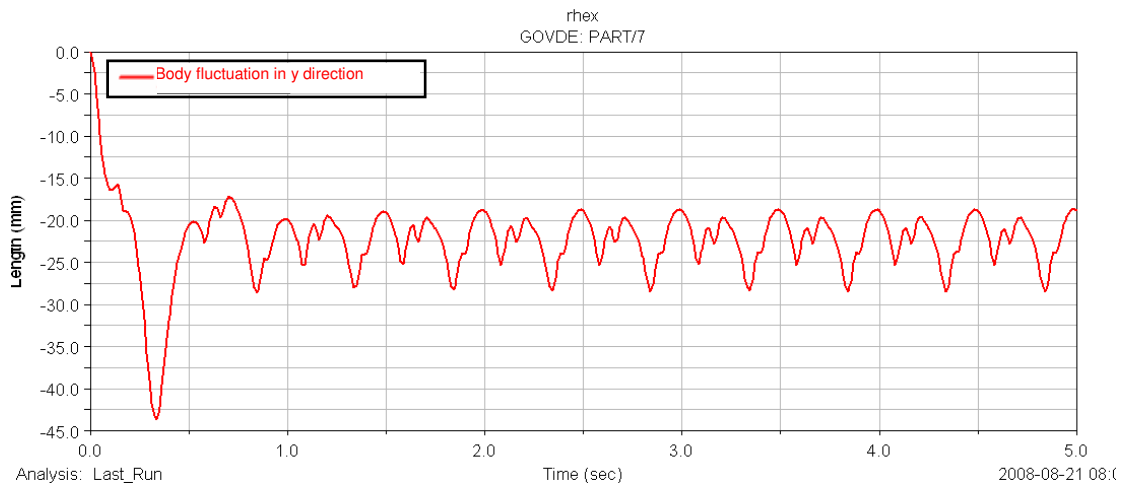


Figure 76 Body fluctuation in y direction

Figure 76 shows the body fluctuation in y direction. The flexible legs' elastic behavior results in this fluctuation. The difference between minimum and maximum height of the body during the simulation is approximately 10mm. The fluctuation profile repeats itself in every half seconds which is the total time for one leg to complete one revolution.

Another graph (Figure 77) represents the torque requirement of one leg about z direction (i.e., the hip axis). Although in real case the rotation is caused by torque input, in this simulation the input is leg angular velocity. In real case the torque input is given to the motors and a closed loop position control is performed. Although this simulation is not the same with the real case, investigating the torque requirement of one leg, it can be observed if there is a handicap to provide angular velocity input to the system.

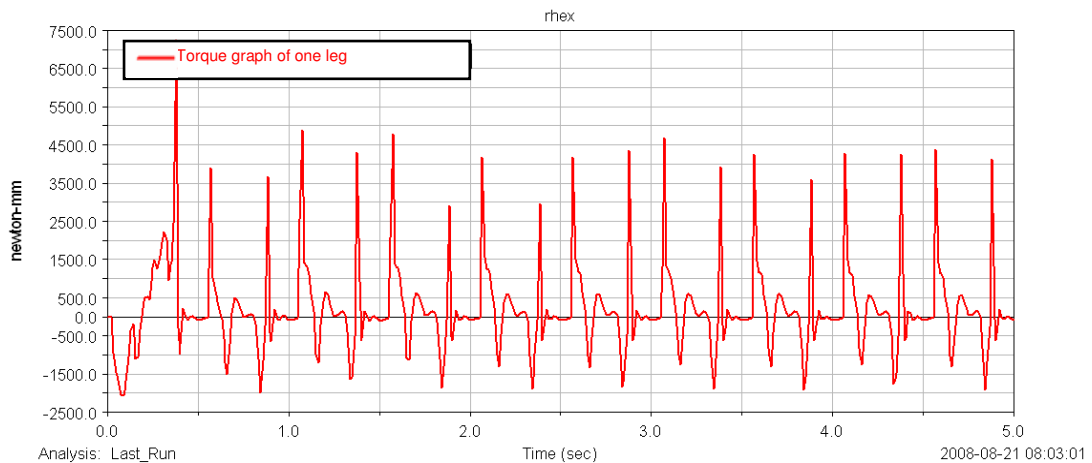


Figure 77 Torque graph of one leg

The maximum torque requirement is approximately 4500 Nmm. The torque speed curve of the motor is represented in Figure 78. The torque need of the leg to follow the reference angular position profile has some peaks. These peaks could be afforded by the motor by taking the risk of briefly overloading.

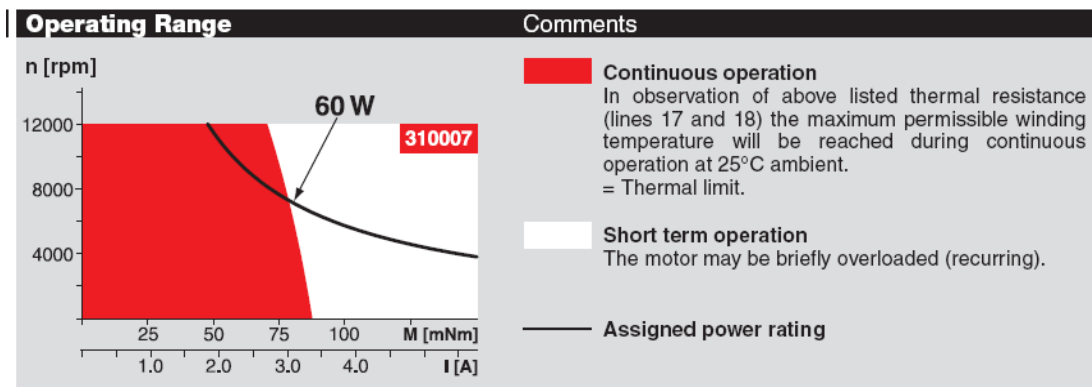


Figure 78 Torque-speed curve of RE30 motor [48]

Another graph, velocity in x direction of the body being the x axis versus height of the body being the y axis, is plotted (Figure 79). As mentioned before, because the simulation starts from stationary state, after half second the motion is stabilized. Therefore ignoring the first 0.5 second, the graph shows that the system settles into a stable limit cycle type oscillation.

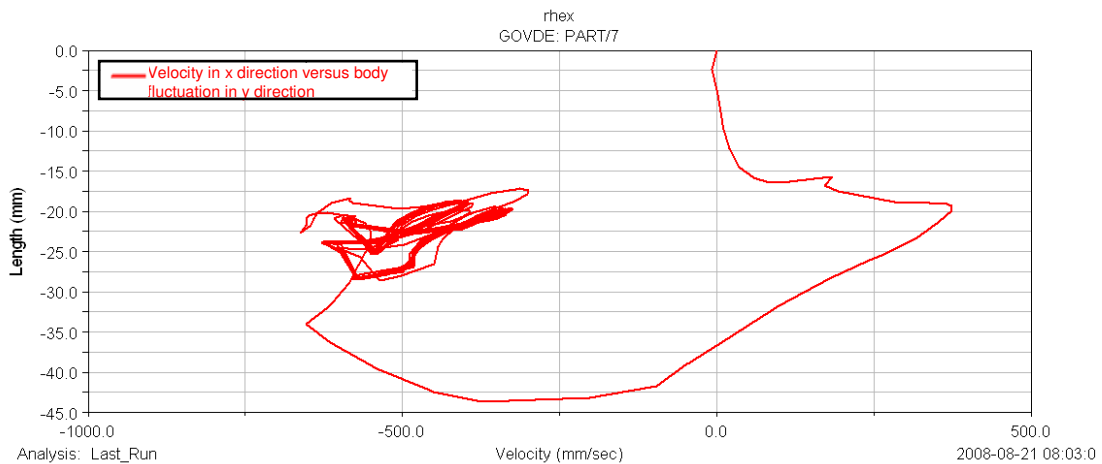


Figure 79 Velocity in x direction versus body fluctuation in y direction

4.2. Simulation trial with MATLAB interaction

As mentioned in the previous chapter the aim of this study is to build a virtual prototype of RHex. The dynamic model is assembled in MSC ADAMS software, which includes also the flexible members. The compliant legs are added to the model with the help of MSC NASTRAN, a finite element program. The final step is adding control structure to the model. Using MATLAB software the motor and closed loop control model is built and the interaction between MSC ADAMS and MATLAB is accomplished.

The control structure and the interaction between ADAMS and MATLAB are mentioned in Chapter 3.4. The final “Adams Sub Block” looks like as in Figure 80. There are six inputs and six outputs. Torques are the inputs of the system and the angular positions of the legs are the outputs.

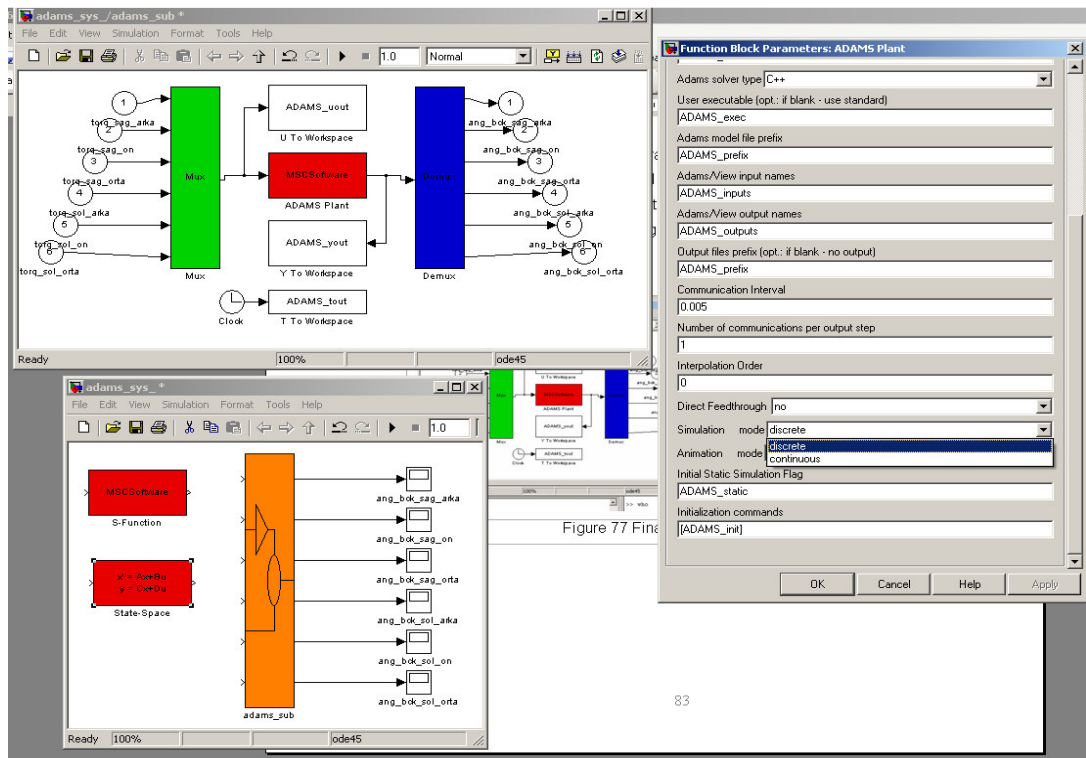


Figure 80 Final ADAMS Sub Block

The ADAMS Sub-Block lets the user to choose the “Simulation Mode”. This property determines that which program will solve the equations in ADAMS. The discrete mode lets ADAMS to solve the equations which is preferred because ADAMS has specific solver types for complicated systems and they are probably more accurate. In the other mode which is called “continuous mode”, MATLAB program solves the equation of motion as well as managing the control structure. MATLAB offers fixed step and variable step solver type with different kinds such as ode45, ode113, ode3, ode5.

A simple pendulum model was mentioned in chapter 3. The control structure and the dynamic model is a very straightforward one. The discrete mode is chosen for ADAMS to solve the equation of motion and variable step ode45 solver type is selected in MATLAB in order to manage the control structure.

The complex flexible dynamical simulation of RHex has been attempted with the same selected features as the simple pendulum model. The different

solver types and discrete mode do not allow achieving a good solution. The reference angle input could not be followed because of an incompatibility.

Another trial is made with the continuous mode and variable step ode45 solver type. This combination results in a good solution but the simulation time is enormous. Normally, a complete 5 s. simulation would take place in ADAMS approximately 20-30 minutes, whereas the same simulation lasts more than 60 hours.

The discrete mode and fixed step ode3 solver type combination is tried in order to decrease the simulation time. The default step size is 0.005. One trial is made without changing the step size. The result is not as expected; the reference angle input could not be followed with enough accuracy. Then the step size is decreased to 0.0005 and 0.00005. Although the final trial with 0.00005 step size gives accurate results, the simulation time is not decreased.

There are previous studies about the ADAMS-MATLAB interaction. The simulation times for different models with different complexity levels are studied [48]. For a simple model the simulation time does not increase incredibly when MATLAB is included but considering a complex system, such as RHex a flexible dynamical model, the simulation time may increase 120 times or more.

Finally the ADAMS MATLAB interaction is completed successfully by the use of extremely fine time steps (0.00005 s.) but because of the huge simulation time it is not feasible to compute all the simulations with MATLAB.

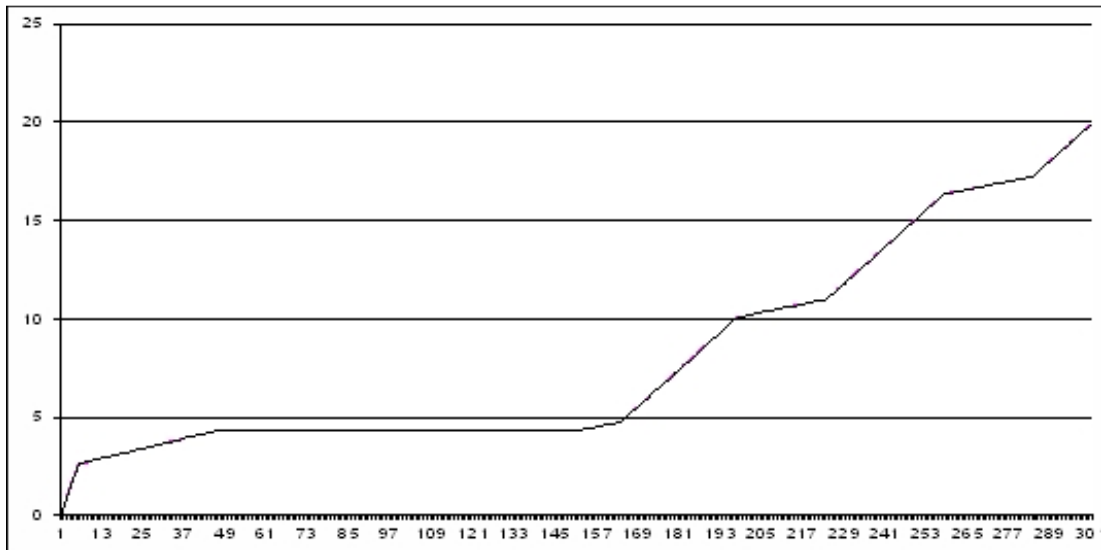


Figure 81 Reference angle input and real angular position of the leg in the same graph

The average difference between the reference angular input and the real angular positions of the legs 0.01 rad. for the 3 s. simulation. Figure 81 shows both the reference angles and the real angular positions.

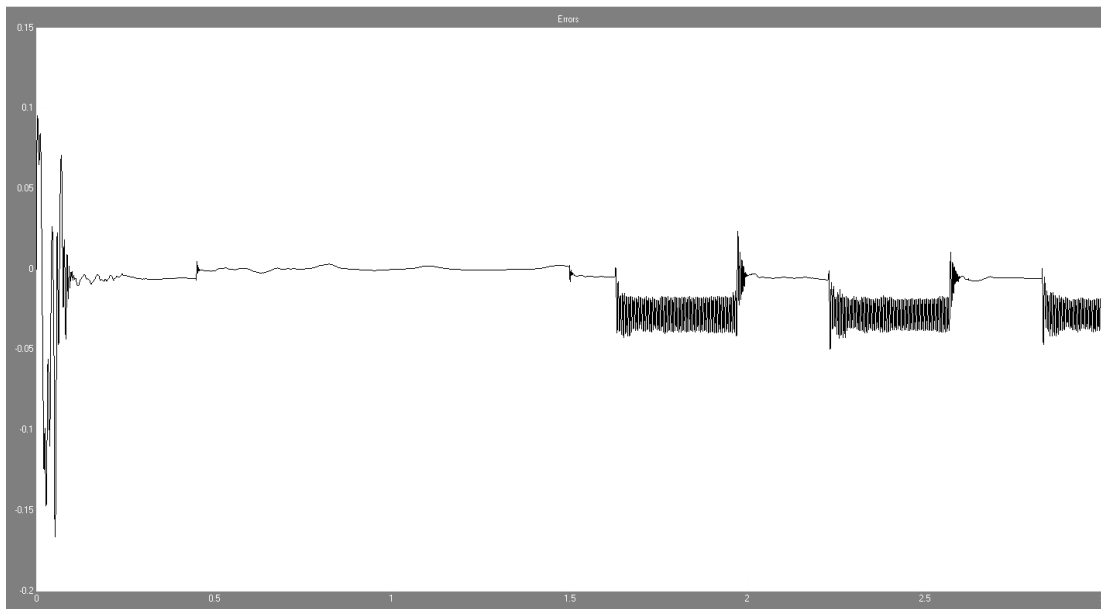


Figure 82 The difference between reference and real angular position of the left tripod

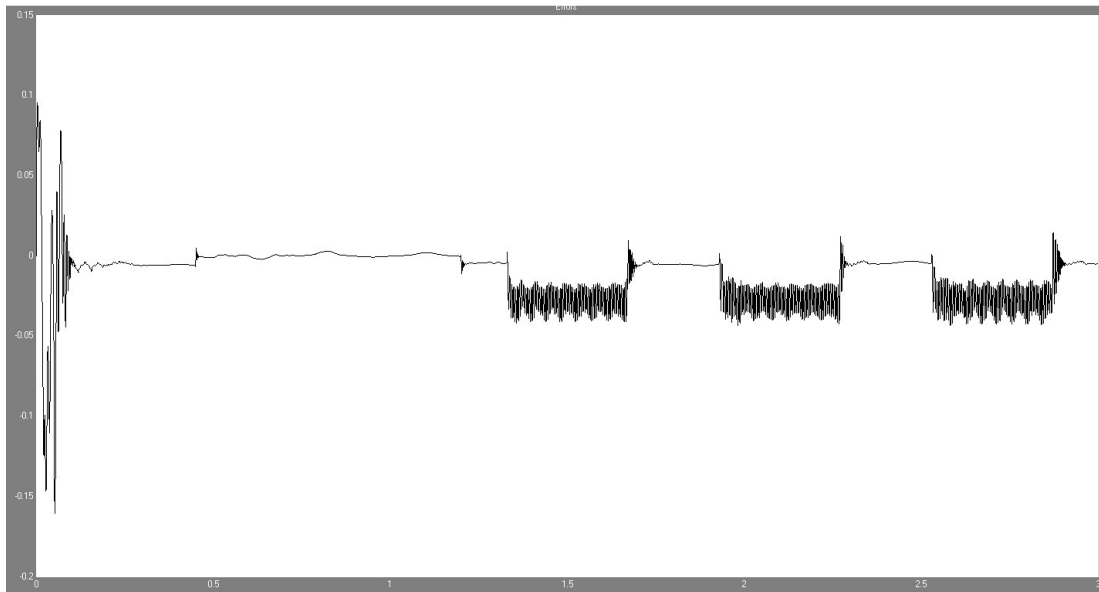


Figure 83 The difference between reference and real angular position of the right tripod

The result of the 3 s. simulation is represented in Figure 82 and Figure 83. The difference between reference and real angular positions are plotted. The graphs show that the PID controller could follow the reference angular position inputs with enough accuracy. The accuracy is dependent on the PID controller gains, which are obtained using Ziegler-Nicholas Method and then tuned manually for further refinement.

The result is that the control model works fine and could follow the reference angle input while stable tripod walking. The simulation time and managing with enormous result data is not feasible to lead optimization study. Further trials may be made with the new version of MSC ADAMS or with super computers or by the way of model simplification.

The other simulation studies which will be mentioned in the next chapters are computed in MSC ADAMS. MATLAB interaction is not included as the results shows that the reference angle input could be followed with high accuracy.

4.3. Stable tripod walking with arbitrary parameters

Before this section, the first simulation trial is done in order to compare ADAMS model results with the results in literature. The validation is successful since the results are comparable. Then ADAMS – MATLAB interaction is tested in the second section. The control structure is able to follow the reference angular position with a high accuracy, but the disadvantage of this structure is that the simulation time is very long. Therefore the following simulation trials do not include MATLAB interaction.

The third simulation trial is done by choosing arbitrary parameters. As in the previous section, the reference angle profile is defined by four parameters, which are chosen as $t_c = 0.6$ s, $\Phi_s = 0.9$ rad, $t_{ratio} = 0.75$ s and $\Phi_0 = 0$ rad.

$\Phi_s: 0.9$	$t_c: 0.6$	$t_{ratio}: 0.75$	$t_f: 0.342857$
$t_s: 0.257143$	$\Phi_0: 0$	$t_0: 0$	

These parameters are selected such that the input to the legs results in a stable tripod walking. The input step function for these parameters is given in Appendix B.

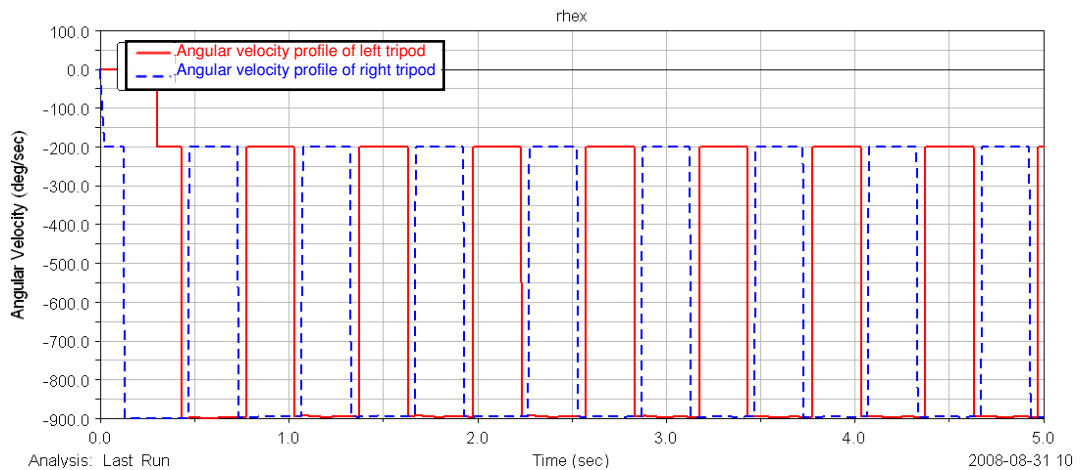


Figure 84 Angular velocity profile of left and right tripods

The above functions are defining the angular velocity of the right and left tripod in the form of step function. The corresponding angular position and velocity profile are shown in Figure 84 and Figure 85 respectively. After setting the motions the simulation is started for five seconds.

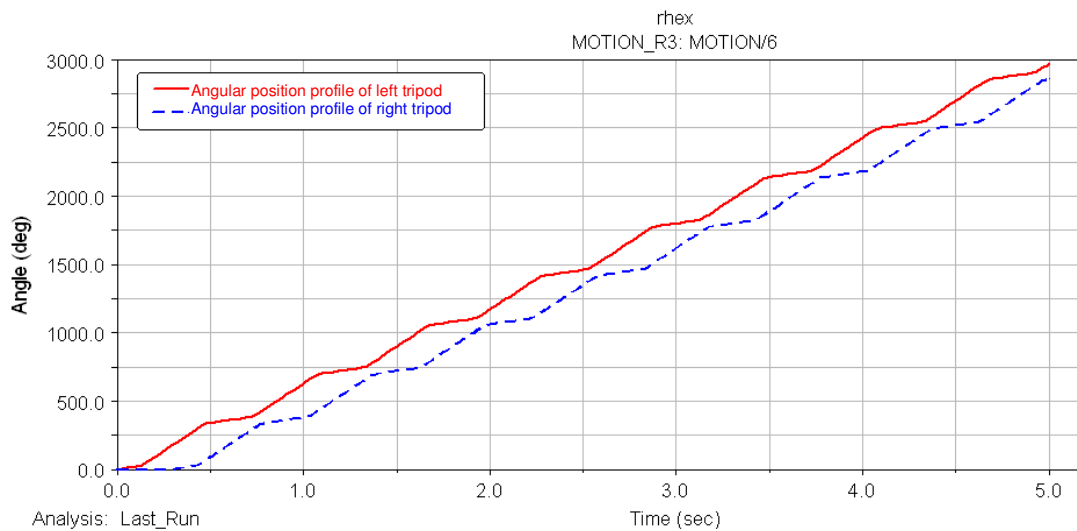


Figure 85 Angular position profile of left and right tripod

The results of the simulation are presented in the following graphs. The first graph is about the position and velocity of the body in x direction (Figure 86). The velocity in x direction has a fluctuating profile and repeats itself in every

0.6 seconds which is the time to complete one revolution. The maximum and the minimum value of the velocity are approximately 1040mm/s and 740mm/s, respectively. The average velocity is approximately 950mm/s.

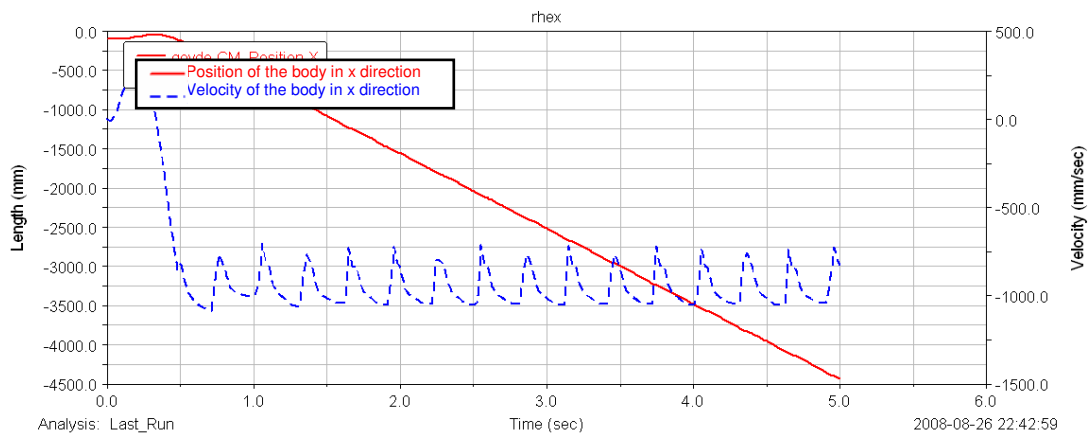


Figure 86 Position and velocity of the body in x direction

The velocity profile is as expected. The fluctuating and periodic profile is the same with the result in literature which is represented in the previous section. The average velocity is more than the velocity in the previous simulation. Although the time to complete one revolution is 0.6 seconds in this simulation which is more than the previous one, the achieved average velocity is double. That means the optimization of the other parameters is very important, comparing the result of the two simulations.

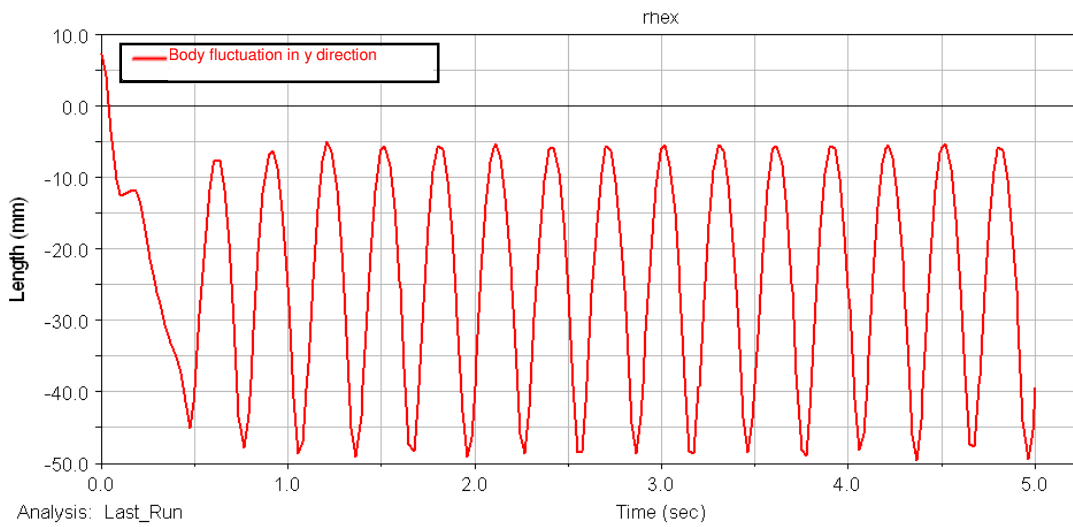


Figure 87 Body fluctuation in y direction

Figure 87 shows the height of the center of mass (CM) of the body during the simulation time. The center of mass fluctuates between -5mm and -50mm in y direction. The previous result represents a fluctuation of approximately 10mm while the fluctuation is 45mm now. There is a connection between the speed of the robot and the fluctuation of the body in y direction. The fluctuation increases when the robot speeds up. Another difference between the two fluctuations is that the second simulation result is smoother than the first one.

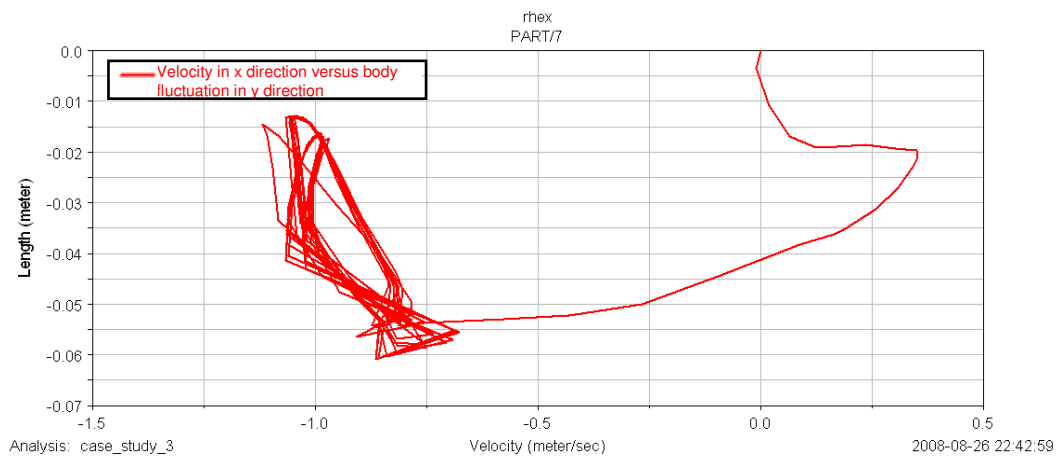


Figure 88 Velocity in x direction versus body fluctuation in y direction

Figure 88 shows the relationship between velocity and the position of the center of mass. As seen from the graph almost the same path is followed during the simulation time.

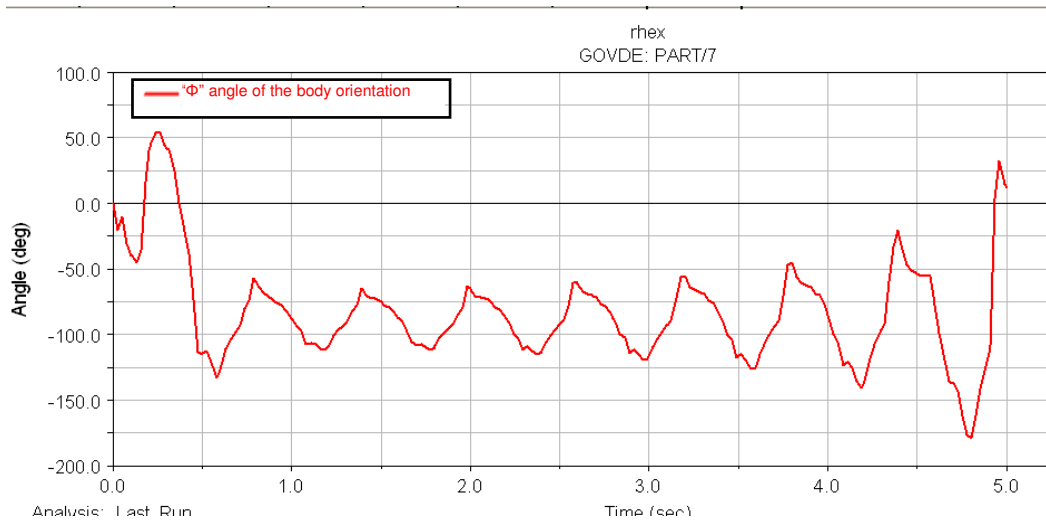


Figure 89 “Φ” angle of the body orientation

Figure 89 and Figure 90 show the body orientation during the simulation time in “Φ” and “θ” Euler Angles. The results are the same, fluctuating and periodic profile.

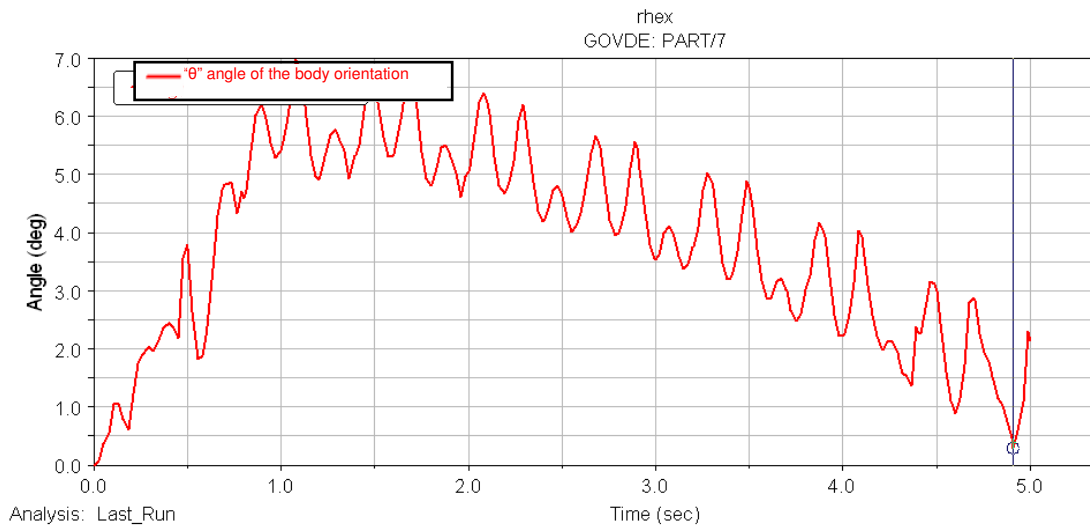


Figure 90 “θ” angle of the body orientation

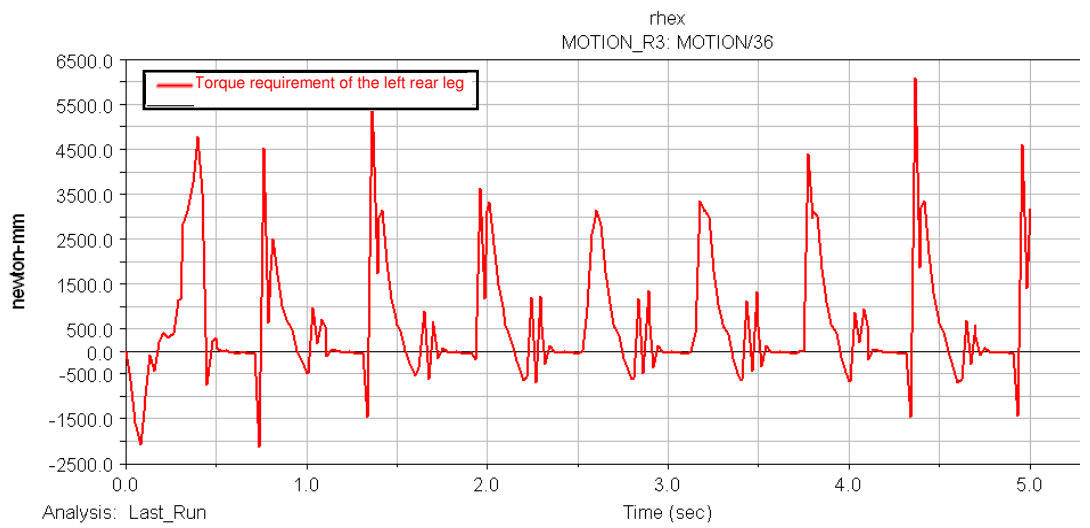


Figure 91 Torque requirement of the left rear leg

Finally the torque requirement of one leg is inspected (Figure 91). The peaks are exceeding 5000 Nmm. The torque profile is discussed in the previous section. The maximum torque requirements could be afforded by the motors sacrificing motor life and energy.

4.4. The effect of leg compliance

In section 3.3, modeling of the flexible legs is described. Figure 47 shows the material properties which define the mechanical behavior of the legs. The elastic modulus of the flexible legs is approximately 10 GPa. The simulation in the previous section is performed with a flexible leg whose elastic modulus is set to 7.5 GPa. In order to see the effect of the elastic modulus, the simulation is run twice again, first with 5 GPa and second 10 GPa elastic modulus value. The results are discussed in the following section.

4.4.1 Simulation run with 5 GPa Elastic Modulus

The four parameters which define the reference angular position of the left and right tripods are the same with the parameters in the previous section. The only difference is that the elastic modulus of the flexible leg is changed to 5 GPa.

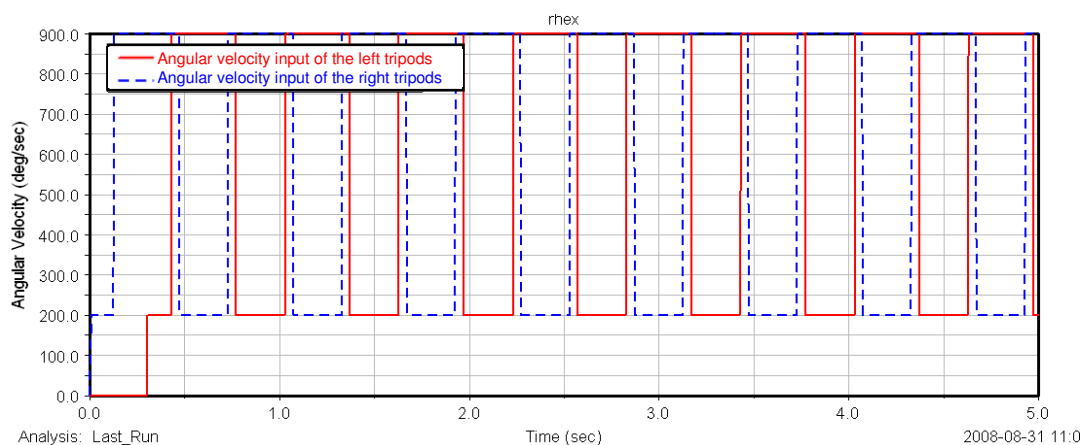


Figure 92 Angular velocity input of the left and right tripods

Figure 92 shows the angular velocity input of the right and left tripods which are the same with the inputs in the previous section.

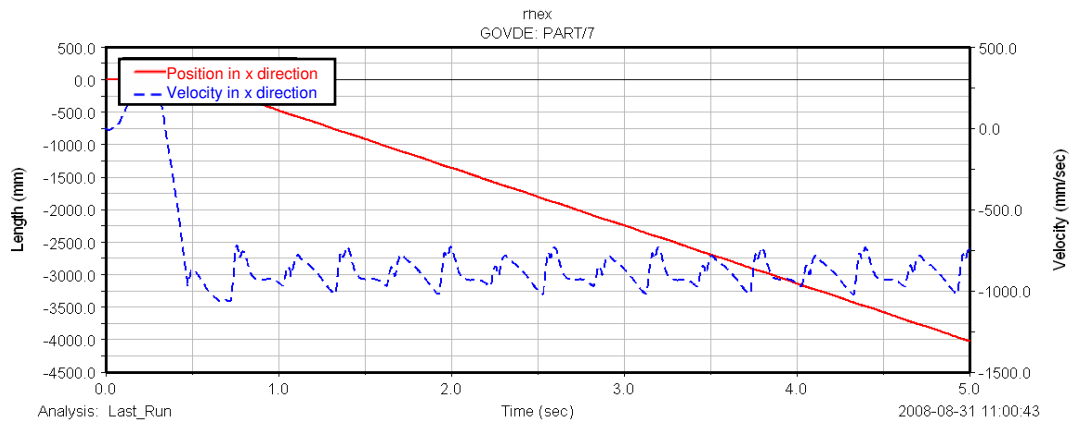


Figure 93 Position and velocity in x direction

The velocity in x direction shows the similar profile and it fluctuates between 730mm/s and 1020mm/s (Figure 93). The average velocity is approximately 880mm/s. The maximum, minimum and average velocity values are less than the previous run result. This means decreasing the elastic modulus value the average velocity of the robot will also decrease. In the following simulation the elastic value will be set 10 GPa. The resulting average velocity will be discussed. The expectation is that the velocity increases while increasing the elastic modulus value.

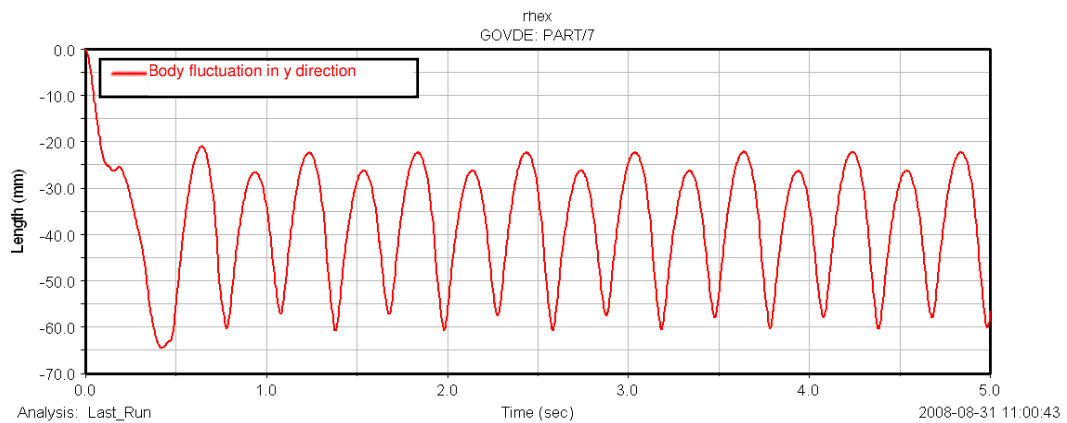


Figure 94 Body fluctuation in y direction

Figure 94 shows the height of the center of mass of the body during the simulation time. The center of mass fluctuates between -25mm and -60mm in y direction. The previous result represents a fluctuation of approximately 45mm while the fluctuation is 35mm now. As mentioned in the previous section there is a connection between the speed of the robot and the fluctuation of the body in y direction. The fluctuation increases when the robot speeds up.

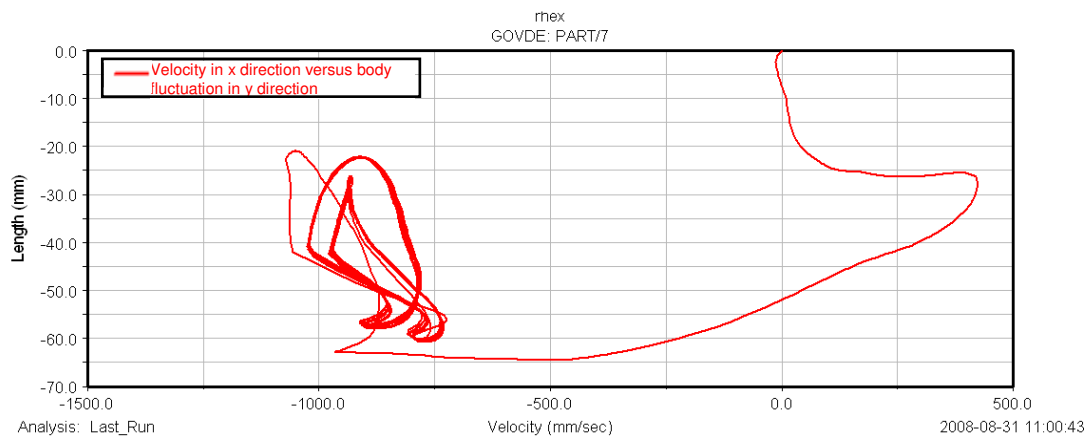


Figure 95 Velocity in x direction versus body fluctuation in y direction

The CM of the body fluctuates in the y direction between -25mm and -65mm. This fluctuation is related to the velocity in x direction. In order to show the relationship between the body fluctuation and the velocity in x direction a graph is drawn (Figure 95). This graph shows that every velocity value represents a point in the y direction and this path is periodic during the five seconds simulation. Dynamic stability property of RHex results in periodic and bounded phase diagrams.

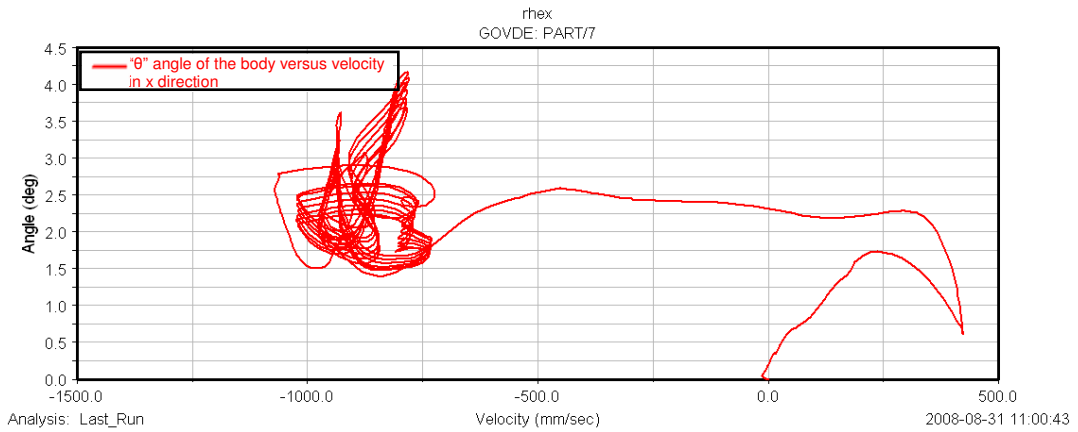


Figure 96 “ θ ” angle of the body versus velocity in x direction

Figure 96 is also a phase diagram, which shows the relationship between the Euler Angle “ θ ” of the body and the velocity in x direction. There is a deviation from the periodic path during the simulation when compared to the previous graph.

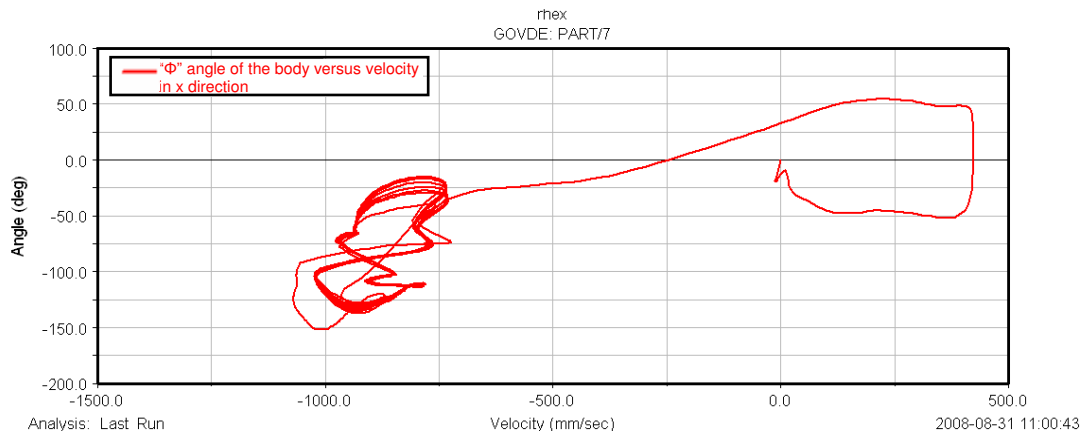


Figure 97 “ Φ ” angle of the body versus velocity in x direction

The above graph (Figure 97) is plotted for “ Φ ” Euler Angle of the body versus the velocity of RHex in “x” direction. The same path is repeated for the whole

simulation. This means that the behavior of robot is stable when the “ Φ ” angle parameter is concerned.

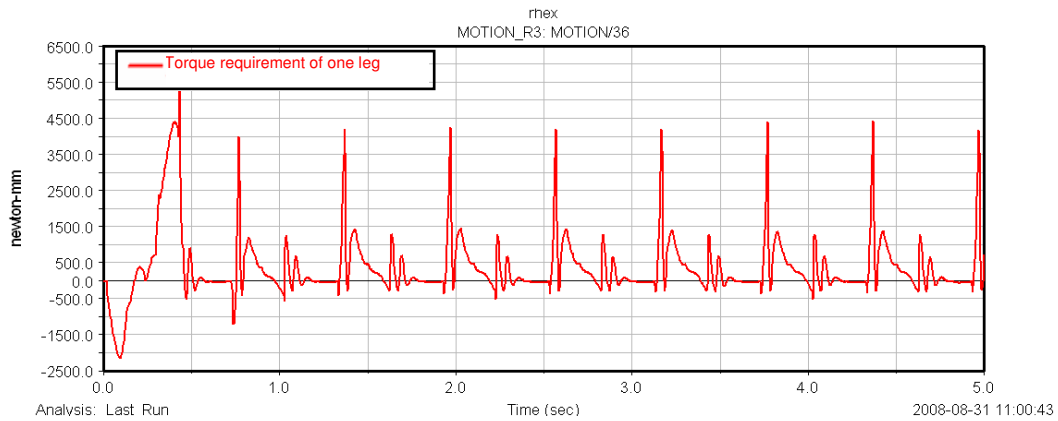


Figure 98 Torque requirement of one leg

Finally the torque requirement of the legs is inspected. The graph (Figure 98) shows the periodic torque profile of one leg. Comparing this result with the previous one, which is the result for 7.5 GPa elastic modulus, the profile is more stable. In Figure 91 the torque requirement of the leg does not repeat itself for every rotation. There are several peaks which are different for every rotation. Although the torque profile for the last simulation run has similar peaks the maximum values are the same.

4.4.2 Simulation run with 10 GPa Elastic Modulus

The last simulation run is performed for an elastic modulus value of 10 GPa. The effect of the elastic modulus property of the legs and the relationship of this property with the velocity, body fluctuation and torque requirements are studied for 5 GPa and 7.5 GPa. This simulation results will emphasize these dependencies.

The observation about the relationship between the elastic modulus value and velocity is that increasing the elastic modulus of the leg results in rise in the velocity. Figure 99 shows the velocity profile of the robot. As expected the maximum, minimum and average values of the velocity are increased. The minimum and maximum values are 720mm/s and 1120 mm/s, respectively. The average velocity is 1022 mm/s which is calculated with the same method.

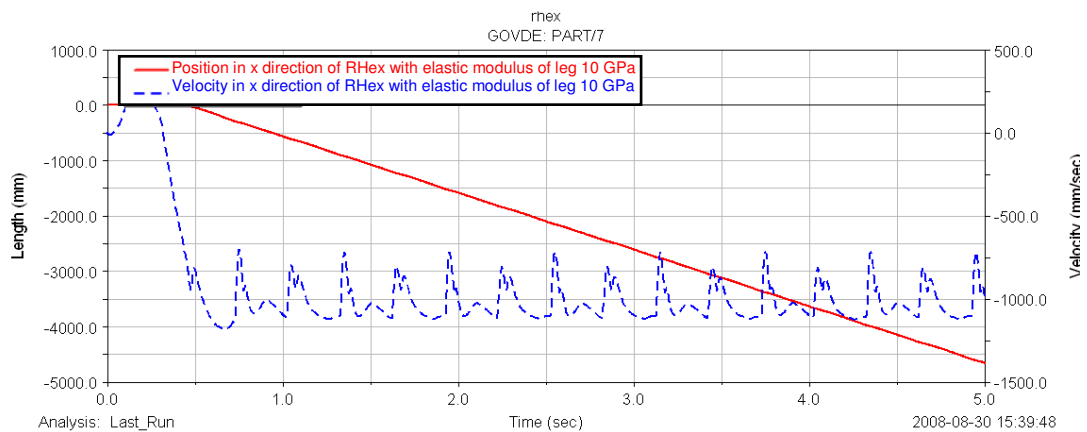


Figure 99 Position and velocity in x direction of RHex with elastic modulus of leg 10 GPa

Although there is an advantage of legs with high elastic modulus which is the speed up of the robot, the body fluctuation in the y direction increases when the elastic modulus gets higher.

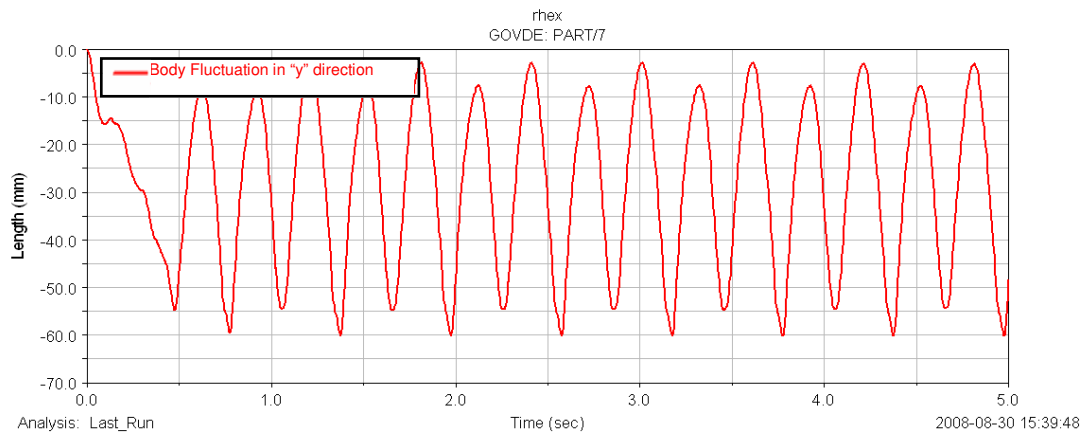


Figure 100 Body Fluctuation in “y” direction

Figure 100 shows the CM position of the body in y direction. The minimum and maximum values are -60mm and -3mm, respectively. So the resulting fluctuation is approximately 55mm, which is the highest value among the three simulation run. This fluctuation should be kept small for the structural integrity of the inner electronic parts. Therefore an optimization may be made concerning the velocity and body fluctuation.

Finally the torque requirement of one leg is considered. The result is also acceptable for this simulation run. The average velocity of the robot increases, when the elastic modulus of the leg increases, so it results in higher torque requirement. The torque requirement increases with the high elastic modulus value. The resulting periodic torque profile of one leg is shown in Figure 101.

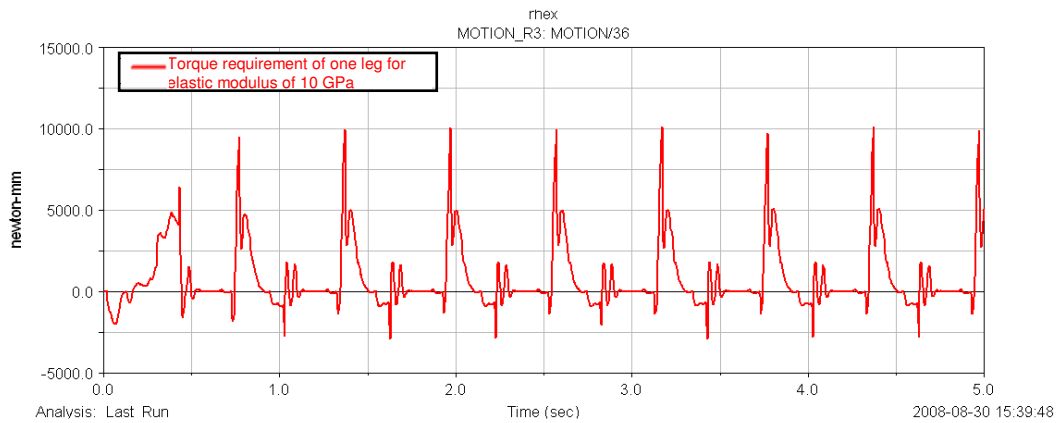


Figure 101 Torque requirement of one leg for elastic modulus of 10 GPa

The comparison of the three simulation results is shown in Figure 102. The observation is that increasing the elastic modulus of the leg results in increasing the velocity and this is confirmed by the three simulations. The theory could be explained with energy conservation. In the last example the elastic modulus of the leg is 10 GPa which means higher stiffness of the leg. The energy given to the system, actually to the legs, is converted to rotational motion. There is a portion of energy which is used to deform the legs. When the leg is stiffer the deformation is less. Therefore in this case there is more energy left which is converted to rotational motion.

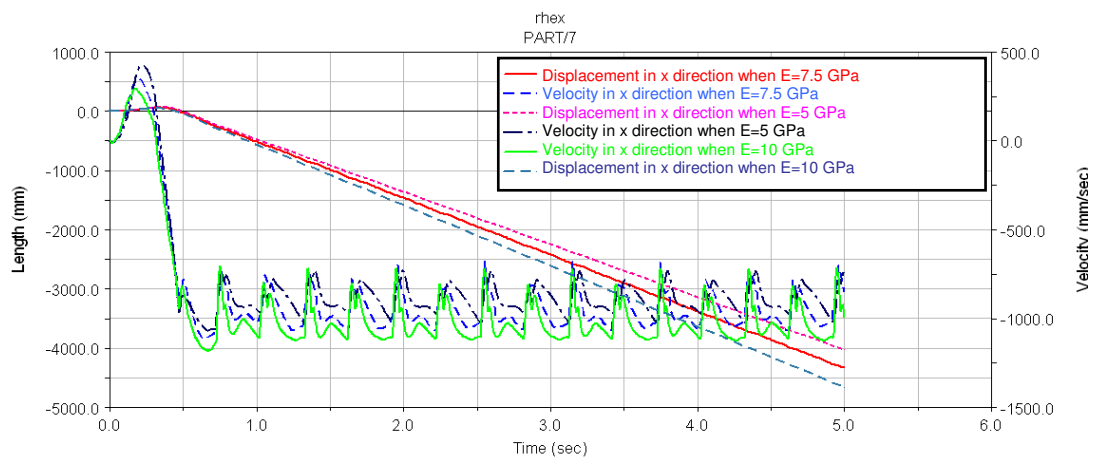


Figure 102 The velocity profile comparison of the three simulation results

4.5. The effect of t_{ratio} parameter

In previous chapter it is mentioned that the reference angle input is defined by means of several parameters. Here, t_c is the time for one leg to complete one revolution. The slow swing phase and fast swing phase times are represented t_s and t_f respectively. The rate of these two parameters, t_{ratio} , is changed in order to see the effect of this parameter while the other three parameters are kept same which are Φ_s , t_c and Φ_s .

4.5.1. Simulation study with $t_{ratio}= 0.5$

The parameters are set as in the table below and the resulting step input function of the right and left tripods are calculated and given in Appendix C.

$\Phi_s: 0.9$	$t_c: 0.6$	$t_{ratio}: 0.5$	$t_f: 0.4$
$t_s: 0.2$	$\Phi_0: 0$	$t_0: 0$	

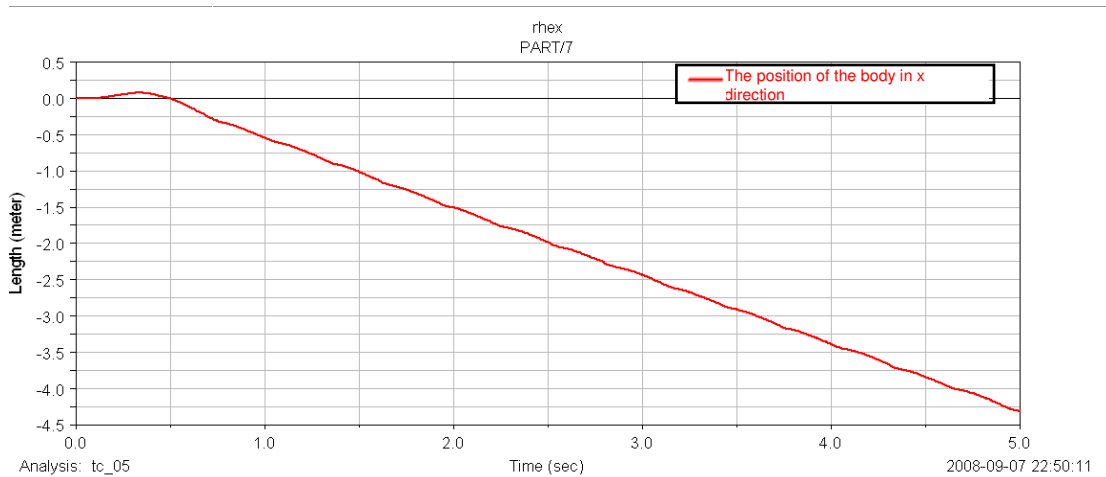


Figure 103 The position of the body in x direction

The simulation result (Figure 103) shows that RHex travels approximately 4300 mm at the end of 5 seconds. The average velocity is calculated as

943mm/s. This value is considerably high when compared with the other simulation results.

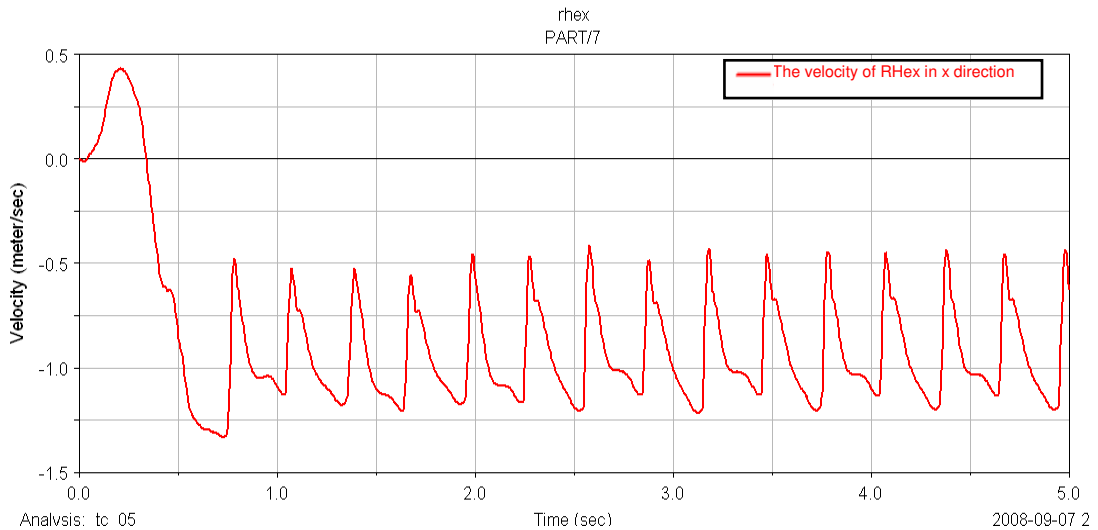


Figure 104 The velocity of RHex in x direction

The velocity profile of RHex is plotted in Figure 104. Maximum velocity of the body is 1210 mm/s while minimum velocity is 430 mm/s. This periodic velocity profile proves that RHex walks in a stable fashion during the 5s. simulation.

Another important characteristic of the robot is the position of the body in the y direction. This represents the body fluctuation. As mentioned in the previous sections the fluctuation is important because the vibration of the robot is undesirable.

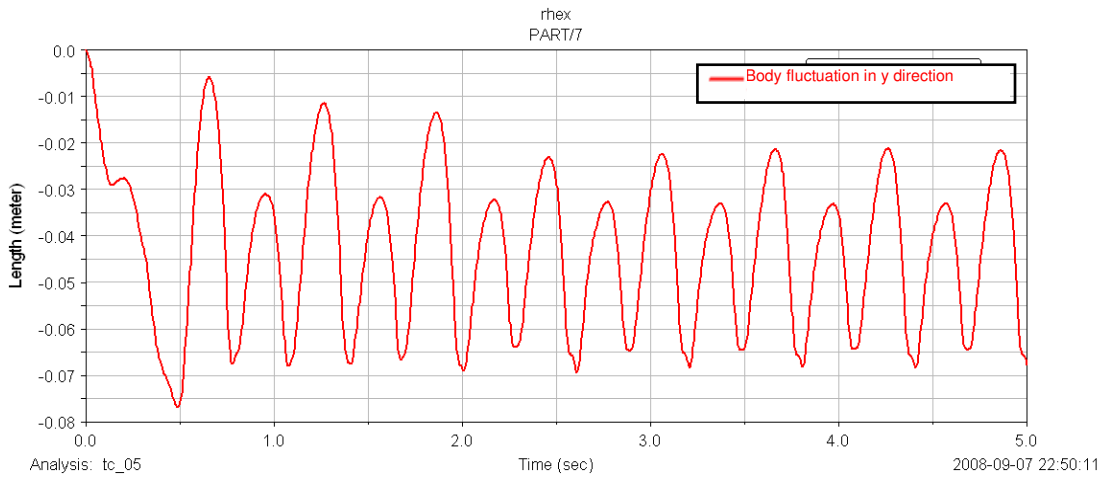


Figure 105 Body fluctuation in y direction

The body fluctuation in y direction is plotted in Figure 105. The center of mass of RHex travels between 20mm and 70mm in y direction. This result shows resemblance with the previous study. The average velocity was 1020 mm/s and the fluctuation is 55mm in y direction. The velocity of RHex in x direction is proportionally related with the body fluctuation in y direction.

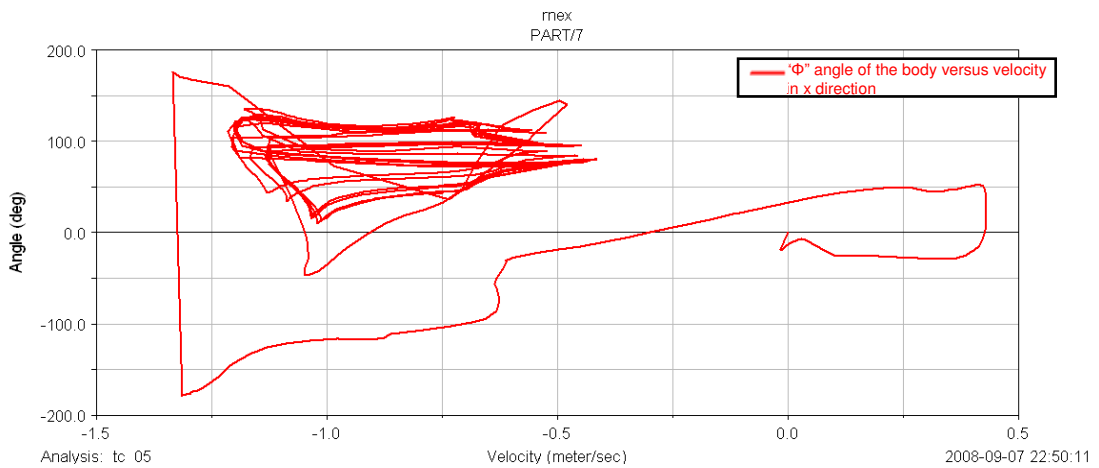


Figure 106 “Φ” angle of the body versus velocity in x direction

Figure 106 and Figure 107 show the variation of “Φ” and “θ” angles versus velocity in x direction. It is expected that the same path is observed for every cycle. In this case, the path which is followed every cycle changes slightly.

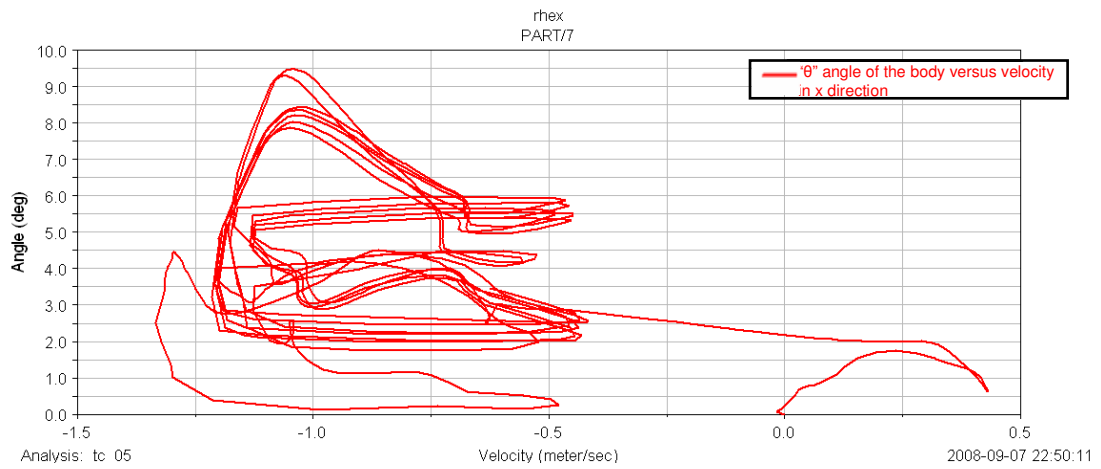


Figure 107 “θ” angle of the body versus velocity in x direction

4.5.2. Simulation study with $t_{ratio} = 1$

The parameters are set as in the table below and the resulting step input function of the right and left tripods are calculated and given in Appendix D.

$\Phi_s: 0.9$	$t_c: 0.6$	$t_{ratio}: 1$	$t_f: 0.3$
$t_s: 0.3$	$\Phi_0: 0$	$t_0: 0$	

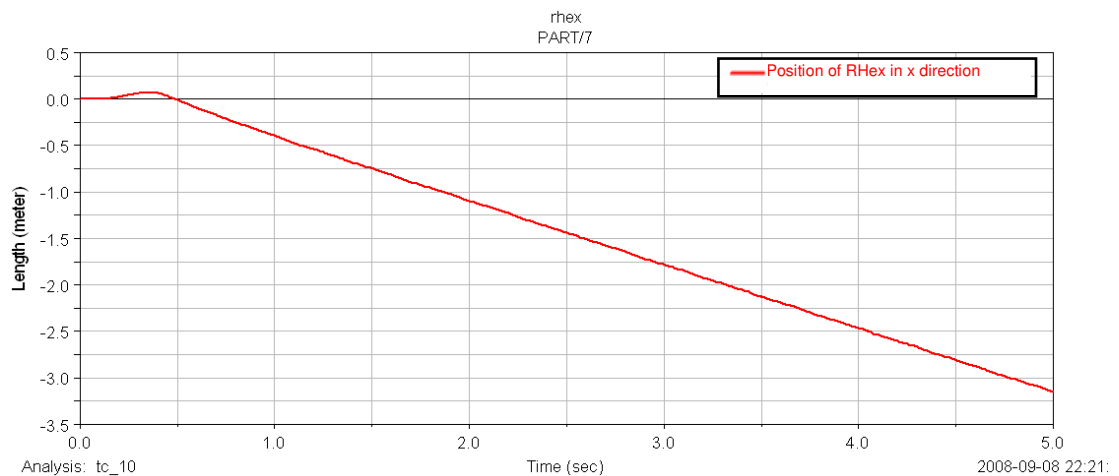


Figure 108 Position of RHex in x direction

The only difference between the previous and this simulation is the t_s and t_f times. The rate of the slow and fast swing phase is increased from 0.5 to 1. So t_s and t_f are equal when t_{ratio} is 1. This means the time passed to complete slow phase increased. The step input function with t_{ratio} equals to 1 results in traveling RHex 3200mm in 5 seconds in x direction (Figure 108).

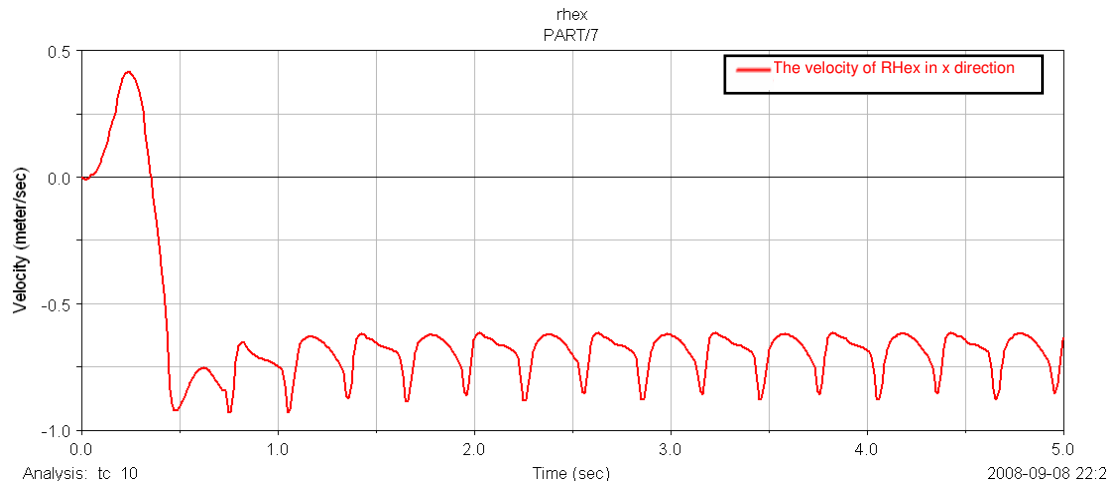


Figure 109 The velocity of RHex in x direction

The maximum velocity that RHex reaches is 880 mm/s and the minimum value of the velocity is 610 mm/s (Figure 109). The rate of slow swing phase and fast swing phase is increased, so the average velocity of the robot decreased to approximately 690mm/s.

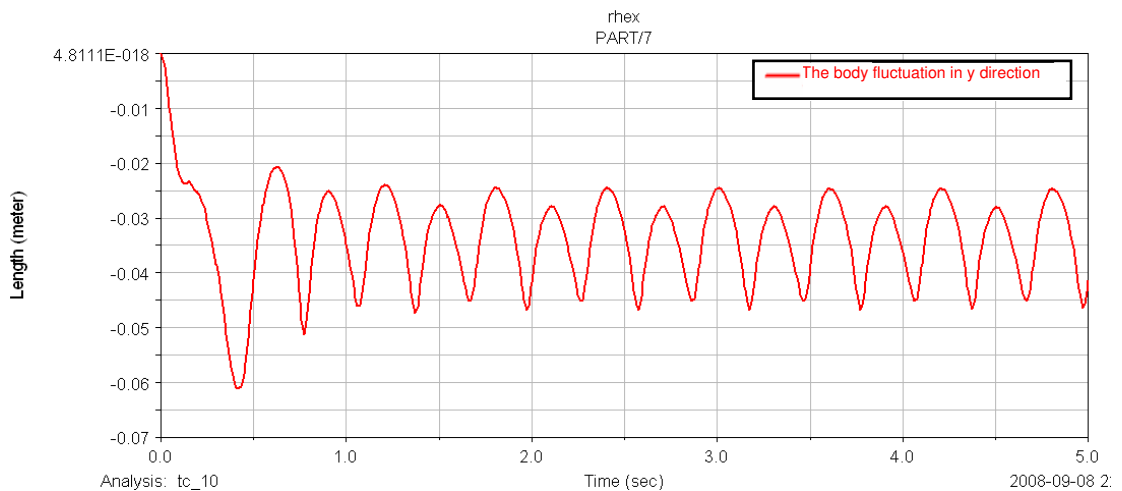


Figure 110 The body fluctuation in y direction

The position of the center of mass changes from 23 mm to 47mm. The body fluctuation is approximately 25mm. This result is an expected one. If the velocity of the robot increases, the fluctuation in y direction also increases.

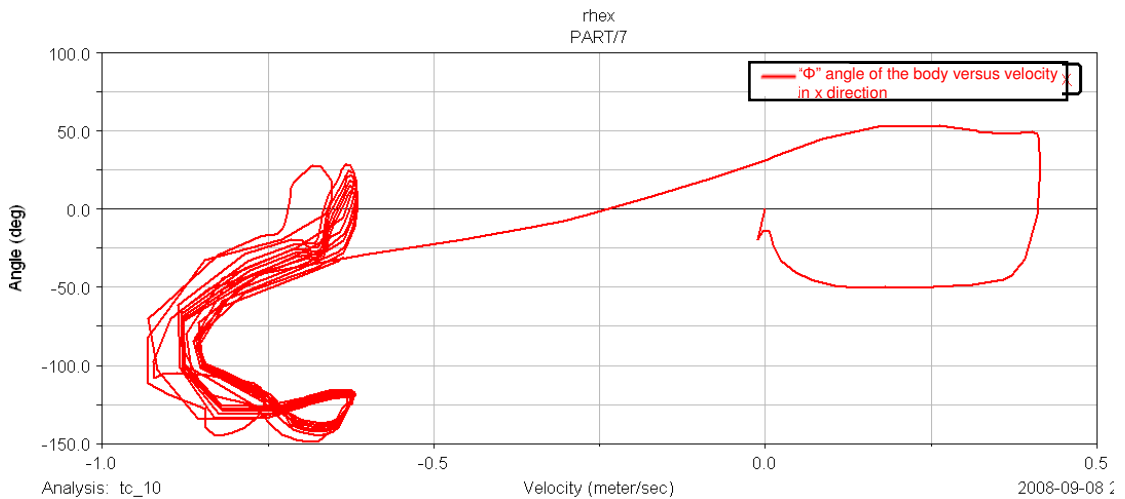


Figure 111 “ Φ ” angle of the body versus velocity in x direction

The relationship between “ Φ ”, “ θ ” angles and velocity in “x” direction are represented in Figure 111 and Figure 112, respectively. The path does not change in the “ Φ ” angle graph when compared to the “ θ ” angle graph.

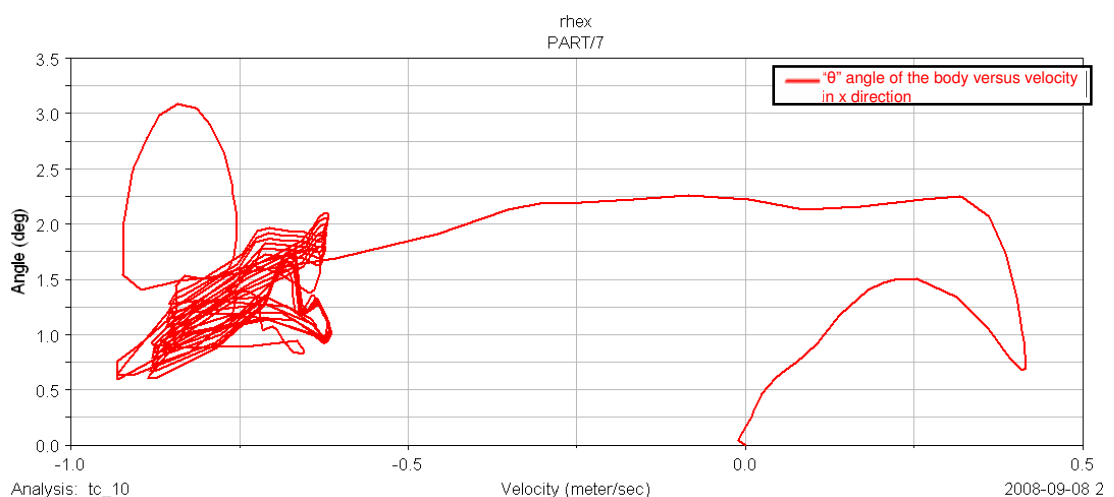


Figure 112 “ θ ” angle of the body versus velocity in x direction

4.5.3. Simulation study with $t_{ratio} = 1.5$

The parameters are set as in the table below and the resulting step input function of the right and left tripods are calculated and given in Appendix E.

$\Phi_s: 0.9$	$t_c: 0.6$	$t_{ratio}: 1.5$	$t_f: 0.24$
$t_s: 0.36$	$\Phi_0: 0$	$t_0: 0$	

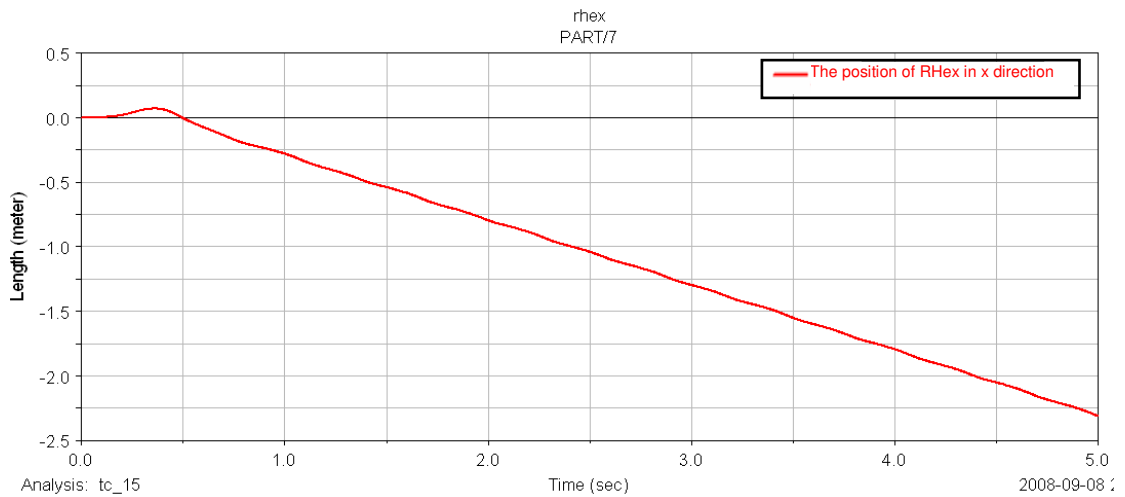


Figure 113 The position of RHex in x direction

Figure 113 shows the displacement of RHex in x direction. As “ t_{ratio} ” parameter is increased the total displacement and the velocity of the robot has decreased. The position of RHex at the end of 5 seconds simulation is approximately 2300mm. The results of the previous studies are 4300mm and 3200mm respectively.

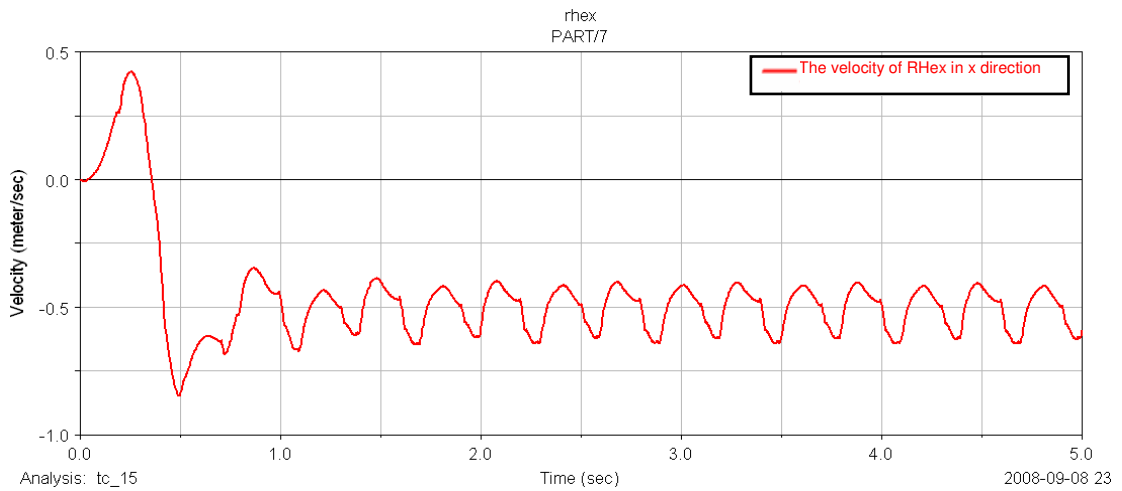


Figure 114 The velocity of RHex in x direction

The lowest velocity has occurred in this simulation. The minimum and maximum velocities are 410mm/s and 640mm/s respectively. The previous velocity results are 943 mm/s and 690 mm/s while the last study result is 508 mm/s.

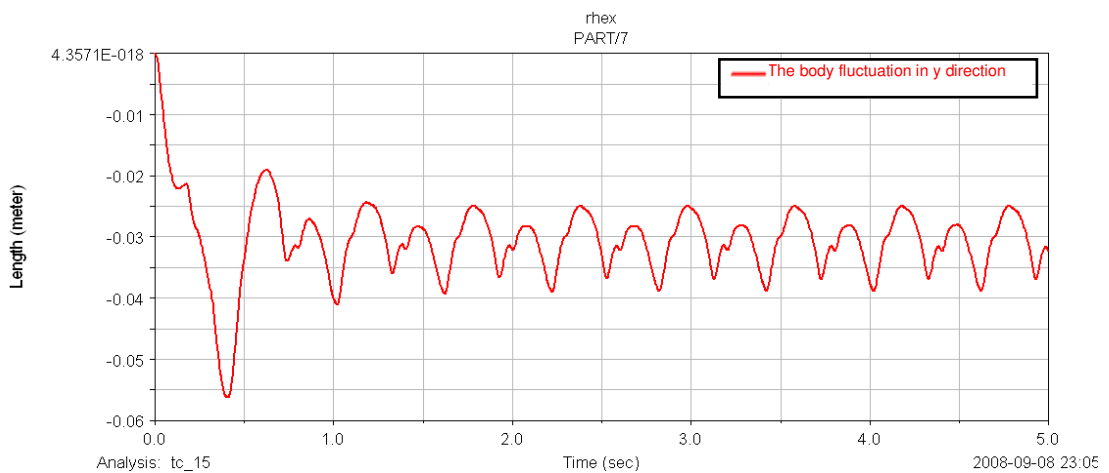


Figure 115 The body fluctuation in y direction

The displacement of the center of mass is shown in Figure 115. In this case the total displacement is approximately 15mm which is the lowest result among the last three simulations. The relationship between velocity and body fluctuation is shown one more time, decreasing the velocity results in decrease of the body fluctuation.

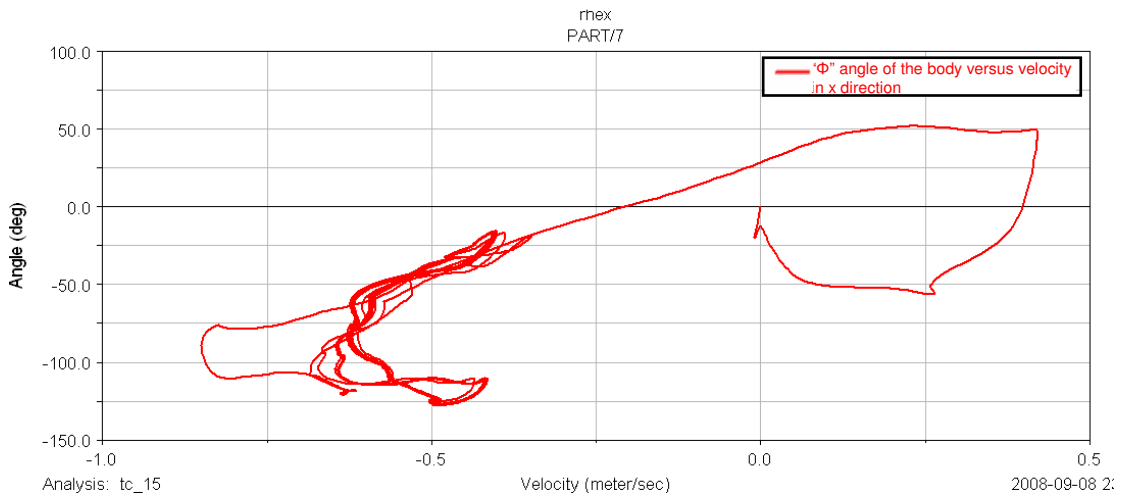


Figure 116 “ Φ ” angle of the body versus velocity in x direction

Figure 116 and Figure 117 show how the “ Φ ” and “ θ ” angles of the body are related with the speed of the robot. The paths, which are observed for every revolution of the legs, are almost the same.

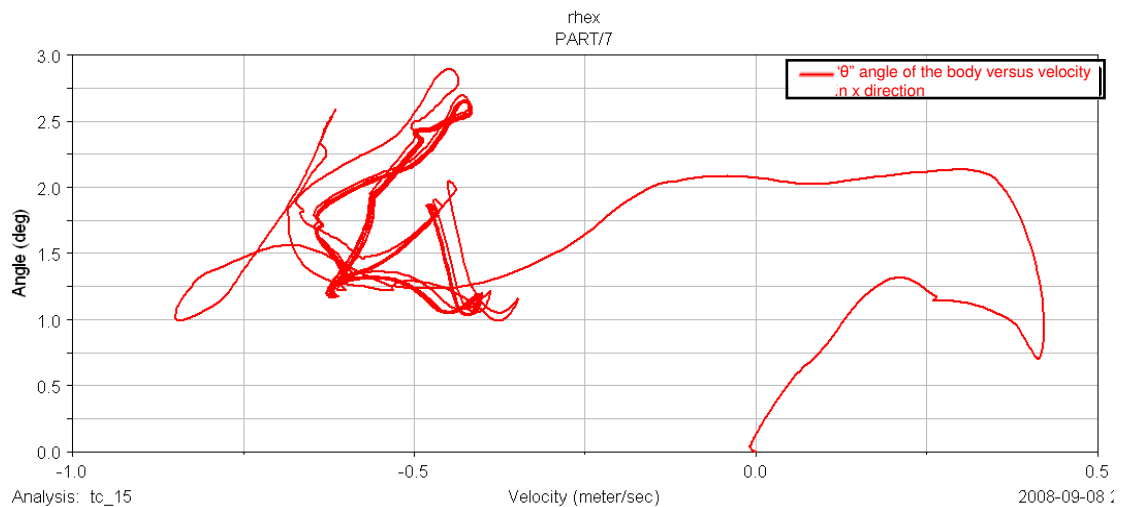


Figure 117 “ θ ” angle of the body versus velocity in x direction

4.5.4. Comparison of the three simulation results

In chapter 4.5, the effect of the “ t_{ratio} ” parameter is inspected. Three different value of this parameter is set while the other parameters are kept

unchanged. The simulation studies are made with 0.5, 1 and 1.5 t_{ratio} values in sequence.

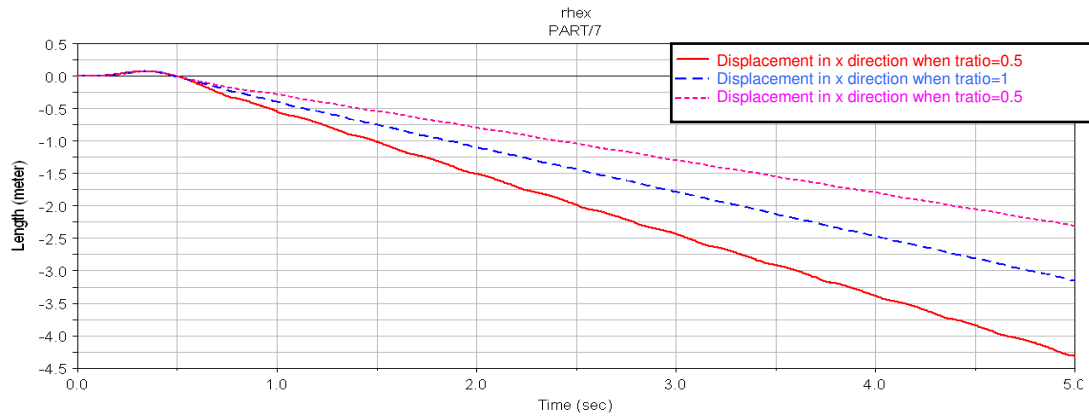


Figure 118 The comparison of the displacement in x direction

Figure 118 shows the relationship between the displacement in x direction and t_{ratio} parameter. The position of the robot in x direction at the end of the 5 seconds simulation increases when t_{ratio} decreases. The t_{ratio} parameter means the rate of slow swing time over fast swing time. The complete one cycle time t_c has not changed for these three simulations, so decreasing t_{ratio} means decreasing the slow swing time and increasing the fast swing time. It is obvious that when the slow phase time decreases the robot's velocity in x direction will increase. Although there is a proportional relationship between these two parameters there should be a lower limit. Figure 119 shows the velocity comparison of these three simulation results. Since the first simulation has run with t_{ratio} parameter equals 0.5, the result of that simulation is the fastest one. But one should note that the difference between the maximum and minimum velocity value is highest in this simulation. This means more fluctuation in velocity profile. Therefore there should be an optimum point that the velocity is high enough and the tripod walking is stable.

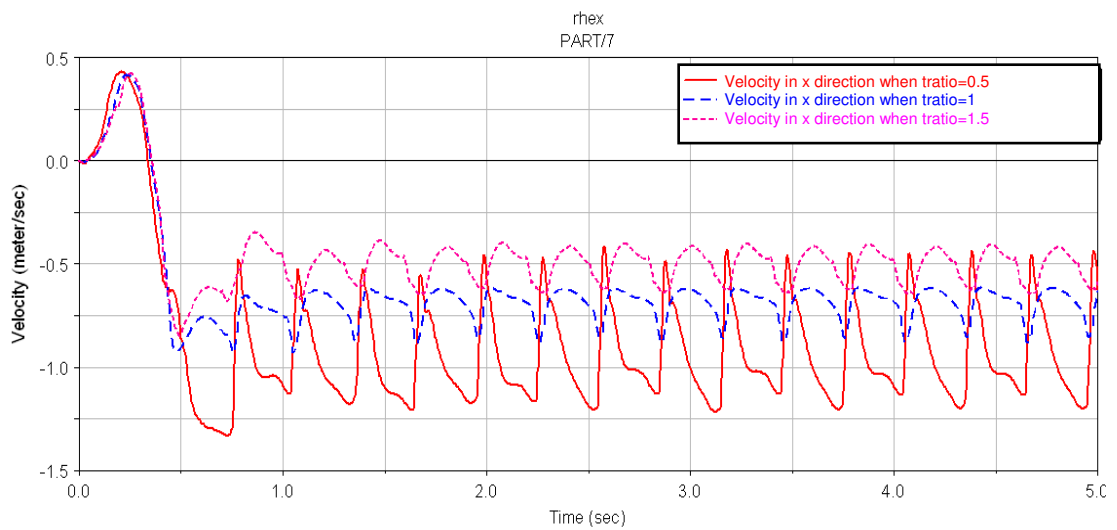


Figure 119 The comparison of the velocity in x direction

Finally the body fluctuation will be discussed. The relationship between the velocity and the body fluctuation is proportional. The results are consistent with this relationship. Decreasing the t_{ratio} parameter increases the velocity of the robot. Increased velocity results in more vibration of the body. The three results of the body fluctuation is plotted in the same graph in Figure 120. The movement of the center of mass is higher when the speed of the robot increases.

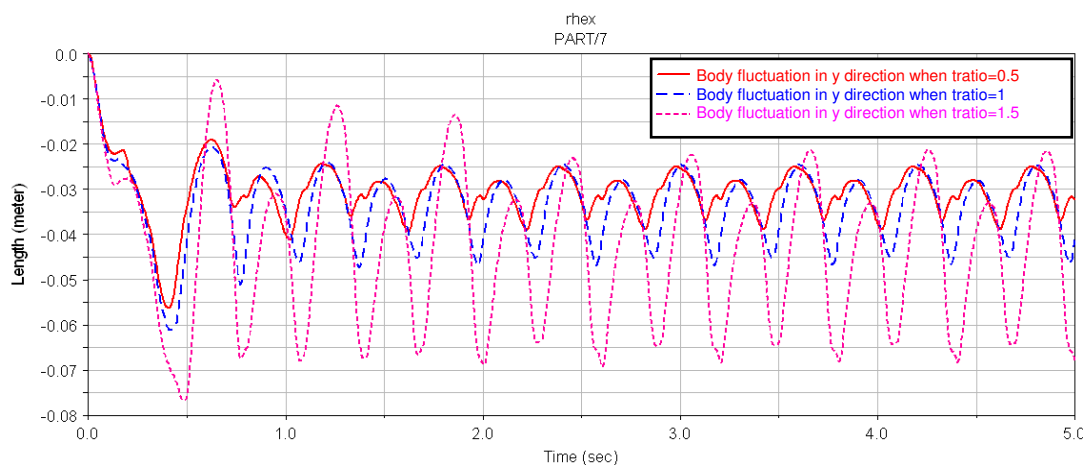


Figure 120 The comparison of the body fluctuation in y direction

4.6. The effect of Φ_s parameter

So far the validation of the dynamic model is made with the parameters and results in literature. Then a stable tripod walking profile is simulated. Using this profile, the effect of the elastic modulus of the legs is studied. Finally the effect of t_{ratio} parameter is observed. Now the effect of Φ_s parameter will be inspected. The parameters in the previous runs are $t_c = 0.6$ s, $\Phi_s = 0.9$ rad, $t_{ratio} = 0.75$ s and $\Phi_0 = 0$ rad. In order to see the effect of Φ_s parameter, it is set to 0.3 rad. Φ_s is the angle which is swept by leg in the slow swing phase. The other parameters are kept unchanged so decreasing the Φ_s angle will also decrease the angular velocity of the slow phase. This means the angular velocity of the fast phase increases.

Φ_s : 0.3	t_c : 0.6	t_{ratio} : 0.75	t_f : 0.342857
t_s : 0.257143	Φ_0 : 0	t_0 : 0	

The above functions are the new inputs of the legs. The angular velocity of the slow phase is decreased while the angular velocity of fast phase increased. The angular velocities of left and right tripods are shown in Figure 121.

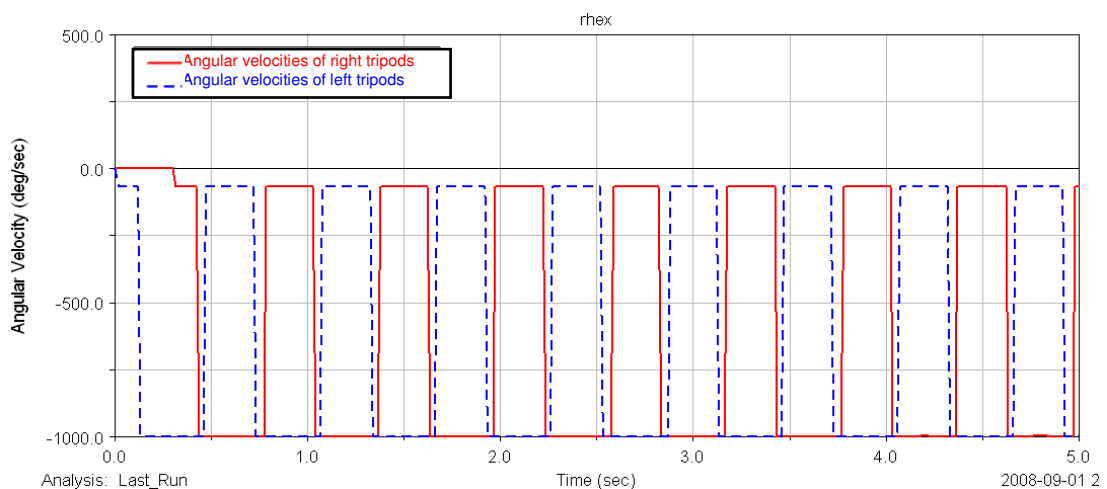


Figure 121 Angular velocities of left and right tripods

Figure 122 shows the velocity and position of the robot in x direction during the simulation. The velocity profile fluctuates between 405mm/s and 610mm/s and the average velocity is approximately 450mm/s. The only difference between the previous parameters and current parameters is Φ_s which is the angle, swept by leg in the slow swing phase. The sharp decrease in the velocity of robot could be only explained by the decrease in Φ_s parameter.

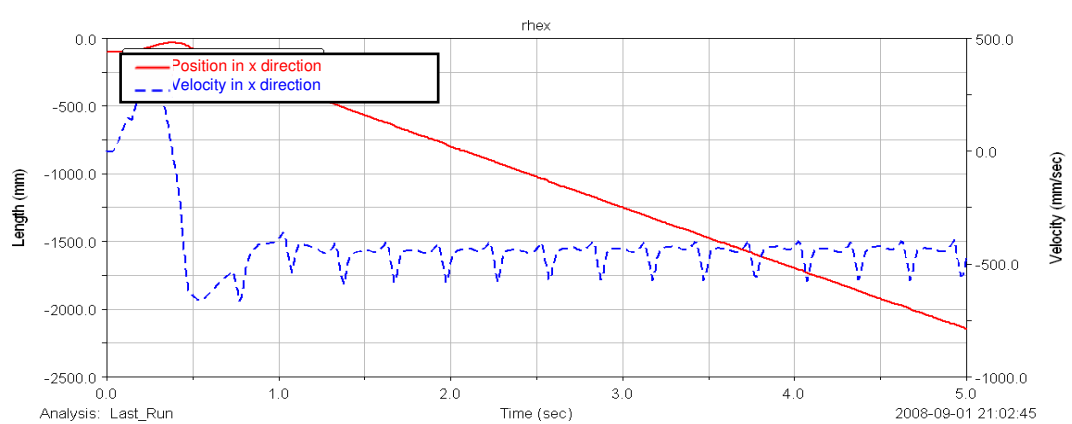


Figure 122 Position and velocity in x direction

The angular velocities in the slow and fast phase of the leg are 200deg/s and 700deg/s, respectively for previous parameters. The new velocities are 66deg/s and 933deg/s. The velocity of the robot has decreased dramatically when the angle which is swept by the slow phase is changed.

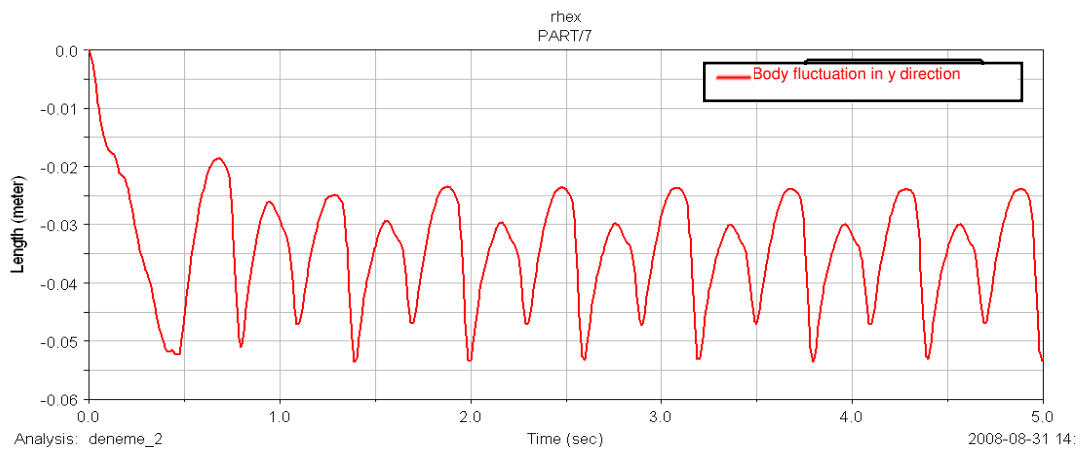


Figure 123 Body fluctuation in y direction

The position of the body fluctuates between -25mm and -55 mm (Figure 123). The total vibration is about 30mm. This is comparable with the previous results. The speed of the robot has decreased, so the vibration is also decreased.

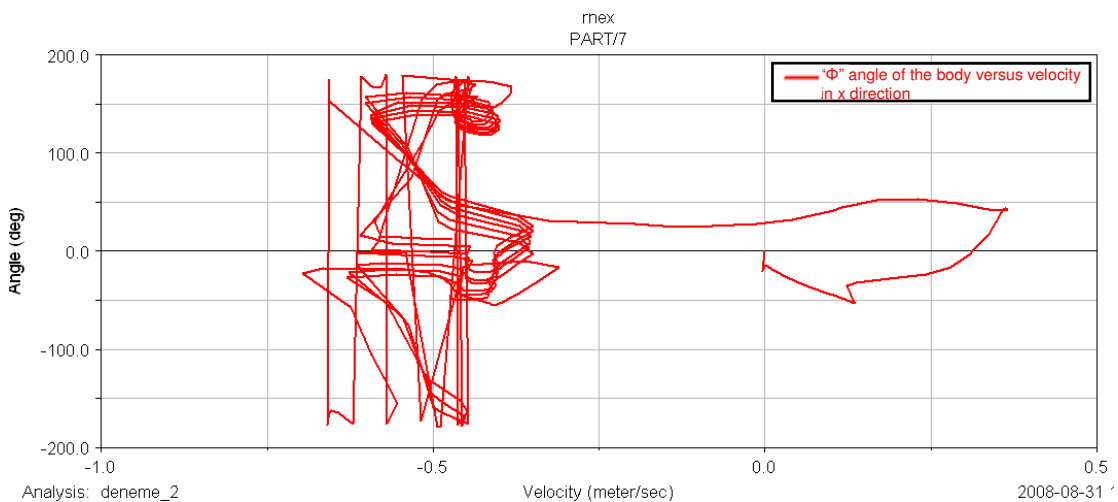


Figure 124 "Φ" angle of the body versus velocity in x direction

Figure 124 and Figure 125 show the variation of "Φ" and "θ" Euler Angles of the body versus velocity in "x" direction, respectively. The paths are not similar. It could be seen that they have changed for every cycle and the graph moves upward.

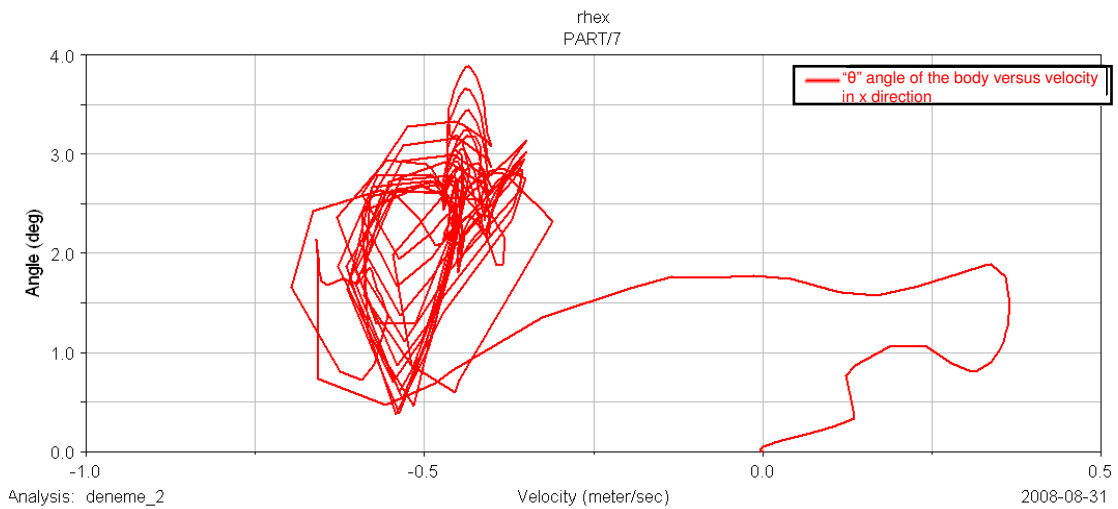


Figure 125 “ θ ” angle of the body versus velocity in x direction

Figure 126 is a captured picture from the simulation and shows the start of the slow phase. The touching point of the leg to the ground is very close to the end. RHex could roll only a few degrees over the legs because of this situation. Therefore the velocity in x direction is sharply decreased. The start of the slow phase in the previous simulation is investigated. The touching point is approximately the center of the half circle. So the rolling motion is more than in the current run.

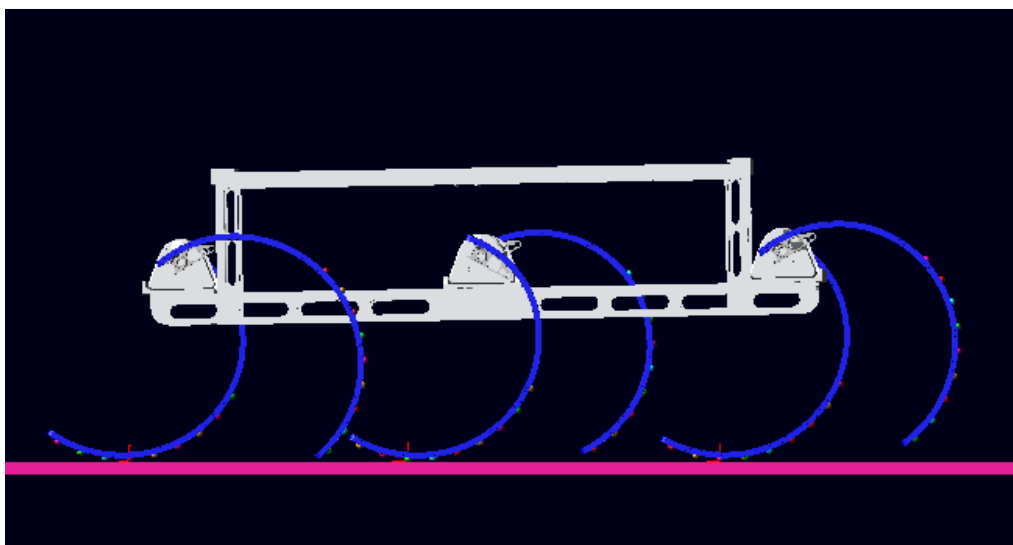


Figure 126 Screenshot of the start of the slow phase

Although RHex is a legged robot, because of the half circular shape and the mounting type to the hip assembly, the legs could act as wheels. The touching point of the leg to the ground could be changed, adjusting the four parameters, especially Φ_s . The last two simulations show that further is the touching point from the end faster is the robot. The legs act as wheels when they touch to the ground at the center of the half circle. In the literature survey it is mentioned that the wheeled robots are faster and energy efficient than the legged robots. These two advantages of the wheeled robots could be used in RHex by choosing appropriate parameters which result in the legs act like wheels.

So far three important parameter effects are discussed. The first one is the elastic modulus of the flexible leg. The result of the three simulations is that increasing the elastic modulus of the leg which means harder the leg is, faster is the robot. On the other hand the body fluctuation of the robot in y direction increases. This is a disadvantage because the inner electronic components are vibrating more. Therefore an optimization should be made. Secondly t_{ratio} parameter effect is studied. The time which is passed to complete slow and fast swing phase affects the stability and speed of the robot directly. The last parameter whose effect is studied is the angle swept by the leg in the slow phase. Φ_s parameter is changed such that the velocity of the robot decreases sharply. The simulation result shows the importance of the touching point of the leg to the ground. This parameter should be adjusted such that the touching point is far from the end of the leg results in the leg acts like wheel. So the speed and efficiency of the robot increases.

CHAPTER 5

CONCLUSION

The aim of this study is to build a virtual prototype of RHex robot. As is known, RHex is a hexapod robot with flexible legs, which are manufactured from composite material with a special process. Therefore the dynamic model of RHex should include compliant parts. This means a dynamic simulation program should interact with a finite element software. MSC ADAMS is used in order to build the dynamic model. The flexible members are added with the use of MSC PATRAN and MSC NASTRAN programs. At this stage the flexible multi body dynamic model is ready to simulate RHex. Finally it is needed to control the robot with a control structure. The real case could be fully simulated after completing the ADAMS – MATLAB interaction. A closed loop control structure is built in MATLAB, which also includes the motor model.

First, the model is tested with the results in literature. In this case MATLAB interaction is not included, because the validation of the model should be made. The parameters in literature are set and a simulation run has been performed. The results in literature are for the previous version of RHex. The differences are that the body dimensions, motors, weight and flexible leg dimensions and properties have been changed. The simulation results are comparable with results in literature considering the version difference of the robot.

Second, MATLAB program is included as a closed loop controller. In that case the solver types and step times are very important. The synchronization of the two programs should be adjusted very carefully. Otherwise the

controller could not be able to follow the reference angular velocity. ADAMS software has only one solver type, fixed step. There are two choices. One is that MATLAB solves the dynamic model and the controller equations. The second choice is that ADAMS solves the dynamic model and MATLAB deals with the controller part. The two choices are tried to simulate the dynamic model. In both cases step time should be less than 0.00005s. This results in enormous number of equations and huge simulation time. A “3s. simulation” is performed in order to see that the controller could follow the reference angular position input accurately. Although the result is satisfactory, the error between the real and reference angular position is less than 0.01 rad., the total simulation has taken place in approximately 3 days. Therefore the other simulation trials do not include MATLAB, closed loop controller.

A stable tripod walking parameter set is found and used for inspecting the effect of the elastic modulus of the flexible legs. The elastic modulus of the flexible legs is calculated as 10 GPa. Three simulations are performed with three different elastic modulus values, 5 GPa, 7.5 GPa, 10 GPa. The results show that if the elastic modulus is higher, the velocity of the robot would increase. Another observation is about the body fluctuation. The position of the center of mass is plotted. This parameter is important because vibration of the electronic components is not wanted. The plotted graphs show the speed of the robot is directly related with the body fluctuation. When the speed of the robot increases, so does the fluctuation. Therefore an optimization can be made here. In these three case studies, the torque requirements are observed. MATLAB is not included for these simulations; so it is assumed that the reference angular position is exactly followed and motor torque is unlimited. Therefore torque graphs are very important. The torque speed curve of the motor is used as a reference in order to see that the torque requirement could be afforded by the motors. It is seen that the peaks of the torque graphs is less than the motor maximum torque. So, as a result, if MATLAB was included in this simulation there should be minimal differences in the behavior of the robot.

Another parameter, t_{ratio} , is inspected in order to see its effect. Actually the four parameters which are used to define the reference angular position are t_c , t_s , Φ_s , Φ_0 . " t_{ratio} " is not one of them. It is the ratio of the slow swing time, t_s , over fast swing time, t_f . A meaningful parameter is tried to derive. This ratio is set 0.5, 1 and 1.5 respectively and three simulations are performed. The results are inspected to comment on the effect of this parameter. The increase of t_{ratio} parameter means decreasing the fast swing time. Although the time which is passed to complete one revolution of the leg, t_c , is kept unchanged, decreasing t_{ratio} parameter results in increase of the speed of the robot. It is related with the difference between slow and fast swing angular velocities. If this difference increases, the speed of the robot decreases dramatically.

Finally the effect of Φ_s parameter is inspected. This parameter defines the angle which is swept by the slow swing phase. It is more related with the touching point of the leg to the ground. So far Φ_s parameter is used as 0.9 rad. and in this trial the parameter is set to 0.3 rad. In this case the touching point of the leg to the ground is very close to the end of the leg. This results in decreasing of the speed of the robot. Farther the touching point from the end of the leg, higher is the velocity in "x" direction. At this stage, the rolling motion increases the speed of the robot.

So far a virtual prototype of RHex robot is built and the validation of this model is done. Then a stable tripod walking parameter set is found. The effects of leg stiffness, t_{ratio} and Φ_s parameters are inspected using the stable parameter set, while the other parameters are kept unchanged. The behavior of the RHex robot is observed under different circumstances.

For future work the refinement of this model could be made in order to decrease the simulation time. In that case a mathematical approach could be used in order to find the most efficient stable tripod walking parameters with running multiple simulations.

REFERENCES

- [1] Manuel F. Silva and J.A. Tenreiro Machado. A Historical Perspective of Legged Robots. *Journal of Vibration and Control* 2007; 13; 1447
- [2] Rosheim M. E., 1994, *Robot Evolution: The Development of Anthrobotics*, 1st edition, Wiley, New York
- [3] K. J. Waldron and V. J. Vohnout. Configuration design of the Adaptive Suspension Vehicle. *International Journal of Robotics Research*, 3(2):37{48, 1984
- [4] Saranli, U., *Dynamic locomotion with a Hexapod Robot*, A dissertation submitted in partial fulfillment of the requirements for the degree of Doctor of Philosophy, Computer Science and Engineering in The University of Michigan, 2002
- [5] Bekker, M. G., 1960, *Off-The-Road Locomotion*, University of Michigan Press, Ann Arbor, MI.
- [6] Kaneko, M., Mizuno, A. and Harada, K., 2002, "Torque distribution for achieving a hugging walk," in *Proceedings of the 2002 IEEE/RSJ International Conference on Intelligent Robots and Systems*, Lausanne, Switzerland, September 30–October 4, pp. 2613–2618
- [7] Yang, J.-M. and Kim, J.-H., 1998, "A strategy of optimal fault tolerant gait for the hexapod robot in crab walking," in *Proceedings of the 1998 IEEE International Conference on Robotics and Automation*, Leuven, Belgium, May 16–20, pp. 1695–1700

- [8] Hirose, S. and Kato, K., 1998, "Development of quadruped walking robot with the mission of mine detection and removal – proposal of shape-feedback master-slave arm," in Proceedings of the 1998 IEEE International Conference on Robotics and Automation, Leuven, Belgium, May 16–20, pp. 1713–1718
- [9] Lee, Y.-J. and Hirose, S., 2000, "Three-legged walking for fault tolerant locomotion of a quadruped robot with demining mission," in Proceedings of the 2000 IEEE/RSJ International Conference on Intelligent Robots and Systems, Takamatsu, Japan, October 30–November 5, pp. 973–978
- [10] Yang, J.-M., 2003, "Fault-tolerant gait generation for locked joint failures," in Proceedings of the 2003 IEEE International Conference on Systems, Man and Cybernetics, Washington, DC, USA, October 5–8, pp. 2237–2242.
- [11] Spenneberg, D., McCullough, K., and Kirchner, F., 2004, "Stability of walking in a multilegged robot suffering leg loss," in Proceedings of the 2004 IEEE International Conference on Robotics and Automation, NewOrleans, LA, April 26–May 1, pp. 2159–2164
- [12] Nonami, K. and Huang, Q.-J., 2001, "Humanitarian mine detection six-legged walking robot COMET-II with two manipulators," in Proceedings CLAWAR'2001 – 4th International Conference on Climbing and Walking Robots, Karlsruhe, Germany, September 24–26, pp. 989–996.
- [13] Ihme, T., 2003, "Posture control and distributed force sensing for technical applications of walking robots," in Proceedings of the ICAR 2003 – 11th International Conference on Advanced Robotics, Coimbra, Portugal, June 30–July 3, pp. 1032–1037.

[14] Takita, K., Katayama, T., and Hirose, S., 2003, "Development of dinosaur-like robot TITRUS—the efficacy of the neck and tail of miniature dinosaur-like robot TITRUS-III," in Proceedings of the 2003 IEEE International Conference on Robotics and Automation, Taipei, Taiwan, September 14–19, pp. 2466–2471.

[15] Hirose, S. and Kato, K., 1998, "Development of quadruped walking robot with the mission of mine detection and removal – proposal of shape-feedback master-slave arm," in Proceedings of the 1998 IEEE International Conference on Robotics and Automation, Leuven, Belgium, May 16–20, pp. 1713–1718.

[16] Omata, T., Tsukagoshi, K., and Mori, O., 2002, "Whole quadruped manipulation," in Proceedings of the 2002 IEEE International Conference on Robotics and Automation, Washington, DC, May 11–15, pp. 2028–2033.

[17] Takahashi, Y., Arai, T., Mae, Y., Inoue, K., and Koyachi, N., 2000, "Development of multi-limb robot with omnidirectional manipulability and mobility," in Proceedings of the 2000 IEEE/RSJ International Conference on Intelligent Robots and Systems, Takamatsu, Japan, October 30–November 5, pp. 2012–2017.

[18] Koyachi, N., Adachi, H., Senjo, N., Murata, R., Izumi, M., Hirose, T., and Arai, T., 2002, "Control of walk and manipulation by a hexapod with integrated limb mechanism: MELMANTIS-1," in Proceedings of the 2002 IEEE International Conference on Robotics and Automation, Washington, DC, May 11–15, pp. 3553–3558.

[19] Janrathitikarn, O., The Use of a Cognitive Architecture To Control A Six-legged Robot, A dissertation submitted in Partial Fulfillment of the Requirements for the Degree of Master of Science, Aerospace Engineering in The Pennsylvania State University, 2007.

- [20] Matsuoka, K., 1979, "A model of repetitive hopping movements in man," in Fifth World Congress on Theory of Machines and Mechanisms, International Federation for Information Processing
- [21] Raibert, M. H., 1986, Legged Robots that Balance, The MIT Press, Cambridge, MA.
- [22] Ahmadi, M. and Buehler, M., 2006, "Controlled passive dynamic running experiments with ARL Monopod II," IEEE Transactions on Robotics 22(5), 974–986
- [23] Iida, F., Dravid, R., and Paul, C., 2002, "Design and control of a pendulum driven hopping robot," in Proceedings of the 2002 IEEE/RSJ International Conference on Intelligent Robots and Systems, Lausanne, Switzerland, September 30–October 4, pp. 2141–2146
- [24] Hirai, K., Hirose, M., Haikawa, Y. and Takenaka, T., 1998, "The development of Honda humanoid robot," in Proceedings of the 1998 IEEE International Conference on Robotics and Automation, Leuven, Belgium, May 16–20, pp. 1321–1326.
- [25] Sakagami, Y., Watanabe, R., Aoyama, C., Matsunaga, S., Higaki, N., and Fujimura, K., 2002, "The intelligent ASIMO: system overview and integration," in Proceedings of the 2002 IEEE/RSJ International Conference on Intelligent Robots and Systems, Lausanne, Switzerland, September 30–October 4, pp. 2478–2483.
- [26] P. G. d. Santos, E. Garcia, and J. Estremera, "Quadrupedal locomotion: An introduction to the control four-legged robots," Germany: Springer, 2006, pp. 3, 29-31.

- [27] D. J. Todd, *Walking Machines: An Introduction to Legged Robots*. New York: Chapman and Hall, 1985.
- [28] Raibert, M. H., 1986, *Legged Robots that Balance*, The MIT Press, Cambridge, MA.
- [29] Liston, R. A. and Mosher, R. S., 1968, "A Versatile Walking Truck," in *Proceedings of the Transportation Engineering Conference*, Institute of Civil Engineers, London.
- [30] Mosher, R. S., 1968, "Test and evaluation of a versatile walking truck," in *Proceedings of the Off-Road Mobility Research Symposium*, International Society for Terrain Vehicle Systems, Washington, DC, May, pp. 359–379.
- [31] McGhee, R. B., 1966, "Finite state control of quadruped locomotion," in *Second International Symposium on External Control of Extremities*.
- [32] Frank, A. A., 1968, *Automatic Control Systems for Legged Locomotion*. USCEE Report No. 273, University of Southern California, Los Angeles, CA.
- [33] Buehler, M., Cocosco, A., Yamazaki, K., and Battaglia, R., 1999, "Stable open loop walking in quadruped robots with stick legs," in *Proceedings of the 1999 IEEE International Conference on Robotics and Automation*, Detroit, MI, May 10–15, pp. 2348–2353.
- [34] Poulakakis, I., Smith, J. A., and Buehler, M., 2005, "Modeling and experiments of untethered quadrupedal running with a bounding gait: The Scout II robot," *International Journal of Robotics Research* 24(4), 239–256.
- [35] Papadopoulos, D. and Buehler, M., 2000, "Stable running in a quadruped robot with compliant legs," in *Proceedings of the 2000 IEEE International*

Conference on Robotics and Automation, San Francisco, CA, April 24–28, pp. 444–449.

[36] Hawker, G. and Buehler, M., 2000, “Quadruped trotting with passive knees—design, control, and experiments,” in Proceedings of the 2000 IEEE International Conference on Robotics and Automation, San Francisco, CA, April 24–28, pp. 3046–3051.

[37] A. A. Yumaryanto, J. An, and L. Sangyoon, "A cockroach-inspired hexapod robot actuated by LIPCA," in IEEE Conference on Robotics, Automation and Mechatronics, 2006, pp. 1-6.

[38] P. G. d. Santos, E. Garcia, and J. Estremera, "Quadrupedal locomotion: An introduction to the control four-legged robots," Germany: Springer, 2006, pp. 3, 29-31.

[39] D. J. Todd, *Walking Machines: An Introduction to Legged Robots*. New York: Chapman and Hall, 1985.

[40] F. Ozguner and S.-J. Tsai, "Design and implementation of a binocular-vision system for locating footholds of a multi-legged walking robot," *IEEE Transactions on Industrial Electronics*, vol. IE- 32, pp. 26-31,

[41] Binnard, M. B., 1995, *Design of a Small Pneumatic Walking Robot*. MSc thesis, Massachusetts Institute of Technology – Department of Mechanical Engineering, Cambridge, MA.

[42] Pfeiffer, F., Eltze, J., and Weidemann, H.-J., 1995, “The TUM-walking machine,” *Intelligent Automation and Soft Computing* 1(3), 307–323.

[43] Quinn, R. D., Offi, J. T., Kingsley, D. A., and Ritzmann, R. E., 2002, “Improved mobility through abstracted biological principles,” in Proceedings

of the 2002 IEEE/RSJ International Conference on Intelligent Robots and Systems, Lausanne, Switzerland, September 30–October 4, pp. 2652–2657.

[44] Saranli, U., Buehler, M., and Koditschek, D. E., 2001, “RHex—a simple and highly mobile hexapod robot,” *The International Journal of Robotics Research* 20(7), 616–631.

[45] Potesil, A., Hanzlik, V. Application of Expert Systems ANSYS and ADAMS in Optimization of Mechanisms With Elastic Member

[46] Albers, A., Emmrich, D. and Häußler, P. Automated Structural Optimization of Flexible Components using MSC.Adams/Flex and MSC.Nastran Sol200

[47] Joldes, G. R., Improved Linear Tetrahedral Element for Surgical Simulation, Intelligent Systems for Medicine Lab., The University of Western Australia

[48] R.J. Pulles Controller Design for ADAMS models using MATLAB/SIMULINK interaction DCT-2003-29

[49] Maxon motor, RE 30 _30 mm, Graphite Brushes, 60 Watt catalog. www.maxonmotor.com

APPENDIX A

VELOCITY INPUT FOR LEFT AND RIGHT TRIPOD FOR VALIDATION WITH THE LITERATURE RESULTS

The right tripod input:

STEP(time,0,0,0.0001,133.63d)+
STEP(time,0.137143,0,0.137243,1465.84d)-
STEP(time,0.337143,0,0.337243,1465.84d)+
STEP(time,0.637143,0,0.637243,1465.84d)-
STEP(time,0.837143,0,0.837243,1465.84d)+
STEP(time,1.13714,0,1.13724,1465.84d)-
STEP(time,1.33714,0,1.33724,1465.84d)+
STEP(time,1.63714,0,1.63724,1465.84d)-
STEP(time,1.83714,0,1.83724,1465.84d)+
STEP(time,2.13714,0,2.13724,1465.84d)-
STEP(time,2.33714,0,2.33724,1465.84d)+
STEP(time,2.63714,0,2.63724,1465.84d)-
STEP(time,2.83714,0,2.83724,1465.84d)+
STEP(time,3.13714,0,3.13724,1465.84d)-
STEP(time,3.33714,0,3.33724,1465.84d)+
STEP(time,3.63714,0,3.63724,1465.84d)-
STEP(time,3.83714,0,3.83724,1465.84d)+
STEP(time,4.13714,0,4.13724,1465.84d)-
STEP(time,4.33714,0,4.33724,1465.84d)+

STEP(time,4.63714,0,4.63724,1465.84d)-
STEP(time,4.83714,0,4.83724,1465.84d)+
STEP(time,5.13714,0,5.13724,1465.84d)-

The left tripod input:

STEP(time,0.237143,0,0.237243,133.63d)+
STEP(time,0.374286,0,0.374386,1465.84d)-
STEP(time,0.574286,0,0.574386,1465.84d)+
STEP(time,0.874286,0,0.874386,1465.84d)-
STEP(time,1.07429,0,1.07439,1465.84d)+
STEP(time,1.37429,0,1.37439,1465.84d)-
STEP(time,1.57429,0,1.57439,1465.84d)+
STEP(time,1.87429,0,1.87439,1465.84d)-
STEP(time,2.07429,0,2.07439,1465.84d)+
STEP(time,2.37429,0,2.37439,1465.84d)-
STEP(time,2.57429,0,2.57439,1465.84d)+
STEP(time,2.87429,0,2.87439,1465.84d)-
STEP(time,3.07429,0,3.07439,1465.84d)+
STEP(time,3.37429,0,3.37439,1465.84d)-
STEP(time,3.57429,0,3.57439,1465.84d)+
STEP(time,3.87429,0,3.87439,1465.84d)-
STEP(time,4.07429,0,4.07439,1465.84d)+
STEP(time,4.37429,0,4.37439,1465.84d)-
STEP(time,4.57429,0,4.57439,1465.84d)+
STEP(time,4.87429,0,4.87439,1465.84d)-
STEP(time,5.07429,0,5.07439,1465.84d)+

APPENDIX B

VELOCITY INPUT FOR LEFT AND RIGHT TRIPOD FOR ARBITRARY PARAMETER SET

The right tripod input:

STEP(time,0.3,0,0.3001,200.445d)+
STEP(time,0.428571,0,0.428671,699.169d)-
STEP(time,0.771429,0,0.771529,699.169d)+
STEP(time,1.02857,0,1.02867,699.169d)-
STEP(time,1.37143,0,1.37153,699.169d)+
STEP(time,1.62857,0,1.62867,699.169d)-
STEP(time,1.97143,0,1.97153,699.169d)+
STEP(time,2.22857,0,2.22867,699.169d)-
STEP(time,2.57143,0,2.57153,699.169d)+
STEP(time,2.82857,0,2.82867,699.169d)-
STEP(time,3.17143,0,3.17153,699.169d)+
STEP(time,3.42857,0,3.42867,699.169d)-
STEP(time,3.77143,0,3.77153,699.169d)+
STEP(time,4.02857,0,4.02867,699.169d)-
STEP(time,4.37143,0,4.37153,699.169d)+
STEP(time,4.62857,0,4.62867,699.169d)-
STEP(time,4.97143,0,4.97153,699.169d)

The left tripod input:

STEP(time,0,0,0.0001,200.445d)+
STEP(time,0.128571,0,0.128671,699.169d)-
STEP(time,0.471429,0,0.471529,699.169d)+
STEP(time,0.728571,0,0.728671,699.169d)-
STEP(time,1.07143,0,1.07153,699.169d)+
STEP(time,1.32857,0,1.32867,699.169d)-
STEP(time,1.67143,0,1.67153,699.169d)+
STEP(time,1.92857,0,1.92867,699.169d)-
STEP(time,2.27143,0,2.27153,699.169d)+
STEP(time,2.52857,0,2.52867,699.169d)-
STEP(time,2.87143,0,2.87153,699.169d)+
STEP(time,3.12857,0,3.12867,699.169d)-
STEP(time,3.47143,0,3.47153,699.169d)+
STEP(time,3.72857,0,3.72867,699.169d)-
STEP(time,4.07143,0,4.07153,699.169d)+
STEP(time,4.32857,0,4.32867,699.169d)-
STEP(time,4.67143,0,4.67153,699.169d)+
STEP(time,4.92857,0,4.92867,699.169d)

APPENDIX C

VELOCITY INPUT FOR LEFT AND RIGHT TRIPOD FOR $t_{ratio} = 0.5$

The right tripod input:

STEP(time,0.3,0,0.3001,257.715d)+STEP(time,0.4,0,0.4001,513.383d)-
STEP(time,0.8,0,0.8001,513.383d)+STEP(time,1,0,1.0001,513.383d)-
STEP(time,1.4,0,1.4001,513.383d)+STEP(time,1.6,0,1.6001,513.383d)-
STEP(time,2,0,2.0001,513.383d)+STEP(time,2.2,0,2.2001,513.383d)-
STEP(time,2.6,0,2.6001,513.383d)+STEP(time,2.8,0,2.8001,513.383d)-
STEP(time,3.2,0,3.2001,513.383d)+STEP(time,3.4,0,3.4001,513.383d)-
STEP(time,3.8,0,3.8001,513.383d)+STEP(time,4,0,4.0001,513.383d)-
STEP(time,4.4,0,4.4001,513.383d)+STEP(time,4.6,0,4.6001,513.383d)

The left tripod input:

STEP(time,0,0,0.0001,257.715d)+STEP(time,0.1,0,0.1001,513.383d)-
STEP(time,0.5,0,0.5001,513.383d)+STEP(time,0.7,0,0.7001,513.383d)-
STEP(time,1.1,0,1.1001,513.383d)+STEP(time,1.3,0,1.3001,513.383d)-
STEP(time,1.7,0,1.7001,513.383d)+STEP(time,1.9,0,1.9001,513.383d)-
STEP(time,2.3,0,2.3001,513.383d)+STEP(time,2.5,0,2.5001,513.383d)-
STEP(time,2.9,0,2.9001,513.383d)+STEP(time,3.1,0,3.1001,513.383d)-
STEP(time,3.5,0,3.5001,513.383d)+STEP(time,3.7,0,3.7001,513.383d)-
STEP(time,4.1,0,4.1001,513.383d)+STEP(time,4.3,0,4.3001,513.383d)-
STEP(time,4.7,0,4.7001,513.383d)+STEP(time,4.9,0,4.9001,513.383d)

APPENDIX D

VELOCITY INPUT FOR LEFT AND RIGHT TRIPOD FOR $t_{ratio} = 1$

The right tripod input:

STEP(time,0.3,0,0.3001,171.81d)+STEP(time,0.45,0,0.4501,856.32d)-
STEP(time,0.75,0,0.7501,856.32d)+STEP(time,1.05,0,1.0501,856.32d)-
STEP(time,1.35,0,1.3501,856.32d)+STEP(time,1.65,0,1.6501,856.32d)-
STEP(time,1.95,0,1.9501,856.32d)+STEP(time,2.25,0,2.2501,856.32d)-
STEP(time,2.55,0,2.5501,856.32d)+STEP(time,2.85,0,2.8501,856.32d)-
STEP(time,3.15,0,3.1501,856.32d)+STEP(time,3.45,0,3.4501,856.32d)-
STEP(time,3.75,0,3.7501,856.32d)+STEP(time,4.05,0,4.0501,856.32d)-
STEP(time,4.35,0,4.3501,856.32d)+STEP(time,4.65,0,4.6501,856.32d)-
STEP(time,4.95,0,4.9501,856.32d)

The left tripod input:

STEP(time,0,0,0.0001,171.81d)+STEP(time,0.15,0,0.1501,856.32d)-
STEP(time,0.45,0,0.4501,856.32d)+STEP(time,0.75,0,0.7501,856.32d)-
STEP(time,1.05,0,1.0501,856.32d)+STEP(time,1.35,0,1.3501,856.32d)-
STEP(time,1.65,0,1.6501,856.32d)+STEP(time,1.95,0,1.9501,856.32d)-
STEP(time,2.25,0,2.2501,856.32d)+STEP(time,2.55,0,2.5501,856.32d)-
STEP(time,2.85,0,2.8501,856.32d)+STEP(time,3.15,0,3.1501,856.32d)-
STEP(time,3.45,0,3.4501,856.32d)+STEP(time,3.75,0,3.7501,856.32d)-
STEP(time,4.05,0,4.0501,856.32d)+STEP(time,4.35,0,4.3501,856.32d)-
STEP(time,4.65,0,4.6501,856.32d)+STEP(time,4.95,0,4.9501,856.32d)

APPENDIX E

VELOCITY INPUT FOR LEFT AND RIGHT TRIPOD FOR $t_{ratio} = 1.5$

The right tripod input:

STEP(time,0.3,0,0.3001,143.175d)+STEP(time,0.48,0,0.4801,1141.99d)-
STEP(time,0.72,0,0.7201,1141.99d)+STEP(time,1.08,0,1.0801,1141.99d)-
STEP(time,1.32,0,1.3201,1141.99d)+STEP(time,1.68,0,1.6801,1141.99d)-
STEP(time,1.92,0,1.9201,1141.99d)+STEP(time,2.28,0,2.2801,1141.99d)-
STEP(time,2.52,0,2.5201,1141.99d)+STEP(time,2.88,0,2.8801,1141.99d)-
STEP(time,3.12,0,3.1201,1141.99d)+STEP(time,3.48,0,3.4801,1141.99d)-
STEP(time,3.72,0,3.7201,1141.99d)+STEP(time,4.08,0,4.0801,1141.99d)-
STEP(time,4.32,0,4.3201,1141.99d)+STEP(time,4.68,0,4.6801,1141.99d)-
STEP(time,4.92,0,4.9201,1141.99d)

The left tripod input:

STEP(time,0,0,0.0001,143.175d)+STEP(time,0.18,0,0.1801,1141.99d)-
STEP(time,0.42,0,0.4201,1141.99d)+STEP(time,0.78,0,0.7801,1141.99d)-
STEP(time,1.02,0,1.0201,1141.99d)+STEP(time,1.38,0,1.3801,1141.99d)-
STEP(time,1.62,0,1.6201,1141.99d)+STEP(time,1.98,0,1.9801,1141.99d)-
STEP(time,2.22,0,2.2201,1141.99d)+STEP(time,2.58,0,2.5801,1141.99d)-
STEP(time,2.82,0,2.8201,1141.99d)+STEP(time,3.18,0,3.1801,1141.99d)-
STEP(time,3.42,0,3.4201,1141.99d)+STEP(time,3.78,0,3.7801,1141.99d)-
STEP(time,4.02,0,4.0201,1141.99d)+STEP(time,4.38,0,4.3801,1141.99d)-
STEP(time,4.62,0,4.6201,1141.99d)+STEP(time,4.98,0,4.9801,1141.99d)

APPENDIX F

VELOCITY INPUT FOR LEFT AND RIGHT TRIPOD FOR Φ_s PARAMETER

The right tripod input:

STEP(time,0.3,0,0.3001,66.815d)+
STEP(time,0.428571,0,0.428671,933.021d)-
STEP(time,0.771429,0,0.771529,933.021d)+
STEP(time,1.02857,0,1.02867,933.021d)-
STEP(time,1.37143,0,1.37153,933.021d)+
STEP(time,1.62857,0,1.62867,933.021d)-
STEP(time,1.97143,0,1.97153,933.021d)+
STEP(time,2.22857,0,2.22867,933.021d)-
STEP(time,2.57143,0,2.57153,933.021d)+
STEP(time,2.82857,0,2.82867,933.021d)-
STEP(time,3.17143,0,3.17153,933.021d)+
STEP(time,3.42857,0,3.42867,933.021d)-
STEP(time,3.77143,0,3.77153,933.021d)+
STEP(time,4.02857,0,4.02867,933.021d)-
STEP(time,4.37143,0,4.37153,933.021d)+
STEP(time,4.62857,0,4.62867,933.021d)-
STEP(time,4.97143,0,4.97153,933.021d)

The left tripod input:

STEP(time,0,0,0.0001,66.815d)+
STEP(time,0.128571,0,0.128671,933.021d)-
STEP(time,0.471429,0,0.471529,933.021d)+
STEP(time,0.728571,0,0.728671,933.021d)-
STEP(time,1.07143,0,1.07153,933.021d)+
STEP(time,1.32857,0,1.32867,933.021d)-
STEP(time,1.67143,0,1.67153,933.021d)+
STEP(time,1.92857,0,1.92867,933.021d)-
STEP(time,2.27143,0,2.27153,933.021d)+
STEP(time,2.52857,0,2.52867,933.021d)-
STEP(time,2.87143,0,2.87153,933.021d)+
STEP(time,3.12857,0,3.12867,933.021d)-
STEP(time,3.47143,0,3.47153,933.021d)+
STEP(time,3.72857,0,3.72867,933.021d)-
STEP(time,4.07143,0,4.07153,933.021d)+
STEP(time,4.32857,0,4.32867,933.021d)-
STEP(time,4.67143,0,4.67153,933.021d)+
STEP(time,4.92857,0,4.92867,933.021d)